Theory of Surfactant Self-Assembly: A Predictive Molecular Thermodynamic Approach

R. Nagarajan*

Department of Chemical Engineering, The Pennsylvania State University, University Park, Pennsylvania 16802

E. Ruckenstein

Department of Chemical Engineering, State University of New York at Buffalo, Amherst, New York 14260

Received May 17, 1991. In Final Form: September 19, 1991

A thermodynamic treatment of surfactant self-assembly in aqueous media is developed that allows an a priori quantitative prediction of the aggregation behavior of surfactants, starting from their molecular structures and the solution conditions. The treatment combines the general thermodynamic principles of self-assembly with detailed molecular models for various contributions to the free energy of aggregation. The treatment is employed to predict the aggregation behavior of surfactants that generate narrowly dispersed, small, spherical or globular aggregates; the transition from spherical to large, polydispersed, rodlike aggregates; the aggregation behavior of surfactants containing polymeric head groups such as the widely used poly(oxyethylene)-type nonionic surfactants; the solubilization of hydrophobic molecules in aggregates; the solubilization-induced transition from rodlike to spherical aggregates; the solubilization of binary mixtures of hydrocarbons; and the temperature dependence of micellization and solubilization. For illustrative purposes, calculated results concerning nonionic, zwitterionic, and ionic surfactants are presented and compared with experimental results generated by more than 20 different laboratories. The calculations show that, as a result of solubilization, microemulsion structures are formed with a single surfactant. However, the core of the solubilizate in these structures is rather small. In developing a molecular model for the free energy of aggregation, we consider contributions arising from (i) the transfer of the surfactant tail from water into the hydrophobic core of the aggregate assumed to behave like a liquid hydrocarbon, (ii) the conformational free energy of the tails inside the aggregates due to the constrained location of the head groups on the aggregate surface, (iii) the free energy of formation of the aggregate–water interface, and (iv) the interactions between the head groups of the surfactant at the aggregate surface. In the case of solubilization, the free energy of mixing of the solubilizates with the surfactants also makes a contribution. Expressions for each of the above free energy contributions are derived here. The transfer free energy is expressed as an explicit function of temperature. Analytical free energy expressions are derived for the dependence of the conformational free energy of the surfactant tails inside the aggregates as a function of the size and shape of aggregates. The interfacial tension characteristic of the aggregate–water interface is calculated using the Prigogine theory when more than two distinct molecular species are present as in the case of micellization involving poly(oxyethylene) surfactants and for the case of solubilization of one or more additives into the aggregates. The interactions among the poly(oxyethylene) head groups in nonionic surfactants are calculated on the basis of two limiting models which differ from one another in the description of the mixing and elastic deformation free energies of the poly(oxyethylene)–water region surrounding the aggregates. Also, the head group interactions between ionic surfactants are calculated using an approximate analytical solution for the Poisson–Boltzmann equation available in the literature. The thermodynamic treatment developed here is strictly predictive in the sense that it is free of information extracted from the aggregation behavior of surfactants. In addition, no arbitrary or empirical factors are involved. The only parameters that appear are molecular constants that can be reasonably determined on the basis of known molecular structures and properties.

I. Introduction

Surfactant molecules are composed of a polar head that is compatible with water and a nonpolar or hydrophobic part that is compatible with oil. This dual nature endows the surfactants with their unique solution and interfacial characteristics. Among these, the most noteworthy is the behavior in dilute aqueous solutions, where the surfactant molecules self-assemble to form aggregates so as to achieve segregation of their hydrophobic parts from water.[1] Various molecular architectures result from this self-assembly. Depending upon the type of surfactant and the solution conditions, the aggregates may be spherical, globular, or rodlike or have the structure of spherical bilayers. The closed aggregates with hydrophobic interiors are known as micelles while the spherical bilayers containing an encapsulated aqueous phase are called vesicles (Figure 1).

One of the distinguishable features of the aqueous surfactant solutions is their ability to enhance the solubility of hydrophobic solutes that have otherwise very poor solubilities in water.[2-4] This solubilization is a consequence of the presence of hydrophobic domains in the surfactant aggregates which act as compatible microenvironments for the location of hydrophobic solubilizates. The enhanced solubility of a hydrophobic solute has been found to be orders of magnitude larger than its aqueous solubility

(1) Tanford, C. *The Hydrophobic Effect*; Wiley: New York, 1973; 2nd ed., 1980.

(2) McBain, M. E. L.; Hutchinson, E. *Solubilization and Related Phenomena*; Academic Press: New York, 1955.

(3) Elworthy, P. H.; Florence, A. T.; McFarlane, C. B. *Solubilization by Surface Active Agents*; Chapman and Hall: London, 1968.

(4) Attwood, D.; Florence, A. T. *Surfactant Systems. Their Chemistry, Pharmacy and Biology*; Chapman and Hall: London, 1983.

0743-7463/91/2407-2934$02.50/0

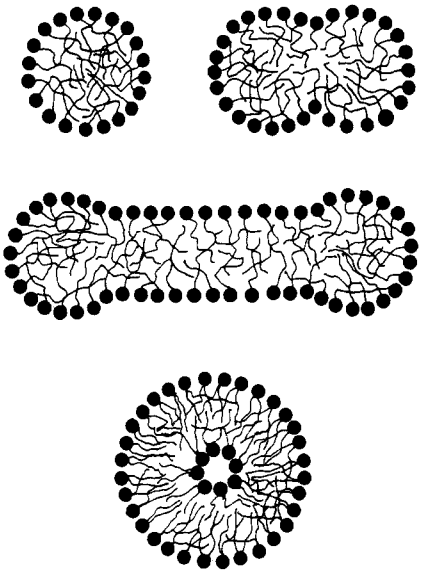

Figure 1. Schematic representation of the structures of surfactant aggregates in dilute aqueous solutions. Shown are aggregates that are spherical, globular, and spherocylindrical micelles and spherical bilayer vesicles.

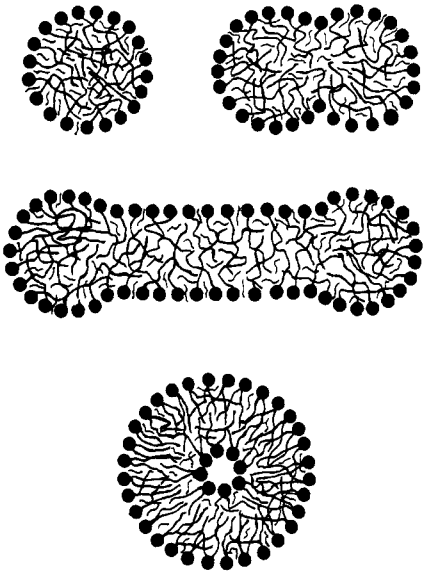

Figure 2. Schematic representation of solubilization of hydrophobic molecules in surfactant aggregates giving rise to type I aggregates, referred to as swollen aggregates. The solubilizates are present in the surfactant tail region which extends over the entire volume of the aggregate. The smaller dimension characterizing the aggregate is limited by the length of the surfactant tail.

in the absence of surfactants. The shapes of the aggregates containing solubilizates may be similar to those in the absence of solubilization if the solubilizate molecules are entirely located in the region of the surfactant tails. This mode of solubilization is designated type I, and the aggregates are referred to as swollen aggregates (Figure 2). Alternately, the solubilizate molecules may constitute a domain themselves in the interior of the aggregates in addition to being present among the surfactant tails. This mode of solubilization is designated as type II, and the aggregates are referred to as microemulsions (Figure 3).

Experimental studies of surfactant solutions reported in the literature are numerous. Representative work in the recent years is well documented in a series of symposia proceedings.[5-9] In general, the experimental studies attempt to determine the critical micelle concentration (cmc) at which the surfactant aggregates come into

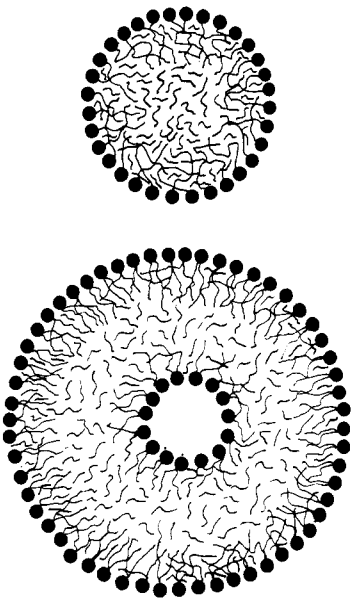

Figure 3. Structure of surfactant aggregates wherein the type II mode of solubilization occurs, also referred to as microemulsions. In these structures, the solubilizates are present both within the surfactant tail region and in a domain made up of only the solubilizate. The solubilizate domain constitutes the core of the aggregate in the first structure shown and is a spherical shell region separating the two surfactant layers in the second structure shown. The dimensions of the aggregates are not limited by the extended length of the surfactant tail.

existence, the average size and the shape of the aggregates, their polydispersity, the internal conformation of the surfactant tails, the conditions under which transitions in the shape of the aggregates occur, and the phase behavior of the surfactant solutions. Studies of solubilization have focused on determining the locus of solubilization and estimating the maximum amount of solubilization possible, the change in the critical micelle concentration as a consequence of solubilization, the change in the size and shape of the aggregates induced by solubilization, and the selectivity for one solubilizate over another displayed by the surfactant solutions.

Many experimentally observed features of surfactant self-assembly are now well-understood qualitatively. Mukerjee[10-12] showed how cooperativity of self-association is responsible for the formation of large aggregates instead of molecular clusters such as dimers, trimers, etc. He also emphasized the important role played by anticooperativity which ensures that micelles remain finite rather than growing without limit. Mukerjee demonstrated how subtle variations in the free energy of micellization control the transition between globular and rodlike micelles using empirical expressions for the free energy.[13] Further, he derived for the first time[14] an expression for the dependence of the average size of the rodlike micelles on the surfactant concentration. The physicochemical features of surfactant self-assembly were elucidated by the pio-

(5) Mittal, K. L., Ed. *Micellization, Solubilization and Microemulsions*; Plenum Press: New York, 1977.
(6) Mittal, K. L., Ed. *Solution Chemistry of Surfactants*; Plenum Press: New York, 1979.
(7) Mittal, K. L., Fendler, E. J., Eds. *Solution Behavior of Surfactants*; Plenum Press: New York, 1981.
(8) Mittal, K. L., Lindman, B., Eds., *Surfactants in Solution. Theoretical and Applied Aspects*; Plenum Press: New York, 1984.
(9) Mittal, K. L., Botherrol, P., Eds. *Surfactants in Solution*; Plenum Press: New York, 1987.
(10) Mukerjee, P. *Adv. Colloid Interface Sci.* **1967**, *1*, 241.
(11) Mukerjee, P. *J. Phys. Chem.* **1969**, *73*, 2054.
(12) Mukerjee, P. *J. Pharm. Sci.* **1974**, *68*, 972.
(13) Mukerjee, P. See ref 5, p 171.
(14) Mukerjee, P. *J. Phys. Chem.* **1972**, *76*, 565.

neering model of Tanford[1,15,16] for the free energy change associated with micellization. Tanford demonstrated that the hydrophobic effect is responsible for the cooperative growth of micelles, while the interactions between the polar head groups of surfactants provide the anticooperativity that constrains the aggregates to remain of finite sizes. It is fair to say that all the free energy models of surfactant self-assembly discussed in the literature have been influenced by Tanford's work. The critical micelle concentration which is usually defined only operationally in terms of the experimental method used for its determination was given a theoretical definition, independent of the experimental method employed, by Ruckenstein and Nagarajan.[17,18] With recognition of the intimate connection between the measurable properties of micellar solutions and the size distribution of the micelles, the critical concentration was defined as the surfactant concentration at which the size distribution of micelles changes from a monotonically decreasing function to a function that exhibits extrema. This theoretically defined critical concentration was shown to be a close lower bound of the experimental critical micelle concentration. Both Tartar[19] and Tanford[1] suggested on the basis of geometrical considerations how the micellar shape and its size are related. This suggestion has received a clear treatment in the work of Israelachvili et al.[20-22] They showed how the type of aggregate formed and its size depend upon the length and the volume of the surfactant tail as well as on the aggregate surface area per molecule obtained from equilibrium free energy considerations. A statistical thermodynamic model of surfactant aggregation was developed by Nagarajan and Ruckenstein.[23,24] In this work, the physical origin of the attractive and repulsive contributions to the free energy of aggregation was clarified and explicit expressions for each of these free energy contributions were formulated. The essential role of steric repulsion between head groups that governs the aggregation behavior of nonionic surfactants was for the first time identified. Gruen,[25-28] Dill and Flory,[29-33] and Ben-Shaul and Gelbart[34-36] have modeled the intraaggregate conformations of the surfactant tail to obtain estimates of the extent of chain ordering inside the aggregates compared to analogous chains in liquid hydrocarbons. These studies also provide information about the extent to which the different parts of the surfactant tail come into contact with water, thus allowing a satisfactory interpretation of various probe-based studies. The problem of intermicellar interactions in concentrated solutions containing globular or rodlike micelles and the phase behavior of such solutions has been treated by Blankschtein and Benedek.[37-41] The consequences of intermicellar interactions for the growth of micelles has been examined in the work of Gelbart et al.[42,43] The aggregation behavior of mixed surfactant systems has been modeled from a molecular point of view by Nagarajan[44,45] and Ruckenstein.[46] The nonideal behavior exhibited by mixed surfactant systems has been traced to the fact that the interactions at the micellar surface depend nonlinearly on the composition of the mixed surfactant systems. The formation of spherocylindrical aggregates in mixed surfactant systems has been shown to be influenced by the asymmetric distribution of the surfactant components in the spherical endcaps and in the cylindrical middle by Gelbart et al.[47] A unitary approach to micellization, solubilization, and microemulsions has been presented by Ruckenstein.[48] He has emphasized the importance of the hydrophobic effect in the occurrence of critical concentrations in aqueous surfactant solutions and suggested a possible explanation for the critical micelle concentration also in nonpolar solutions.[49]

Many of the general principles of surfactant aggregation have now been adequately clarified by the theoretical studies mentioned above. Yet, a majority of these studies have not provided quantitative a priori predictions of the aggregation behavior starting from the molecular structure of the surfactants and the solution conditions such as temperature, ionic strength, surfactant concentration, etc. Very few predictive attempts other than our earlier work and the recent work of Puvvada and Blankschtein[41] can be found in the literature. In our earlier work,[23,24] we developed a molecular thermodynamic treatment of aggregation in dilute aqueous solutions which was used to predict the critical micelle concentration, the average size and shape of aggregates, and the detailed size distribution of aggregates. The predictions were compared with the experimental data for a number of nonionic, anionic, cationic, and zwitterionic surfactants possessing either one or two hydrocarbon chains as tails. The predictions regarding the formation of spherical and rodlike micelles as well as spherical bilayer vesicles were found to be in agreement with the experimental data. The calculations were extended to mixtures of surfactants[44,45] and also to surfactant–alcohol mixtures.[46] The critical micelle concentration of the mixed aggregates and the composition and the size of the mixed micelles were all predicted as a function of the overall composition of the surfactant

(15) Tanford, C. *J. Phys. Chem.* **1974**, *78*, 2469.
(16) Tanford, C. See ref 5, p 119.
(17) Ruckenstein, E.; Nagarajan, R. *J. Phys. Chem.* **1975**, *79*, 2622.
(18) Ruckenstein, E.; Nagarajan, R. *J. Colloid Interface Sci.* **1976**, *57*, 388.
(19) Tartar, H. V. *J. Phys. Chem.* **1955**, *55*, 1195.
(20) Israelachvili, J. N.; Mitchell, D. J.; Ninham, B. W. *J. Chem. Soc., Faraday Trans. 2* **1976**, *72*, 1525.
(21) Israelachvili, J. N.; Mitchell, D. J.; Ninham, B. W. *Biochim. Biophys. Acta* **1977**, *470*, 185.
(22) Israelachvili, J. N.; Marcelja, S.; Horn, R. G. *Q. Rev. Biophys.* **1980**, *13*, 121.
(23) Nagarajan, R.; Ruckenstein, E. *J. Colloid Interface Sci.* **1977**, *60*, 221.
(24) Nagarajan, R.; Ruckenstein, E. *J. Colloid Interface Sci.* **1979**, *71*, 580.
(25) Gruen, D. W. R. *Biochim. Biophys. Acta* **1980**, *595*, 161.
(26) Gruen, D. W. R. *J. Colloid Interface Sci.* **1981**, *84*, 281.
(27) Gruen, D. W. R.; de Lacey, E. H. B. See Ref 8, p 279.
(28) Gruen, D. W. R. *J. Phys. Chem.* **1985**, *89*, 146.
(29) Dill, K. A.; Flory, P. J. *Proc. Natl. Acad. Sci. U.S.A.* **1980**, *77*, 3115.
(30) Dill, K. A.; Flory, P. J. *Proc. Natl. Acad. Sci. U.S.A.* **1980**, *78*, 676.
(31) Dill, K. A.; Cantor, R. S. *Macromolecules* **1984**, *17*, 380.
(32) Cantor, R. S.; Dill, K. A. *Macromolecules* **1984**, *17*, 384.
(33) Dill, K. A.; Koppel, D. E.; Cantor, R. S.; Dill, J. D.; Bendedouch, D.; Chen, S. H. *Nature* **1984**, *309*, 42.
(34) Ben-Shaul, A.; Szleifer, I.; Gelbart, W. M. *Proc. Natl. Acad. Sci. U.S.A.* **1984**, *81*, 4601.
(35) Ben-Shaul, A.; Szleifer, I.; Gelbart, W. M. *J. Chem. Phys.* **1985**, *83*, 3597.
(36) Ben-Shaul, A.; Gelbart, W. M. *Annu. Rev. Phys. Chem.* **1985**, *36*, 179.
(37) Blankschtein, K.; Thurston, G. M.; Benedck, G. B. *Phys. Rev. Lett.* **1985**, *54*, 955.
(38) Thurston, G. M.; Blankschtein, D.; Fisch, M. R.; Benedek, G. B. *J. Chem. Phys.* **1986**, *84*, 4558.
(39) Blankschtein, D.; Thurston, G. M.; Benedek, G. B. *J. Chem. Phys.* **1986**, *85*, 7268.
(40) Huang, Y. X.; Thurston, G. M.; Blankschtein, K.; Benedek, G. B. *J. Chem. Phys.* **1990**, *92*, 1956.
(41) Puvvada, S.; Blankschtein, D. J. *J. Chem. Phys.* **1990**, *92*, 3710.
(42) McMullen, W. E.; Gelbart, W. M.; Ben-Shaul, A. *J. Chem. Phys.* **1985**, *82*, 5615.
(43) Gelbart, W. M.; Ben-Shaul, A.; McMullen, W. E.; Masters, A. *J. Phys. Chem.* **1984**, *88*, 861.
(44) Nagarajan, R. *Langmuir* **1985**, *1*, 331.
(45) Nagarajan, R. *Adv. Colloid Interface Sci.* **1986**, *26*, 205.
(46) Rao, I. V.; Ruckenstein, E. *J. Colloid Interface Sci.* **1986**, *113*, 375.
(47) Gelbart, W. M.; McMullen, W. E.; Masters, A.; Ben-Shaul, A. *Langmuir* **1985**, *1*, 101.
(48) Ruckenstein, E. In *Progress in Microemulsions*; Martellucci, S., Chester, A. N., Eds.; Plenum Press: New York, 1989; p 41.
(49) Ruckenstein, E. In *Progress in Microemulsions*; Martellucci, S., Chester, A. N., Eds.; Plenum Press: New York, 1989; p 31.

solution. The treatment was also applied[50] to the bola surfactants which have two polar groups attached to the two ends of a hydrophobic chain. Further, a predictive theory of solubilization of hydrocarbons and hydrocarbon mixtures in micelles[51-53] was developed. This theory allowed the estimation of the change in the critical micelle concentration as a consequence of solubilization, the maximum amount of solubilization possible in an aggregate, and the solubilizate-induced changes in the size as well as shape of the aggregates. The theory also predicted the selective solubilization of aromatic hydrocarbons compared to aliphatic hydrocarbons of similar size when binary hydrocarbon mixtures were solubilized. Most recently, the thermodynamic treatment of aggregation has been employed to investigate how the presence of polymer molecules in surfactant solutions influences their self-assembly.[54] Interesting predictions result from these calculations, namely, that rodlike micelles may transform into smaller globular micelles and spherical bilayer vesicles can transform into closed disklike aggregates.

Our earlier treatments of micellization and solubilization were not strictly a priori predictive in nature, since a few of the contributions to the free energy of aggregation were estimated by utilizing experimental data available for micellar solutions. Firstly, the free energy change associated with the conformational constraints on the surfactant tail when incorporated within an aggregate was calculated using an empirical expression chosen to provide agreement with the experimental cmcs. However, despite its empirical nature, the expression had universality in the sense that it was not altered from one surfactant to another but was considered valid for all surfactants. This empirical expression assumed the chain conformation energy to be independent of the aggregate size and shape, which is contrary to the results obtained from the treatments of Gruen, Dill and Flory, and Ben-Shaul and Gelbart referred to above. Secondly, the free energy contribution due to the electrostatic interactions between the polar head groups of ionic surfactants was estimated using the Debye–Huckel approximation in which an empirical correction was incorporated. A constant numerical factor of 0.46 was employed in view of Tanford's observation[1] that the ionic interaction free energy estimated on the basis of the Debye–Huckel expression is roughly twice that necessary to describe the experimental cmc data. Again, the empirical constant was not changed for different surfactants but displayed universality by retaining the value of 0.46 for all surfactants. Thirdly, for the nonionic surfactants containing poly(oxyethylene) chain polar head groups, the interactions among the head groups was computed without a detailed modeling of the polymeric polar group but by merely visualizing it as similar to other surfactants having compact head groups. Finally, in the solubilization calculations, a negative excess free energy had to be included for the predicted solubilization behavior of aromatic solubilizates to agree with experimental data in contrast to the positive excess free energy typical for such hydrocarbon–hydrocarbon mixtures.

The main goal of the present paper is to develop a molecular thermodynamic treatment that allows an a priori prediction of micellization and solubilization. The free energy model does not utilize any information derived from experiments on surfactant solutions. As part of this goal, firstly we develop an analytical equation for the chain conformation free energy that is dependent on the size and the shape of the aggregates by borrowing results from the analysis of the chain conformation in polymer microdomains.[55,56] This free energy contribution allows new predictions to be made that were overlooked by the empirical, shape-independent free energy expression used earlier. Secondly, the electrostatic interactions in ionic micelles are computed by using an approximate analytical solution to the Poisson–Boltzmann equation that incorporates curvature corrections. This result has been derived recently and applied to spherical and spherocylindrical micellar systems.[57-59] The use of this equation is found to provide a satisfactory estimate of the ionic interaction free energy and avoids the earlier use of the empirical coefficient of 0.46 in conjunction with the Debye–Huckel approximation. Thirdly, the interactions among poly(oxyethylene) head groups in nonionic micelles is treated by taking into account the polymeric nature of the polar head group and considering the mixing and deformation free energies in polymer solutions in addition to the steric repulsions at the micellar core surface. Two alternate models have been developed for this purpose. One assumes a constant segment density in the region surrounding the micellar core and, correspondingly, a nonuniform deformation of the poly(oxyethylene) chain. The other assumes a uniform deformation of the polymer chain and, consistent with it, a nonuniform segment density in the micellar shell region. Fourthly, the excess free energies of mixing of solubilizates and surfactant tails are computed on the basis of the molecular properties of the surfactant tail and the solubilizate and no empirical free energy corrections are introduced. Finally, the temperature dependence of all the free energy contributions are explicitly described and have been employed to calculate the temperature dependence of the aggregation behavior. To summarize, in developing the theories of micellization and solubilization in this paper, we have not made use of any information obtained a posteriori from experimental aggregation data. Instead, we have chosen to examine how well the a priori predictions of the present model compare with the experimental results. Obviously, various molecular constants are involved in the calculations, and we show how they have been estimated on the basis of available molecular property information.

This paper is organized as follows. In section II, the general principles of surfactant self-assembly are summarized along with the geometrical relations characterizing various kinds of aggregates. The contributions to the free energy of micelle formation are considered in section III. Only brief discussions are presented for those contributions which are modeled as in our earlier work while the new free energy expressions are presented in greater detail. In section IV, the model predictions are compared with the available experimental data. For illustrative purposes, examples of nonionic, ionic, and zwitterionic surfactants are considered. The formation and characteristics of both globular and rodlike micelles are predicted. Extensive calculations of the temperature dependence of the cmc have been carried out. Also the parameter K accounting for the preferential formation of rodlike micelles over globular micelles has been predicted for a variety of solution conditions. The aggregation behaviors of nonionic surfactants with poly(oxyethylene) head groups are modeled in section V where two complementary treatments of

(50) Nagarajan, R. *Chem. Eng. Commun.* **1987**, *55*, 261.
(51) Nagarajan, R.; Ruckenstein, E. *Sep. Sci. Technol.* **1981**, *16*, 1429.
(52) Nagarajan, R.; Ruckenstein, E. See ref 8, p 923.
(53) Nagarajan, R.; Chaiko, M. A.; Ruckenstein, E. *J. Phys. Chem.* **1984**, *88*, 2916.
(54) Nagarajan, R. *J. Chem. Phys.* **1989**, *90*, 1980.
(55) Semenov, A. N. *Sov. Phys.—JETP (Engl. Transl.)* **1985**, *61*, 733.
(56) Nagarajan, R.; Ganesh, K. *Macromolecules* **1989**, *22*, 4312.
(57) Evans, D. F.; Ninham, B. W. *J. Phys. Chem.* **1983**, *87*, 5025.
(58) Chao, Y.; Sheu, E. Y.; Chen, S. H. *J. Phys. Chem.* **1985**, *89*, 4862.
(59) Missel, P. J.; Mazer, N.; Carey, M. C.; Benedek, G. B. *J. Phys. Chem.* **1989**, *93*, 8354.

the poly(oxyethylene) chain region are developed. The predictions of the two models are examined in section VI for surfactants containing a range of poly(oxyethylene) chain lengths as head groups. In section VII, a theory of solubilization is formulated. Solubilizations leading to swollen globular and rodlike micelles as well as microemulsions are considered. The free energy of solubilization is then modeled in section VIII. The predictions of the solubilization model for ionic and nonionic surfactants are presented in section IX and compared with the experimental data. Also, the phenomenon of rod to sphere transition induced by solubilization is examined. Section X extends the treatment of solubilization to binary solubilizate mixtures. The predicted solubilization of aliphatic–aromatic hydrocarbon mixtures is compared with our experimental data reported earlier. The last section summarizes the main conclusions.

II. Thermodynamics of Micellization

Size Distribution of Micelles and the Cmc. The surfactant solution consists of water molecules, singly dispersed surfactant molecules, and surfactant aggregates of all possible sizes and shapes. Each size and shape of aggregate is viewed as corresponding to a distinct chemical component, and the entire surfactant solution is visualized as a multicomponent solution. The standard state for water is defined to be the pure liquid while the standard states for all the other components are defined as the infinitely dilute solution conditions. Further, because of the dilute nature of the solution, the interspecies interactions are considered negligible. One may note that the (important) interactions of all the components with the solvent water are properly taken into account in the infinitely dilute standard states. The Gibbs free energy of the solution must be a minimum at equilibrium, and this condition yields the following relation for any total surfactant concentration:[1]

$$\mu_g^\circ + kT \ln X_g = g[\mu_1^\circ + kT \ln X_1] \tag{1}$$

In the above equation, μ_g° is the standard chemical potential of a surfactant aggregate containing g surfactant molecules and X_g is the mole fraction of these aggregates in the solution. The above relation states that the chemical potential of the surfactant molecule in the singly dispersed state is equal to the chemical potential per molecule of the surfactant aggregate. This relation can be rewritten in the form of the aggregate size distribution equation.

$$X_g = X_1^g \exp\left(-\frac{\mu_g^\circ - g\mu_1^\circ}{kT}\right) = X_1^g \exp\left(-\frac{g\Delta\mu_g^\circ}{kT}\right) \tag{2}$$

where $\Delta\mu_g^\circ$ is the difference in the standard chemical potentials between a surfactant molecule present in an aggregate of size g and a singly dispersed surfactant in water.

From the size distribution one can compute the average sizes of the aggregates via the relations

$$g_n = \frac{\sum gX_g}{\sum X_g}, \quad g_w = \frac{\sum g^2X_g}{\sum gX_g} \tag{3}$$

where g_n and g_w denote the number and the weight average aggregation numbers. The summations in eq 3 extend from 2 to ∞. The critical micelle concentration X_{cmc} can be obtained by constructing a plot of one of the functions X_1, $\sum gX_g$, or $\sum g^2X_g$ (which are proportional to different experimentally measured properties of the surfactant solution) against the total concentration X of the surfactant in solution, $X = X_1 + \sum gX_g$. The cmc can be determined as that value of the total surfactant concentration at which a sharp change in the plotted function (representing a physical property) occurs.[18,60,61] In practice, the cmc is usually taken to be the total surfactant concentration at which about 5–10% of the surfactant is in the form of aggregates.[1] The cmc has also been estimated[62] as that value of X_1 for which the concentration of the singly dispersed amphiphiles is equal to that of the surfactant present in the form of aggregates, namely, $X_1 = \sum gX_g = X_{cmc}$.

An alternative to the size distribution view of micellar solutions emerges from the observation that the aggregation number g of micelles is typically large. Therefore, one can rewrite eq 1 by noting that the concentrations X_1 and X_g are of the same order of magnitude.

$$\mu_g^\circ/g = \mu_1^\circ + kT \ln X_1 \tag{4}$$

This equation can be interpreted as implying that the aggregates constitute a pseudophase in equilibrium with the singly dispersed surfactant molecules. The standard Gibbs free energy of this pseudophase depends on the size g of the phase, as expected for small systems such as the surfactant aggregates. Thus, the pseudophase view of aggregates differs from the size distribution view through the neglect of the contribution to the solution entropy provided by the aggregates.

When globular micelles form, usually they are narrowly dispersed in size. For such conditions, it is possible to identify two well-defined limits both for the average aggregation number and for the cmc. One of the limits is provided by the theoretical critical concentration defined earlier by us[17,18] corresponding to an inflection point in the size distribution function. The curve with an inflection point separates the monotonically decreasing size distributions from those that exhibit a minimum and a maximum. On the basis of this definition, the critical point is given by

$$dX_g/dg = d^2X_g/dg^2 = 0 \tag{5}$$

Equation 5 is satisfied at a critical aggregation number g_{crit}. This critical aggregation number can be found by combining eqs 2 and 5 to obtain

$$\frac{d^2}{dg^2}\left[\frac{g\Delta\mu_g^\circ}{kT}\right] = 0 \text{ at } g = g_{crit} \tag{6}$$

Correspondingly, the critical concentration X_{crit} is given by

$$\ln X_{crit} = \frac{d}{dg}\left[\frac{g\Delta\mu_g^\circ}{kT}\right] \text{ at } g = g_{crit} \tag{7}$$

The critical aggregation number g_{crit} provides a lower bound for the average aggregation number. In general, the critical aggregation number is closer to the minimum in the aggregate size distribution which corresponds to the most unstable aggregates that play an important role in the kinetics of micellization.[63,64] Since the average aggregation number is closer to the maximum in the size distribution, the critical aggregation number is usually much smaller than the average aggregation number. The critical surfactant concentration X_{crit} constitutes a lower bound of the X_{cmc} defined above on the basis of the

(60) Ruckenstein, E.; Nagarajan, R. *J. Phys. Chem.* **1981**, *85*, 3010.
(61) Nagarajan, R.; Ruckenstein, E. *J. Colloid Interface Sci.* **1983**, *91*, 500.
(62) Hartley, G. S. *Aqueous Solutions of Paraffin Chain Salts*; Hermann: Paris, 1936.
(63) Aniansson, E. A. G.; Wall, S. N. *J. Phys. Chem.* **1974**, *78*, 1024.
(64) Zana, R.; Lang, J.; Yiv, S. H.; Djavanbakt, A.; Abad, C. see ref 5, p 291.

complete aggregate size distribution. The two critical concentrations are found to differ by only a factor of 1.31[61] when realistic free energy models such as those of Tanford[1] or of Israelachvili et al.[20] are considered. Using an arbitrary free energy model, Ben-Naim and Stillinger[65] found that the two critical concentrations X_{cmc} and X_{crit} deviate substantially from one another by a factor as large as 20. We have demonstrated,[60] however, that their free energy model is physically unreasonable and is thus responsible for the large difference between the two critical concentrations.

A second well-defined limit for the cmc and the average aggregation number is provided by the pseudophase description of the aggregates. Since the micelle is viewed as a distinct phase, the free energy per molecule of this phase must be a minimum at equilibrium. Therefore, the micellar aggregation number at equilibrium, g_{opt}, is obtained from the condition

$$\frac{d}{dg}\left[\frac{\Delta\mu_g^\circ}{kT}\right] = 0 \text{ at } g = g_{opt} \tag{8}$$

The above relation when combined with eqs 2 and 4 provides the following critical concentration:

$$\ln X_{opt} = \frac{\Delta\mu_g^\circ}{kT} = \frac{d}{dg}\left[\frac{g\Delta\mu_g^\circ}{kT}\right] \text{ at } g = g_{opt} \tag{9}$$

One may observe that the functional dependencies on the free energy of micellization for the two critical concentrations X_{crit} and X_{opt} in eqs 7 and 9 are the same. They differ however in magnitude since the free energies of micellization are evaluated at two different aggregation numbers, g_{crit} and g_{opt}, respectively. The aggregation number g_{opt} is an upper bound of the average aggregation number determined from the aggregate size distribution. Usually, it is up to 20% larger than that calculated via eq 3. The critical concentration X_{opt} provides an upper bound of the critical micelle concentration X_{cmc} calculated using the size distribution equation.

Sphere to Rod Transition. Micelles that are sufficiently small in size pack into spherical aggregates or into somewhat distorted globular aggregates. Usually, such micelles are narrowly dispersed in sizes. A different realm of micellization behavior is, however, observed when micelles grow larger in size and rodlike micelles are generated.[14,20,66-69] These aggregates can be visualized as having a cylindrical middle part with two spherical endcaps. The standard chemical potential of a rodlike aggregate of size g containing g_{cap} molecules in the two spherical endcaps and $g - g_{cap}$ molecules in the cylindrical middle can be written[20,66-69] as

$$\mu_g^\circ = (g - g_{cap})\mu_{cyl}^\circ + g_{cap}\,\mu_{cap}^\circ \tag{10}$$

where μ_{cyl}° and μ_{cap}° are the standard chemical potentials of the molecules in the two regions of the spherocylindrical aggregate, respectively. Introduction of the above relation in the aggregate size distribution eq 2 yields

$$X_g = \left[X_1 \exp\left(-\frac{\Delta\mu_{cyl}^\circ}{kT}\right)\right]^g \exp\left[-g_{cap}\left(\frac{\Delta\mu_{cap}^\circ - \Delta\mu_{cyl}^\circ}{kT}\right)\right] \tag{11}$$

As before, $\Delta\mu_{cyl}^\circ$ and $\Delta\mu_{cap}^\circ$ are the differences in the standard chemical potentials between the surfactant molecules in the cylindrical middle and the endcaps of the spherocylindrical micelle and the singly dispersed surfactant molecule. With Y and K denoting the following functions

$$Y = \left[X_1 \exp\left(-\frac{\Delta\mu_{cyl}^\circ}{kT}\right)\right]$$

$$K = \exp\left[g_{cap}\left(\frac{\Delta\mu_{cap}^\circ - \Delta\mu_{cyl}^\circ}{kT}\right)\right] \tag{12}$$

the size distribution equation becomes

$$X_g = (1/K)\,Y^g \tag{13}$$

One may note that K is a measure of the free energy advantage of molecules present in the cylindrical portion of the micelle when compared to molecules present in the spherical endcaps. The value of the parameter Y indicates the possibility of occurrence of rodlike aggregates at a given concentration of the singly dispersed surfactant molecules. The average aggregation numbers can be computed using eqs 3 and 13. Performing the analytical summation of the series functions, one obtains[20]

$$g_n = g_{cap} + \left(\frac{Y}{1-Y}\right)$$

$$g_w = g_{cap} + \frac{Y}{1-Y}\left[1 + \frac{1}{Y + g_{cap}(1-Y)}\right] \tag{14}$$

The total concentration of surfactant present in the aggregated state can also be analytically calculated and is given by the expression

$$\sum gX_g = \frac{1}{K}\left(\frac{g_{cap}Y^{g_{cap}}}{1-Y}\right)\left[1 + \frac{Y}{g_{cap}(1-Y)}\right] \tag{15}$$

Equations 14 and 15 show that, for values of Y very close to unity, very large aggregates are formed.[20] Equation 15 reduces in the limit of Y close to unity, to

$$\sum gX_g = \frac{1}{K}\left(\frac{1}{1-Y}\right)^2 = X - X_1 \tag{16}$$

Taking into account eq 16, eq 14 becomes for Y close to unity

$$g_n = g_{cap} + \left(\frac{1}{1-Y}\right) = g_{cap} + [K(X - X_1)]^{1/2}$$

$$g_w = g_{cap} + 2\left(\frac{Y}{1-Y}\right) = g_{cap} + 2[K(X - X_1)]^{1/2} \tag{17}$$

From eq 17, it is clear that the weight and the number average aggregation numbers substantially deviate from one another, indicating high polydispersity in the sizes of the equilibrium aggregates. Further, eq 16 shows that large, polydispersed aggregates form at finite surfactant concentrations X, when the factor K is large. Typically, K should be in the range of 10^8–10^{12} for polydispersed rodlike micelles to form at physically realistic surfactant concentrations.[14,20,69] Extremely large values of K imply that almost infinitely long rodlike micelles form even in infinitely dilute solutions. This may correspond to the formation of a separate phase. For systems in which rodlike micelles form, the critical micelle concentration can be calculated from the condition that Y should tend to unity.[20] Then, from eq 12 one obtains

$$X_1 = X_{cmc} = \exp(\Delta\mu_{cyl}^\circ/kT) \tag{18}$$

Determination of Equilibrium Solution Properties. The critical micelle concentration and the average aggregation number can be precisely estimated by computing the concentrations of all aggregates using the formal size

(65) Ben-Naim, A.; Stillinger, F. H. *J. Phys. Chem.* **1980**, *84*, 2872.
(66) Tausk, R. J. M.; Oudshoorn, C.; Overbeek, J. Th. G. *Biophys. Chem.* **1974**, *2*, 53.
(67) Tausk, R. J. M.; Overbeek, J. Th. G. *Biophys. Chem.* **1974**, *2*, 175.
(68) Mazer, N. A.; Benedek, G. B.; Carey, M. C. *J. Phys. Chem.* **1976**, *80*, 1075.
(69) Nagarajan, R. *J. Colloid Interface Sci.* **1982**, *90*, 477.

distribution equation as described earlier. Obviously, such computations are time consuming, though not complicated. Alternatively, one can calculate either of the two limiting solutions (corresponding to the inflection point in size distribution or the pseudophase model) mentioned before that are easier to obtain but are only approximate. A simpler approach yielding reasonably precise results is possible for systems displaying narrow size dispersions. In such systems, one can approximate the entire size distribution of aggregates by a single aggregate size that corresponds to a maximum in the aggregate concentration, $\sum X_g = X_g(\text{maximum})$. Aggregates that are different from this most probable size provide only small contributions to the total surfactant concentration. Consequently, the average aggregation number is determined to be that value of the aggregation number g at which the aggregate concentration X_g is a maximum. The cmc is then estimated using any one of the methods mentioned before. This approach is utilized in this paper for calculating the average aggregation number. The cmc is estimated as suggested by Hartley,[62] $X_1 = gX_g(\text{maximum}) = X_{\text{cmc}}$.

In contrast, when rodlike micelles form, the aggregate size distribution is very broad as can be seen from the size distribution eq 13. In this case, the entire size distribution should be taken into account. The average aggregation number is directly obtained from eq 17 while the cmc can be estimated using eq 18. For this purpose, one needs to know the magnitudes of g_{cap}, $\Delta\mu^{\circ}_{\text{cap}}$, and $\Delta\mu^{\circ}_{\text{cyl}}$. The standard chemical potential difference $\Delta\mu^{\circ}_{\text{cyl}}$ is that between a molecule present in an infinitely long cylinder and a singly dispersed surfactant and is calculated by its minimization with respect to the radius of the cylinder. $\Delta\mu^{\circ}_{\text{cap}}$ and g_{cap} are determined as those corresponding to a minimum in the standard chemical potential difference with respect to the radius of the endcap, considered here as different from that of the cylinder.

To proceed further and calculate the aggregation behavior of surfactants, models for the standard free energy differences associated with micelle formation are necessary. This, in turn, requires the specification of the shapes of the aggregates and of their geometrical characteristics.

Geometrical Characteristics of Aggregates. The hydrophobic interiors of the surfactant aggregates are constituted of the surfactant tails. Consequently, irrespective of the shape of the aggregates, no point within the aggregate can be farther than l_s from the aggregate core–water interface, where l_s is the extended length of the surfactant tail.[1,20] This implies that at least one dimension of the surfactant micelles should be smaller than or at most equal to $2l_s$. One can assume that the small micelles are spherical in shape. When large rodlike micelles form, it will be assumed that the middle portion is cylindrical while the endcaps are parts of spheres. The cylindrical and the endcap regions are allowed to have different diameters, the actual values being determined from minimum free energy considerations. When micelles cannot pack into spheres anymore, namely, for aggregation numbers for which a spherical aggregate will have a radius larger than l_s, and if at the same time the rodlike micelles are not yet favored, small globular aggregates that are not much larger than the largest spheres should form. The shapes of these aggregates have been examined by Israelachvili et al.[20] on the basis of local and overall molecular packing considerations. For a shape to be allowed, they showed that the local geometrical characteristics of the shape rather than its average geometrical characteristics should satisfy the molecular packing requirements. By using this criterion, they demonstrated that ellipsoidal shapes which satisfy the packing criterion on the average

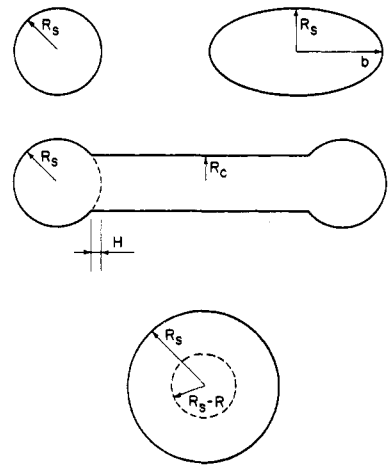

Figure 4. Geometrical variables defining the structures of surfactant aggregates considered in this work. As explained in the text, the prolate ellipsoid structure is used to obtain the average properties of the globular aggregate depicted in Figure 1. The spherocylinder is allowed to have differing radii for the cylindrical middle and the spherical endcaps. The bottom structure denotes a spherical microemulsion (shown in Figure 3) with a core of solubilizate surrounded by a shell consisting of both surfactant tails and solubilizate.

do not satisfy the packing criterion locally anywhere on the aggregate. For aggregates in the transition region between spheres and spherocylinders, they have suggested globular shapes generated via ellipses of revolution. We note that, for aggregation numbers that are up to 3 times as large as that of the largest spherical micelles, the average area per molecule for globular aggregates (ellipses of revolution) suggested by Israelachvili et al.[20] is practically the same as for prolate ellipsoids. Therefore, the average geometrical properties of the aggregates in the transition regime will be computed as for prolate ellipsoids. It should be emphasized, however, that this does not imply that prolate ellipsoidal micelles form, but only that the micelles are nonspherical and globular. The geometrical relations for each kind of aggregate shape are given below. The shapes of the aggregates considered in this paper are depicted in Figure 4.

Spherical Micelles. Small micelles are considered spherical with a radius of the hydrophobic core R_s smaller than or equal to l_s. For spherical micelles containing g surfactant molecules, the total volume of the aggregate, V_g, and the aggregate surface area, A_g, are given by

$$V_g = 4\pi R_s^3/3 = g v_s \tag{19}$$

$$A_g = 4\pi R_s^2 = ga \tag{20}$$

respectively. Here, v_s denotes the volume of the hydrophobic tail of the surfactant molecule and a the surface area of the aggregate per surfactant molecule. A different area per molecule a_δ defined at a distance δ from the hydrophobic core of the micelle (which plays a role in the calculation of the ionic interaction energy at the micellar surface) is given by

$$A_{g\delta} = 4\pi(R_s + \delta)^2 = ga_\delta \tag{21}$$

A geometrical ratio P that characterizes the average molecular packing in the aggregates is defined via the expression

$$P = V_g/A_g R_s = v_s/aR_s \tag{22}$$

This packing parameter will be shown later to affect the free energy of deformation of the surfactant tails within

the micellar core. Obviously, $P = 1/3$ for spherical aggregates. One may note that the analogous geometrical packing ratio defined by Israelachvili et al.[20] as v_s/al_s will always be less than or equal to $1/3$ for spherical micelles, since $R_s \leq l_s$.

Globular Micelles. The micelles whose sizes are somewhat larger than allowed by the spherical shape are called globular, and their average geometrical characteristics are computed as for prolate ellipsoids. Since one of the dimensions of any aggregate is determined by the extended length of the surfactant tail, the semiminor axis of the globular aggregate is taken to be $R_s = l_s$. The semimajor axis is denoted by b. The eccentricity E of the aggregate is given by

$$E = [1 - (R_s/b)^2]^{1/2} \tag{23}$$

The total volume of the hydrophobic core of the aggregate can be computed from

$$V_g = 4\pi R_s^2 b/3 = g v_s \tag{24}$$

and the total surface area of the hydrophobic core is given by

$$A_g = 2\pi R_s^2 \left[1 + \frac{\sin^{-1} E}{E(1-E^2)^{1/2}}\right] = ga \tag{25}$$

With E_δ denoting the eccentricity of the aggregate at a distance δ from the hydrophobic core

$$E_\delta = \left[1 - \left(\frac{R_s + \delta}{b + \delta}\right)^2\right]^{1/2} \tag{26}$$

the area of the aggregate at that surface can be calculated from

$$A_{g\delta} = 2\pi(R_s + \delta)^2 \left[1 + \frac{\sin^{-1} E_\delta}{E_\delta(1-E_\delta^2)^{1/2}}\right] = ga_\delta \tag{27}$$

Further, we define an equivalent radius R_{eq} of the globular aggregate by considering the volume of the aggregate to be the same as that of an equivalent spherical aggregate:

$$R_{eq} = (3V_g/4\pi)^{1/3} \tag{28}$$

The packing factor P for the globular aggregate defined as in eq 22 is given by

$$P = V_g/A_g R_s = v_s/aR_s \tag{29}$$

Obviously, P will always be greater than $1/3$. One may note that the radius R_s rather than R_{eq} is used in the definition of P. The packing factor P, as discussed later, is employed in the estimation of chain conformation free energies. Since the chains in globular micelles do not have to extend beyond the radius R_s in order to pack the aggregate core with liquid hydrocarbon density, this radius is relevant in the calculation of P.

Cylindrical Part of Spherocylinders. The cylindrical middle portion of a spherocylindrical micelle is similar to an infinitely long cylindrical rod. The radius of the hydrophobic cylindrical core is denoted by R_c. The volume and the total surface area of the cylindrical part per unit length of the cylinder can be calculated from

$$V_g = \pi R_c^2 = g v_s \qquad A_g = 2\pi R_c = ga \tag{30}$$

where g represents the number of surfactant molecules contained within a unit length of the cylinder. The packing factor P, defined as before, is

$$P = V_g/A_g R_c = v_s/aR_c \tag{31}$$

One may note that P will always be equal to $1/2$ in view of eq 30. One can also define an area per unit length of the cylinder at a distance δ from the hydrophobic core via the relation

$$A_{g\delta} = 2\pi(R_c + \delta) = ga_\delta \tag{32}$$

This area will be used later in the calculation of some contributions to the free energy of aggregation. Equations 30 and 32 can be used to obtain the following explicit expressions for the area per molecule in the cylindrical middle part:

$$a = \frac{2v_s}{R_c} \qquad a_\delta = a\frac{(R_c + \delta)}{R_c} \tag{33}$$

Endcaps of Spherocylinders. The two ends of the spherocylindrical aggregate are considered to be parts of spheres. In contrast to our earlier treatment of rodlike micelles where the endcaps and the cylindrical middle part of the micelle were assigned the same radius,[23,24,45] here the spherical endcaps are allowed to have a radius R_s that can be different from the radius R_c of the cylindrical middle. As already noted, the two radii can be determined from the condition of minimum free energy. Calculations discussed later show that they are found to be almost always different from one another. The total volume and the surface area of the two endcaps together can be calculated from

$$V_g = \left[\frac{8\pi R_s^3}{3} - \frac{2\pi}{3}H^2(3R_s - H)\right] = g v_s \tag{34}$$

$$A_g = [8\pi R_s^2 - 4\pi R_s H] = ga \tag{35}$$

where the quantity H is defined by

$$H = R_s[1 - \{1 - (R_c/R_s)^2\}^{1/2}] \tag{36}$$

The packing factor P for the endcaps is given by

$$P = V_g/A_g R_s = v_s/aR_s \tag{37}$$

It can be seen that P is always greater than $1/3$. The area of the two endcaps at a distance δ from the hydrophobic core surface can be computed from

$$A_g\delta = [8\pi(R_s + \delta)^2 - 4\pi(R_s + \delta)(H + \delta)] = ga_\delta \tag{38}$$

This area will be employed later in the calculation of some contributions to the free energy of aggregation.

III. Model for the Free Energy of Micellization

Having specified the geometries of the various aggregate shapes, we formulate now explicit expressions for the standard free energy difference between a surfactant molecule present in an aggregate and one present in the singly dispersed state in water. This free energy difference is composed of a number of contributions, each of which is examined below.

Transfer Free Energy of the Surfactant Tail. When aggregation occurs, the hydrophobic tail of the surfactant is transferred from its contact with water to the hydrophobic core of the aggregate. The contribution to the free energy from this transfer process is estimated by considering the aggregate core to be like a liquid hydrocarbon. The fact that the aggregate core differs somewhat from a liquid hydrocarbon gives rise to an additional free energy contribution that is evaluated immediately below.

The transfer free energy of the surfactant tail from water to a liquid hydrocarbon state can be estimated from independent experimental data regarding the solubility of hydrocarbons in water. Using the solubility data for hydrocarbon gases ranging from methane to octane as a function of temperature, the standard free energy differ-

ence between the hydrocarbon gas at 1 atm pressure (ideal gas conditions) and the hydrocarbon in its saturated state in water can be calculated.[70,71] From these, one can estimate the group contributions of methylene and methyl groups as functions of temperature. On this basis, the standard free energy change for transfer from the aqueous phase to the ideal gas phase for the methylene and the methyl groups, respectively, are given by

$$(\Delta\mu^\circ/kT)(\text{aq}\rightarrow\text{gas}) = 3.61 \ln T + 1326/T - 25.3 \quad (39)$$

and

$$(\Delta\mu^\circ/kT)(\text{aq}\rightarrow\text{gas}) = 19.84 \ln T + 7361/T - 142.8 \quad (40)$$

In the above two relations, the temperature T is expressed in Kelvin. The functional forms for the temperature dependence in the above expressions describe not only the gas solubility (or equivalently, the free energy) data well, but also yield accurate values for other thermodynamic quantities such as the specific heat and changes in enthalpy as well as entropy for hexane, heptane, and octane.

The difference in the standard free energies for hydrocarbons in their ideal gas state at 1 atm pressure and their pure liquid state can be computed from vapor pressure data:

$$(\Delta\mu^\circ/kT)(\text{gas}\rightarrow\text{liq}) = \ln P \quad (41)$$

where P is the vapor pressure expressed in atmospheres. Using the vapor pressure–temperature data available for hydrocarbons,[72] the methylene and methyl group contributions to this free energy difference can be estimated. For methylene groups one obtains

$$(\Delta\mu^\circ/kT)(\text{gas}\rightarrow\text{liq}) = 2.24 \ln T - 430/T - 10.85 - 0.0056T \quad (42)$$

and for the methyl groups

$$(\Delta\mu^\circ/kT)(\text{gas}\rightarrow\text{liq}) = -16.46 \ln T - 3297/T + 98.67 + 0.02595T \quad (43)$$

where T is expressed in Kelvin. One may note that the functional forms of eqs 42 and 43 are those used to describe the temperature dependence of the vapor pressure of hydrocarbons.

The free energy change of transfer from an aqueous phase to a liquid hydrocarbon phase can now be calculated by summing the free energies for the two transfer processes described above. Consequently, the transfer free energy for a methylene group in an aliphatic tail as a function of temperature can be written as

$$(\Delta\mu_g^\circ)_{tr}/kT = 5.85 \ln T + 896/T - 36.15 - 0.0056T \quad (44)$$

For a methyl group in the aliphatic chain, the temperature-dependent transfer free energy is

$$(\Delta\mu_g^\circ)_{tr}/kT = 3.38 \ln T + 4064/T - 44.13 + 0.02595T \quad (45)$$

Deformation Free Energy of the Surfactant Tail. The surfactant tails inside the hydrophobic core of the aggregate are not in a state identical to that in liquid hydrocarbons. This is because one end of the surfactant tail in the aggregate is constrained to remain at the aggregate–water inferface, while the entire tail has to assume a conformation consistent with the maintenance of a uniform density equal to that of liquid hydrocarbon in the aggregate core. Consequently, the formation of aggregates is associated with a positive free energy contribution stemming from the conformational constraints on the surfactant tails which is referred to here as the tail deformation free energy. In our earlier work, this free energy was taken to be a function of the length of the surfactant tail, but was considered independent of the aggregate shape. The free energy expression used

$$(\Delta\mu_g^\circ)_{def}/kT = -0.50 + 0.24n_c \quad (46)$$

was empirical and was chosen to provide satisfactory agreement with experimental data regarding the critical micelle concentration of surfactants.

A more detailed examination of these chain conformational constraints has been made by Gruen,[25-28] Dill and Flory,[29-33] and Ben-Shaul et al.[34-36]. For example, Gruen evaluated the conformational free energy of surfactant tails inside the aggregates using the single chain mean field model and the rotational isomeric state approximation. On this basis, he determined the extent of trans and gauche conformations assumed by the surfactant tail within the aggregate in contrast to a hydrocarbon chain in a bulk liquid hydrocarbon and thereby estimated the corresponding free energy contribution associated with the internal chain ordering in micelles. In his treatment, the micelles were considered to have rough surfaces so that a part of some of the hydrocarbon tails can lie outside the hydrophobic core of the micelle. Further, he also allowed holes to exist inside the micelle so that spherical aggregates having radii larger than the extended length of the surfactant chain could exist. The numerical results for the conformational free energy obtained for a C_{11} surfactant were fitted to a polynomial expression for spherical, cylindrical, and lamellar aggregate shapes. The free energy was expressed as a function of the average dimension of the hydrocarbon region of the aggregate, thereby including the small fraction of the chain lying outside the hydrophobic core. Ben-Shaul and co-workers have followed a similar approach adopting, however, a different computational procedure. They concluded that the geometrical packing constraints rather than internal energy (trans–gauche) effects are the dominant factors determining chain conformation. Dill and Flory treated the micelle packing problem using lattice representations for the interior of the aggregate and by considering the placement of the surfactant chains on this lattice. Recently Puvvada and Blankschtein[41] have integrated the approaches of Gruen and Ben-Shaul et al. into their treatment of micellization and phase behavior of surfactant solutions. All these studies indicate that the free energy due to the chain conformational constraint should depend upon the size and shape of the aggregate. While the three studies mentioned above have provided numerical estimates for this free energy for illustrative aggregates having spherical, cylindrical, and lamellar shapes, the free energy estimates have not been expressed as explicit analytical functions of the aggregation number, aggregate shape, and surfactant chain length. An approach that can yield a reasonable analytical expression for this free energy contribution is certainly needed. Here, a lattice picture for the aggregate core is used to develop an expression for the free energy due to the constrained conformation of the surfactant tail. This approach is similar to that suggested by Semenov[55] in the context of block copolymer microdomains and has been used in our earlier work on block copolymer micelles.[56] Following this approach, simple analytical expressions for the chain deformation free energy are obtained as explicit

(70) Abraham, M. H. *J. Chem. Soc., Faraday Trans. 1* **1984**, *80*, 153.
(71) Abraham, M. H.; Matteoli, E. *J. Chem. Soc., Faraday Trans. 1* **1988**, *84*, 1985.
(72) Daubert, T. E.; Danner, R. P. *Physical and Thermodynamic Properties of Pure Chemicals*; Design Institute for Physical Property Data, American Institute of Chemical Engineers; Hemisphere Publishing Corp.: New York, 1988.

functions of the aggregation number for the different aggregate geometries. It may be mentioned that the free energy estimates based on these analytical expressions are found to be larger than those obtained by Gruen for the system illustrated in his paper[28] but are in satisfactory agreement with the results of Puvvada and Blankschtein summarized in Table I of their paper.[41]

A lattice representation is used to model the conformation of the surfactant tails in the interior of the aggregate. The use of a lattice requires the specification of the size of the molecular segment which can be placed on the lattice without any orientational constraints. As suggested by Dill and Flory,[30] a suitable segment is that which contains about 3.6 methylene groups. Correspondingly, the linear dimension of a lattice site, denoted by L, is taken equal to about 4.6 Å. This linear dimension also represents the typical spacing between alkane molecules in the liquid state, and hence, L^2 equals the cross-sectional area of a polymethylene chain. One may also note that L^3 equals the volume of 3.6 methylene groups. Since the volume of the methyl group is twice that of a methylene group, a surfactant tail that contains $n_c - 1$ methylene groups and a terminal methyl group is considered as made up of N segments, where $N = (n_c + 1)/3.6$. One end of the surfactant tail, namely, that attached to the polar head group, is constrained to be located at the aggregate–water interface. The other end (the terminal methyl group) is free to occupy any position in the entire volume of the aggregate as long as a uniform segment density can be maintained within the aggregate core. Obviously, the chains will be locally deformed in order to satisfy both the packing and the uniform density constraints. The conformational free energy per surfactant tail can be determined by calculating the integral of this local deformation energy over the entire volume of the aggregate. This free energy due to the conformational constraint is estimated as a function of the aggregation number of the micelle as follows.

Consider a surfactant chain consisting of N segments placed on a lattice whose sites have a size L. The fixed end of the chain is at a distance 0 from the aggregate–water interface, while the free end (the methyl terminal) is located at a distance r_o from this interface. Let $r(n)$ denote the location of the nth segment from the aggregate–water interface. Therefore, $r(N) = r_o$. The local extension of this chain at r is defined as $E(r,r_o) = dr/dn$, where dr is the actual extension of the perturbed chain consisting of dn segments. Since the unperturbed end to end distance of a chain containing dn segments[73] is $(dn)^{1/2}L$, the local deformation free energy dF for isotropic deformation in all three directions can be written as[73]

$$\frac{dF}{kT} = \frac{3}{2}\frac{(dr)^2}{(dn)L^2} = \frac{3}{2}\frac{1}{L^2}E(r,r_o)\,dr \qquad (47)$$

where the factor 3/2 arises because of the three-dimensional deformation. To calculate the deformation free energy of the aggregate core as a whole, the local free energies of deformation of all the chains should be summed over the entire aggregate core volume taking into account how all the chains are distributed over this volume. For this purpose, the density distribution function $G(r_o)$ of the chain free ends is introduced. $G(r_o)\,dr_o$ represents the number of chains whose free ends (terminal methyl groups) lie between r_o and $r_o + dr_o$. Therefore, the free energy of the aggregate core associated with the nonuniform chain deformation can be written as

$$\frac{F}{kT} = \frac{3}{2}\frac{1}{L^2}\int_0^R dr_o \int_0^{r_o} dr\, E(r,r_o)\, G(r_o) \qquad (48)$$

The yet unknown functions $E(r,r_o)$ and $G(r_o)$ should satisfy the following relations:

$$\int_0^{r_o} dr/E(r,r_o) = N \qquad (49)$$

and

$$\int_r^R dr_o\, L^3[G(r_o)/E(r,r_o)] = 4\pi(R-r)^2, 2\pi(R-r), 2 \qquad (50)$$

Equation 49 specifies that there are N segments in the surfactant chain, while eq 50 states that the segment density in the core of the aggregate is uniform. The three quantities on the right-hand side of eq 50 correspond to spherical, infinite cylindrical, and infinite lamellar aggregates, respectively. The minimization of the deformation free energy eq 48 subject to the constraints eqs 49 and 50 allows the determination of the functional forms of $E(r,r_o)$ and $G(r_o)$, and thus the minimum value of F for any arbitrary aggregation number. Semenov[55] thus obtained

$$E(r,r_o) = \pi(r_o^2 - r^2)^{1/2}/2N \qquad (51)$$

He also provided expressions for the distribution function $G(r_o)$ as well as for the free energy of the aggregate core F.

For spherical aggregates

$$G(r) = (8\pi R^2/NL^3)u[\tanh^{-1}(1-u^2)^{1/2} - (1-u^2)^{1/2}] \qquad (52)$$

where u denotes r/R. Introducing eqs 51 and 52 in eq 48, one obtains

$$\frac{F}{kT} = \left(\frac{3\pi^2}{80}\right)\left(\frac{4\pi R^3}{3NL^3}\right)\left(\frac{R^2}{NL^2}\right) = \left(\frac{3\pi^2}{80}\right)g\left(\frac{R^2}{NL^2}\right) \qquad (53)$$

Here, g is the number of surfactant molecules contained within the spherical micelle. For infinite cylinders

$$G(r) = (2\pi R/NL^3)\, u \tanh^{-1}(1-u^2)^{1/2} \qquad (54)$$

and

$$\frac{F}{kT} = \left(\frac{5\pi^2}{80}\right)\left(\frac{\pi R^2}{NL^3}\right)\left(\frac{R^2}{NL^2}\right) = \left(\frac{5\pi^2}{80}\right)g\left(\frac{R^2}{NL^2}\right) \qquad (55)$$

Here, g is the number of surfactant molecules contained within a unit length of the cylinder. For infinite lamellae

$$G(r) = \frac{2}{NL^3}\frac{u}{(1-u^2)^{1/2}} \qquad (56)$$

and

$$\frac{F}{kT} = \left(\frac{10\pi^2}{80}\right)\left(\frac{2R}{NL^3}\right)\left(\frac{R^2}{NL^2}\right) = \left(\frac{10\pi^2}{80}\right)g\left(\frac{R^2}{NL^2}\right) \qquad (57)$$

Here, g is the number of surfactant molecules contained within a unit area of the lamellae.

One can estimate the chain deformation free energy of the micelle core per surfactant molecule for spheres, cylinders, and lamellae, respectively, from

$$\frac{1}{g}\frac{F}{kT} = \left(\frac{3\pi^2}{80}\right)\left(\frac{R^2}{NL^2}\right), \left(\frac{5\pi^2}{80}\right)\left(\frac{R^2}{NL^2}\right), \left(\frac{10\pi^2}{80}\right)\left(\frac{R^2}{NL^2}\right) \qquad (58)$$

The different numerical coefficients 3, 5, and 10 for the three geometries result from the differences in molecular packing in the respective geometries. By introducing the geometrical packing factor P explicitly in the above equation, the free energy expressions for the three geometries become practically unified since the numerical

(73) Flory, P. J. *Principles of Polymer Chemistry*; Cornell University Press: Ithaca, NY, 1962.

values 3, 5, and 10 become $9P$ for spheres, and $10P$ for cylinders as well as lamellae. Consequently, we estimate the contribution of the chain deformation in the aggregate core to the free energy of micellization for spherical micelles from

$$\frac{(\Delta\mu_g^\circ)_{def}}{kT} = \frac{9P\pi^2}{80}\frac{R_s^2}{NL^2} \quad (59)$$

the same relation being also employed for globular micelles and for the spherical endcaps of the spherocylinders. The relation valid for infinite cylindrical rods

$$\frac{(\Delta\mu_g^\circ)_{def}}{kT} = \frac{10P\pi^2}{80}\frac{R_c^2}{NL^2} \quad (60)$$

is employed for the middle cylindrical part of the spherocylinder. It will be shown later that the use of the size-dependent expressions eqs 59 and 60 for the chain deformation free energy affects both the aggregation number and the cmc. In contrast, our earlier empirical expression had an influence only on the cmc.

Aggregate Core–Water Interfacial Free Energy. The formation of surfactant aggregates generates an interface between the hydrophobic core region consisting of the surfactant tails and the surrounding water medium. The free energy associated with the formation of this interface has been taken in our previous calculations[23,24,45,48] as the product of the area of the interface and the macroscopic interfacial tension of the aggregate core–water interface.

$$(\Delta\mu_g^\circ)_{int}/kT = (\sigma_{agg}/kT)(a - a_o) \quad (61)$$

Here, σ_{agg} is the macroscopic aggregate core–water interfacial tension, a is the surface area of the hydrophobic core per surfactant molecule defined earlier, and a_o is the area per molecule of the core surface shielded from contact with water by the polar head group of the surfactant.

The aggregate core–water interfacial tension σ_{agg} is taken equal to the interfacial tension σ_{sw} between the aliphatic hydrocarbon of the same molecular weight as the surfactant tail (s) and the surrounding water (w). The interfacial tension σ_{sw} can be calculated in terms of the surface tensions σ_s of the aliphatic surfactant tail and σ_w of water via the relation[74]

$$\sigma_{sw} = \sigma_s + \sigma_w - 2.0\psi(\sigma_s\sigma_w)^{1/2} \quad (62)$$

where ψ is a constant with a value of about 0.55.[74,75] For aliphatic hydrocarbon molecules, the surface tension σ_s has a weak dependence on the chain length of the molecule. However, its temperature derivative has been found[76] to be virtually independent of the hydrocarbon chain length as well as temperature (implying a linear dependence on temperature):

$$\partial\sigma_s/\partial T = -0.098 \text{ dyn/(cm K)} \quad (63)$$

Using the above temperature dependence of the surface tension and the experimental surface tension data for aliphatic hydrocarbons at 20 °C summarized in ref 74, the surface tension σ_s can be correlated against the molecular weight of the aliphatic hydrocarbons to within 2% accuracy by the relation

$$\sigma_s = 35.0 - 325M^{-2/3} - 0.098(T - 298) \quad (64)$$

where M is the molecular weight of the surfactant tail, T is in Kelvin, and σ_s is expressed in dynes per centimeter. Such a molecular weight dependence has been already suggested in the literature for homologous series of hydrocarbons as well as polymeric systems.[77,78] The experimentally measured surface tension of water as a function of temperature[79] can be correlated by the expression

$$\sigma_w = 72.0 - 0.16(T - 298) \quad (65)$$

where the surface tension is given in dynes per centimeter and the temperature in Kelvin.

The area a_o that appears in eq 61 depends on the extent to which the polar head group shields the cross-sectional area of the surfactant tail. It has already been noted while defining a lattice for the aggregate core that the lattice size L is based on the typical spacing between alkane molecules in the liquid state. Such a definition of the lattice spacing L implies that L^2 corresponds to the cross-sectional area of the surfactant tail as mentioned earlier. This area is shielded completely from the contact with water if the polar head group has a cross-sectional area a_p larger than L^2. For such a surfactant, a_o is taken equal to L^2. If the polar head group area a_p is less than L^2, then the head group shields only a part of the cross-sectional area of the tail from the contact with water. In this case, a_o is taken equal to a_p.

Head Group Steric Interactions. The formation of the surfactant aggregate brings the polar head groups of the surfactant molecules to the surface of the aggregate where they are crowded when compared to their isolated states as singly dispersed surfactant molecules. The area occupied by the head groups at the aggregate surface is excluded for the translational motion of the surfactant molecules constituting the aggregate. This generates steric repulsions among the head groups. If the head groups are compact in nature with a definable hard core area or hard core volume, then the steric interactions can be estimated as hard particle interactions by using any of the models available in the literature. The simplest is the van der Waals approach, on the basis of which the steric repulsion is given by[23,24,45]

$$\frac{(\Delta\mu_g^\circ)_{steric}}{kT} = -\ln\left(1 - \frac{a_p}{a}\right) \quad (66)$$

Here, a_p is the effective cross-sectional area of the polar head group near the micellar surface as mentioned earlier. This approach is no longer adequate when the polar head groups cannot be considered as compact such as in the case of nonionic surfactants having poly(oxyethylene) chains as head groups. An alternate treatment for head group interactions in such systems is developed in a later section.

Head Group Dipole Interactions. If the polar head groups are zwitterionic, then they are associated with a permanent dipole of appreciable magnitude. The dipoles of the surfactants at the micellar surface are in the proximity of one another, and the mutual interactions between them are expected to provide an important contribution to the free energy of micellization. In general, the dipole–dipole interactions are dependent on the orientation of the dipoles. Because of the chain packing, one expects to find the dipoles oriented normal to the interface and be stacked such that the poles of the dipoles

(74) Girifalco, L. A.; Good, R. J. *J. Phys. Chem.* **1957**, *61*, 904.
(75) Good, R. J.; Elbing, E. *Ind. Eng. Chem.* **1970**, *62*, 54.
(76) Reid, R. C.; Prausnitz, J. M.; Sherwood, T. K. *The Properties of Gases and Liquids*; McGraw-Hill Book Co.: New York, 1977.
(77) LeGrand, D. G.; Gaines, G. L. *J. Colloid Interface Sci.* **1969**, *31*, 162.
(78) LeGrand, D. G.; Gaines, G. L. *J. Colloid Interface Sci.* **1969**, *31*, 430.
(79) *CRC Handbook of Chemistry and Physics*, 60th ed.; CRC Press Inc.: Boca Raton, FL, 1980.

are located on parallel surfaces. The dipole–dipole interactions in such a case are repulsive, and they can be estimated by visualizing the arrangement of the poles of the dipoles as constituting an electrical capacitor. The distance between the planes of the capacitor is equated to the distance of charge separation on the zwitterionic head group. Consequently, the dipole–dipole interactions for dipoles having a charge separation d can be computed for spherical aggregates from[24]

$$\frac{(\Delta\mu_g^\circ)_{\text{dipole}}}{kT} = \frac{2\pi e^2 R_s}{\epsilon a}\left[\frac{d}{d+R_s}\right] \tag{67}$$

In the above relation, e denotes the electronic charge, ϵ is the dielectric constant of the solvent, and R_s is the radius of the spherical micelle. The same equation is employed for globular aggregates and the endcaps of spherocylinders. For the cylindrical part of the spherocylinders

$$\frac{(\Delta\mu_g^\circ)_{\text{dipole}}}{kT} = \frac{2\pi e^2 R_c}{\epsilon a}\ln\left[1+\frac{d}{R_c}\right] \tag{68}$$

where R_c is the radius of the cylindrical part of the micelle. The dielectric constant ϵ is taken to be that of pure water. The dielectric constant as a function of temperature given in ref 79 can be correlated by the relation

$$\epsilon = 87.74\exp[-0.0046(T-273)] \tag{69}$$

where T is expressed in Kelvin.

Head Group Ionic Interactions. Ionic interactions arise at the micellar surface if the surfactant has a charged head group. The theoretical computation of these interactions is complicated by a number of factors such as the size, shape, and orientation of the charged groups, the dielectric constant in the region where the head groups are located, the occurrence of Stern layers, discrete charge effects, etc. Nevertheless, it was found that the use of the simple Debye–Huckel solution obtained by linearizing the Poisson–Boltzmann equation gave consistently a magnitude of the ionic interaction energies approximately twice as large as those necessary to obtain agreement with experiment.[1,44-46] Therefore, in our earlier work, the Debye–Huckel expression was used along with an arbitrary but universal correction factor of 0.46.[44-46] An approximate analytical solution to the Poisson–Boltzmann equation has been derived by Evans and Ninham[57] for spherical and cylindrical micelles assuming that the surfactant molecules are completely dissociated. They obtained an approximate solution for nonplanar geometries by adding to the exact solution for the planar geometry another term that provides a correction for the curvature of the aggregate. Since the derivation is given in detail in the literature,[57-59] only the result is given here

$$(\Delta\mu_g^\circ)_{\text{ionic}}/kT = 2[\ln(s/2+\{1+(s/2)^2\}^{1/2}) - (2/s)(\{1+(s/2)^2\}^{1/2}-1) - (2C/\kappa s)\ln(1/2+(1/2)\{1+(s/2)^2\}^{1/2})] \tag{70}$$

where

$$s = 4\pi e^2/\epsilon\kappa a_\delta kT \tag{71}$$

The area per molecule a_δ which appears in the above equation is evaluated at a distance δ from the hydrophobic core surface. This distance δ is estimated as the distance from the hydrophobic core surface to the surface where the center of the counterion is located. κ is the reciprocal Debye length. The last term in the right-hand side of eq 70 is the curvature correction term while the remaining terms constitute the exact solution of the Poisson–Boltzmann equation for a planar geometry. C is a factor dependent on the curvature and is given by

$$C = \frac{2}{R_s+\delta},\ \frac{2}{R_{eq}+\delta},\ \frac{1}{R_c+\delta} \tag{72}$$

for spheres/spherical endcaps of spherocylinders, globular aggregates, and the cylindrical middle part of spherocylinders, respectively. The reciprocal Debye length κ is related to the ionic strength of the solution via

$$\kappa = \left(\frac{8\pi n_o e^2}{\epsilon kT}\right)^{1/2} \qquad n_o = \frac{(C_1+C_{\text{add}})}{10^3}N_{\text{Av}} \tag{73}$$

In the above equation, n_o is the number of counterions in solution per cubic centimeter, C_1 is the molar concentration of the singly dispersed surfactant molecules, C_{add} is the molar concentration of the salt added to the surfactant solution, and N_{Av} is the Avogadro's number. The temperature dependence of the reciprocal Debye length κ arises from both the variables T and ϵ present in eq 73.

IV. Predictions of the Micellization Model

Computational Approach. The equation for the size distribution of aggregates, in conjunction with the geometrical characteristics of the aggregates and the expressions for the different contributions to the free energy of micellization, allows one to calculate the size distribution of aggregates, the cmc, and various average properties of the surfactant system. In the equation for the aggregate size distribution

$$X_g = X_1^g \exp(-g\Delta\mu_g^\circ/kT) \tag{74}$$

the factor $\Delta\mu_g^\circ$ denotes the difference in the standard chemical potentials between a surfactant molecule present in an aggregate and one in the singly dispersed state. This factor is the sum of various contributions discussed in the previous section, namely

$$\Delta\mu_g^\circ = (\Delta\mu_g^\circ)_{\text{tr}} + (\Delta\mu_g^\circ)_{\text{def}} + (\Delta\mu_g^\circ)_{\text{int}} + (\Delta\mu_g^\circ)_{\text{steric}} + (\Delta\mu_g^\circ)_{\text{dipole}} + (\Delta\mu_g^\circ)_{\text{ionic}} \tag{75}$$

where $(\Delta\mu_g^\circ)_{\text{dipole}}$ is to be included in the case of zwitterionic surfactants and $(\Delta\mu_g^\circ)_{\text{ionic}}$ is to be included in the case of ionic surfactants.

For spherical or globular micelles, the size dispersion is usually narrow. Consequently, one can consider the average aggregation number to be equal to that value of g for which X_g has a maximum.[80] This condition yields results very close to those obtained by accounting for the entire size distribution of aggregates. The maximum in the value of the aggregate concentration X_g and the aggregation number g at which this maximum occurs are both determined as a function of the concentration of the singly dispersed surfactant X_1. The predicted critical micelle concentration reported in this paper is that value of X_1 for which the total amount of the surfactant in the micellized form is equal to that in the singly dispersed form, namely, $X_{\text{cmc}} = X_1 = \sum gX_g$.[62] The prediced average aggregation numbers reported in this paper also correspond to this condition, namely, that the concentration of the surfactant present as aggregates is equal to the concentration of the singly dispersed surfactant.

In the case of spherocylindrical micelles, the standard chemical potential difference between a surfactant molecule in the cylindrical part of the micelle and one in its singly dispersed state is denoted by $\Delta\mu_{\text{cyl}}^\circ$. Similarly, the difference in the standard chemical potentials between a surfactant molecule in the spherical endcaps of the mi-

(80) Rao, I. V.; Ruckenstein, E. *J. Colloid Interface Sci.* **1987**, *119*, 211.

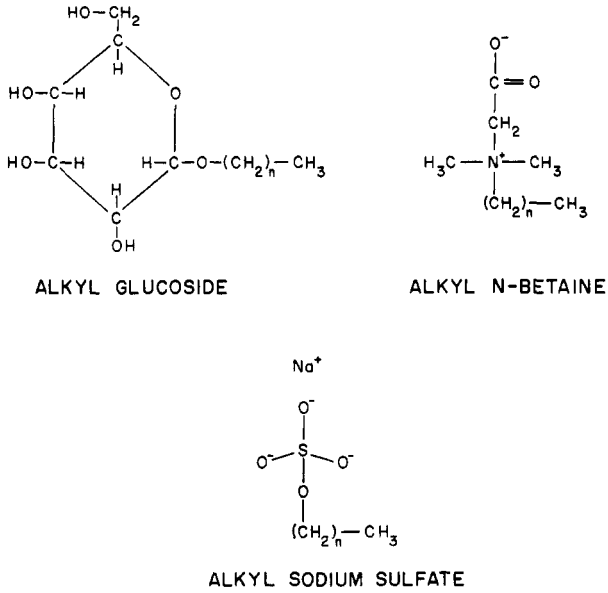

Figure 5. Representation of the polar head groups of nonionic glucoside, zwitterionic *N*-betaine, and ionic sodium sulfate considered in this study.

celle and a singly dispersed surfactant molecule is denoted by $\Delta\mu^{\circ}_{cap}$. Both $\Delta\mu^{\circ}_{cyl}$ and $\Delta\mu^{\circ}_{cap}$ are composed of all the free energy contributions given by eq 75 for $\Delta\mu^{\circ}_{g}$. By minimizing the standard chemical potential difference $\Delta\mu^{\circ}_{cyl}$ for infinitely long cylinders, the equilibrium radius R_c of the cylindrical part of the micelle is determined. Given the radius of the cylindrical part, the number of molecules in the spherical endcaps g_{cap} is found to be that value which minimizes the standard chemical potential difference $\Delta\mu^{\circ}_{cap}$ for the molecules located at the endcaps. Given g_{cap} and the standard free energy differences $\Delta\mu^{\circ}_{cyl}$ and $\Delta\mu^{\circ}_{cap}$, the sphere to rod transition parameter K is calculated from eq 12, the average aggregation number at any total surfactant concentration from eq 17, and the critical micelle concentration from eq 18.

Obviously, when the sphere to rod transition parameter K is smaller than unity, spherical or globular micelles are preferred. For K larger than unity, spherocylinders are preferred. If K is larger than unity but small, then the spherocylinders are small in size and narrowly dispersed. For larger values of K, the spherocylinders are large as well as polydispersed.

The search for the parameter values that maximize the aggregate concentration X_g or minimize the standard chemical potential differences $\Delta\mu^{\circ}_{cyl}$ and $\Delta\mu^{\circ}_{cap}$ was carried out using a standard IMSL (International Mathematical and Statistical Library) subroutine ZXMWD. This subroutine is designed to carry out the search for the global extremum of a function of q independent variables subject to any specified constraints on the variables. Therefore, this subroutine was used not only for the calculations described above involving one independent variable (the aggregation number g for spherical or globular micelles, the core radius R_c for infinite cylinders, or the aggregation number g_{cap} for the endcaps of spherocylinders) but also for calculations involving 2–5 independent variables that are discussed later in this paper.

Properties of Surfactants. Illustrative predictions are presented here for nonionic alkyl β-glucosides, zwitterionic *N*-alkylbetaines, and ionic sodium alkyl sulfates. The polar groups of the surfactant families considered are depicted in Figure 5, and the various molecular constants used in the predictive calculations are summarized in Table I. The glucoside head group in β-glucosides has a compact

Table I. Molecular Constants for Surfactants

surfactant head group	a_p, Å^2	a_o, Å^2	δ, Å	d, Å
glucoside	40	21		
N-betaine	30	21		5
sodium sulfate	17	17	5.45	
sodium sulfonate	17	17	3.85	

ring structure[10] with an approximate diameter of 7 Å, and hence, the effective cross-sectional area of the polar head group a_p is estimated to be approximately 40 Å^2. Correspondingly, the area shielded by the polar head group is taken to be $a_o = L^2 = 21$ Å^2, at 25 °C. For the zwitterionic *N*-betaine head group, the distance d between the separated charges can be estimated from the bond lengths and bond angles for the bonds separating the charges. The computations in this paper are based on an estimate of $d = 5$ Å. The cross-sectional area of the polar head group a_p has been estimated to be 30 Å^2, and correspondingly, the cross-sectional area of the tail shielded by the head group is taken to be $a_o = L^2 = 21$ Å^2, at 25 °C. For sodium alkyl sulfates, the cross-sectional area of the polar group a_p has been estimated to be 17 Å^2 which is smaller than L^2. Consequently, the cross-sectional area of the surfactant tail shielded by the head group a_o is taken equal to the area a_p. The distance δ at which the ionic interactions are computed depends on the size of the ionic head group (approximately 3.6 Å) and the size of the hydrated counterion (approximately 1.85 Å). Therefore, we estimate $\delta = 5.45$ Å. For sodium alkyl sulfonates, the cross-sectional area of the polar group a_p is as for alkyl sulfates. Consequently, the cross-sectional area of the surfactant tail shielded by the head group a_o is taken equal to the area $a_p = 17$ Å^2. The distance δ at which the ionic interactions are computed is smaller than that for alkyl sulfates (by the size of an oxygen atom) and is estimated to be $\delta = 3.85$ Å.

The molecular volume of the surfactant tail containing n_c carbon atoms is calculated from the group contributions of $n_c - 1$ methylene groups and the terminal methyl group:

$$v_s = v(CH_3) + (n_c - 1)v(CH_2) \qquad (76)$$

These group molecular volumes are estimated from the density vs temperature data available[72] for aliphatic hydrocarbons. At 25 °C, the molecular volume of a methylene group is estimated to be 26.9 Å^3 while that of the methyl group is estimated to be 54.6 Å^3. Over the temperature range of 273–373 K, the molecular volume changes approximately linearly with temperature. The increase in volume with an increase in temperature is estimated to be 0.0146 Å^3/K for the methylene group and 0.124 Å^3/K for the methyl group. Therefore, the group molecular volumes are calculated from

$$v(CH_3) = 54.6 + 0.124(T - 298)\ \text{Å}^3$$
$$v(CH_2) = 26.9 + 0.0146(T - 298)\ \text{Å}^3 \qquad (77)$$

where T is in Kelvin. The extended length of the surfactant tail l_s at 298 K has been calculated by Tanford[1] using a group contribution of 1.265 Å for the methylene group and 2.765 Å for the methyl group:

$$l_s = 1.50 + 1.265n_c\ \text{Å} \qquad (78)$$

In the absence of any other information and given the small volumetric expansion of the surfactant tail over the range of temperatures of interest, the extended tail length l_s will be treated as temperature independent. Obviously, the small volumetric expansion of the surfactant tail will be accounted for by small increases in the cross-sectional area of the surfactant tail.

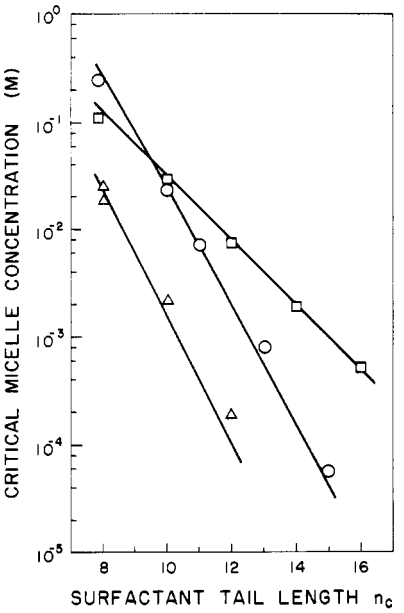

Figure 6. Dependence of the critical micelle concentration on the number of carbon atoms in the surfactant tail for alkyl glucosides (triangles), *N*-alkylbetaines (circles), and sodium alkyl sulfates (squares). The lines represent the predictions of the present theory while the points are experimental data.

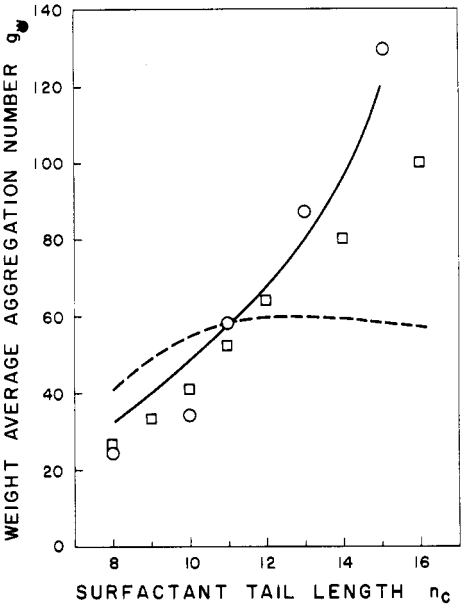

Figure 7. Dependence of the weight average aggregation number of micelles at the cmc, on the chain length of the surfactant tail for sodium alkyl sulfates (squares) and *N*-alkylbetaines (circles). The points are experimental data. The dotted line shows predicted values for sodium alkyl sulfates while the continuous line describes the predictions for *N*-alkylbetaines. See text for comments about the reported experimental aggregation numbers for sodium alkyl sulfates with C_{14} and C_{16} surfactant tails.

Influence of Free Energy Contributions on the Aggregation Behavior. Before the predicted aggregation behavior for different surfactants is discussed, certain general features of the present theory can be extracted from the functional forms of the various contributions to the free energy of micellization (all expressed per molecule of surfactant). Of all the contributions, only the transfer free energy of the surfactant tail is negative. When this contribution is large enough in magnitude to ensure that the total free energy change on micellization is negative, the aggregated state of the surfactant is favored at equilibrium compared to the singly dispersed state. This free energy contribution is thus fundamentally responsible for the formation of micelles as equilibrium entities. However, the surfactant tail transfer free energy is independent of the aggregation number and has thus no influence on the size of the equilibrium aggregate. All the remaining free energy contributions are positive and depend on the aggregation number. Among them, the aggregate core–water interfacial free energy decreases with increasing aggregation number. This is a result of the decrease in the area per molecule of the hydrophobic core of the aggregate with increasing aggregation number. This free energy is thus responsible for the positive cooperativity which favors the growth of aggregates to large sizes. All remaining free energy contributions (namely, the surfactant tail deformation energy, the steric repulsions between the head groups, the dipole–dipole interactions between the head groups, and the ionic interactions between the head groups) increase with increasing aggregation number. These free energy contributions are, therefore, responsible for the negative cooperativity which limits the aggregates to finite sizes. All the free energy contributions affect, however, the magnitude of the cmc.

Predicted Cmc and Micelle Aggregation Numbers. Influence of Surfactant Tail and Head Group. The cmc values predicted at 25 °C for nonionic alkyl β-glucosides, zwitterionic *N*-alkylbetaines, and ionic alkyl sodium sulfates are presented in Figure 6 as a function of the length of the surfactant tail. The cmc decreases with an increase in the chain length of the surfactant. This is primarily a consequence of the increase in the magnitude of the transfer free energy of the surfactant tail with increasing n_c. The incremental variation in cmc is roughly constant for a given homologous family of surfactants. The experimentally measured cmcs[81-86] are in reasonable agreement with the predicted values. For a given length of the surfactant tail, the cmc is smaller for a nonionic surfactant than for an anionic surfactant. This is a consequence of the relative magnitudes of the head group steric interactions and the head group ionic interactions in the surfactants considered.

The predicted average aggregation numbers at the cmc are plotted as a function of the tail length in Figure 7 for the zwitterionic and anionic surfactants. The micelles are spherical or globular and are narrowly dispersed in size. For the zwitterionic *N*-alkylbetaines, the predicted aggregation numbers are in reasonable agreement with the measured values.[85,86] The aggregation number increases with an increase in the chain length of the surfactant tail. This can be understood because the equilibrium area per molecule of the aggregate does not vary appreciably with a change in the tail length. Consequently, given an equilibrium area per molecule of the aggregate, the aggregation number of a spherical or globular micelle must increase with increasing tail length. One can see from eqs 19 and 20 for spherical micelles that the aggregation number g depends on v_s^2 (or alternately on n_c^2) for a given equilibrium area a per molecule. Indeed, the quantitative predictions plotted in Figure 7 show this result. For anionic sodium alkyl sulfates with alkyl chain lengths smaller than the dodecyl chain, a range of experimental data have been reported in the literature.[87-90] From this range, we select

(81) Shinoda, K.; Yamanaka, T.; Kinoshita, K. *J. Phys. Chem.* **1959**, *63*, 648.
(82) Shinoda, K.; Yamaguchi, T.; Hori, R. *Bull. Chem. Soc. Jpn.* **1961**, *34*, 237.
(83) Focher, B.; Savelli, G.; Torri, G.; Vecchio, G.; McKenzie, D. C.; Nicoli, D. F.; Bunton, C. A. *Chem. Phys. Lett.* **1989**, *158*, 491.
(84) Herrman, K. W. *J. Colloid Interface Sci.* **1966**, *22*, 352.
(85) Molyneux, P.; Rhodes, C. T.; Swarbrick, J. *Trans. Faraday Soc.* **1965**, *61*, 1043.
(86) Swarbrick, J.; Daruwala, J. *J. Phys. Chem.* **1970**, *74*, 1293.
(87) Tartar, H. V. *J. Colloid Sci.* **1959**, *14*, 115.

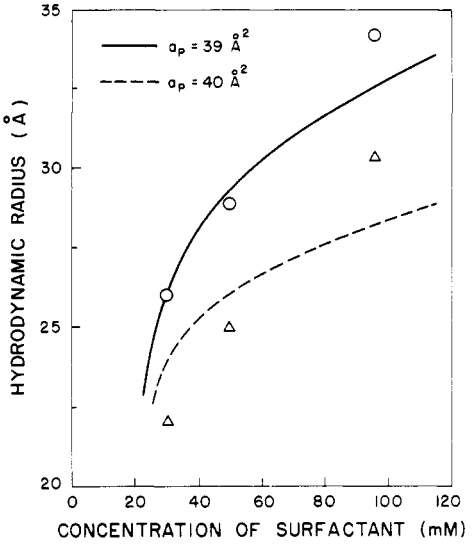

Figure 8. Dependence of the micellar size (expressed as the hydrodynamic radius) on the concentration of the surfactant for octyl glucoside. The two lines correspond to predicted values for marginally different values of the molecular constant a_p. The circles denote the reported experimental data. The triangles correspond to modified experimental data assuming that the reported measurements of hydrodynamic radius had included one layer of water. See text for discussion.

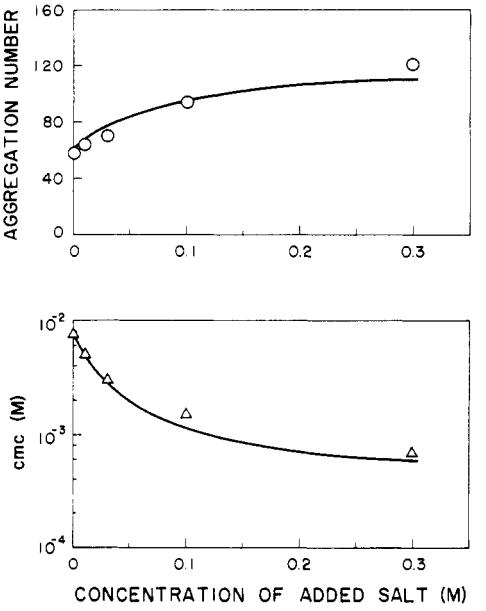

Figure 9. Influence of added NaCl concentration on the cmc and the average aggregation number of sodium dodecyl sulfate micelles. The lines denote the predicted values while the points are the experimental measurements, both at 25 °C.

experimental aggregation numbers that show the largest deviation from the predicted values for plotting in the figure. For tetradecyl and hexadecyl chains, aggregation numbers tabulated by Aniansson et al.[91] have been plotted in the figure. Although Aniansson et al.[91] cite the work of Tartar[87] as the source of their tabulated data, no reference to such experimental aggregation numbers is made in the latter paper. Therefore, the reported aggregation numbers for these two surfactants should be discounted. For alkyl sulfates, the predicted aggregation numbers do not show a significant increase with increasing length of the surfactant tail and remain practically constant for the longer tail lengths. These results can be understood by noting that the cmc for the surfactant with the smaller tail length is large, accounting for an appreciably large ionic strength. Under these conditions, the head group ionic repulsion is decreased, allowing for a smaller equilibrium area per molecule of the aggregate. In contrast, for surfactants with longer tail lengths, the cmc values are low. Therefore, the ionic strength is small and the ionic repulsion between the head groups is correspondingly large. Hence, the equilibrium area per molecule of the aggregate is larger. This increase in the equilibrium area per molecule with increasing tail length is responsible for the relatively small increase in the aggregation number with the increasing tail length in contrast to the behavior exhibited by the zwitterionic surfactant.

The results for nonionic alkyl glucoside indicate that large polydispersed spherocylindrical aggregates form. For the octyl glucoside, the aggregation numbers are still not very large while for larger chain lengths very large spherocylinders are predicted to form. The predicted weight average aggregation number is used to compute the hydrodynamic radius of the micelles using the relation

$$R_h = (3g_w v_s/4\pi)^{1/3} + l_p \qquad (79)$$

where l_p is the length of the polar head group which for the ring structure of the glucoside has been estimated[10] to be 7 Å. The computed hydrodynamic radii as a function of the surfactant concentration are presented in Figure 8. One may note that for conditions which favor the formation of spherocylindrical micelles, the parameter K which is a measure of the propensity for the surfactant molecule to be present in the cylindrical part rather than in the spherical endcaps is large. From eq 12, one can see that the value of K can be substantially altered by small changes in the calculated standard free energy difference $\Delta\mu^\circ_{cap} - \Delta\mu^\circ_{cyl}$ between spherical endcaps and cylinders, since g_{cap} which appears in the definition of K is quite large. For example, assuming a typical value of 90 for g_{cap}, a small change of $0.05kT$ in the free energy difference $\Delta\mu^\circ_{cap} - \Delta\mu^\circ_{cyl}$ will cause a change in K of $e^{4.5} = 90$. Since the magnitude of K affects the aggregation numbers (eq 17), the predicted average aggregation numbers are very sensitive even to small free energy changes whenever spherocylindrical micelles form. This is illustrated by the predictions reported here for two slightly different values of the parameter a_p which affects the magnitude of the head group steric interaction energy. The predictions are compared with the data provided by dynamic light scattering measurements.[83] It is not clear whether the reported hydrodynamic radii correspond to the dry or hydrated aggregates. Therefore, both the reported values of the hydrodynamic radii and the radii obtained by subtracting the diameter of a water molecule are plotted in Figure 8. Given the sensitivity of K to the free energy estimates, the agreement between the measured and predicted aggregate sizes is satisfactory.

Influence of Ionic Strength. An increase in the ionic strength increases the reciprocal Debye length κ. Consequently, the head group ionic interactions at the micelle surface are weakened by the addition of salt to the surfactant solution, as seen from the free energy expression, eq 70. The predicted values of the cmc and the average aggregation number for micelles of anionic sodium dodecyl sulfate are presented in Figure 9 as a function of the amount of added NaCl electrolyte. For the range of ionic strength considered, only narrowly dispersed spherical or globular micelles are formed. As expected, with decreasing ionic repulsion between the head groups, the cmc decreases

(88) Leibler, J. F.; Jacobus, J. *J. Phys. Chem.* **1977**, *81*, 130.
(89) Williams, R. J.; Philips, J. N.; Mysels, K. J. *Trans. Faraday Soc.* **1955**, *51*, 728.
(90) Mysels, K. J.; Princen, L. H. *J. Phys. Chem.* **1959**, *63*, 1696.
(91) Aniansson, E. A. G.; Wall, S. N.; Almgren, M.; Hoffmann, H.; Kielmann, I.; Ulbricht, W.; Zana, R.; Lang, J.; Tondre, C. *J. Phys. Chem.* **1976**, *80*, 905.

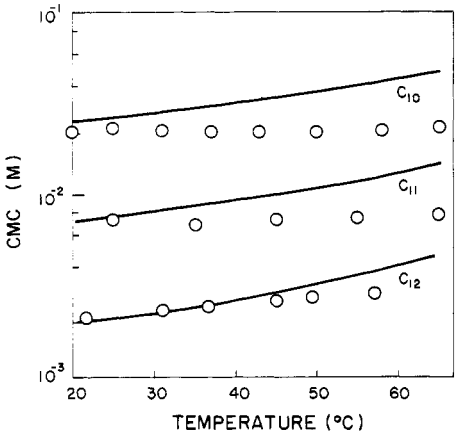

Figure 10. Dependence of cmc on temperature for *N*-alkylbetaines having C_{10}, C_{11}, and C_{12} as surfactant tails. The lines are predictions of the present theory while the points are experimental data.

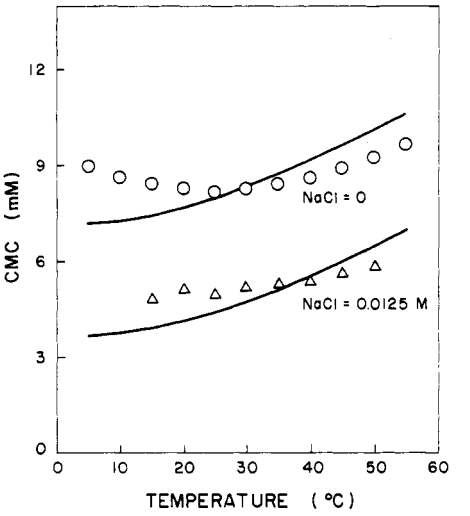

Figure 11. Dependence of cmc on temperature for sodium dodecyl sulfate present in water and in a 0.0125 M solution of NaCl. The lines are predictions of the present theory while the points are experimental data.

and the average aggregation number of the micelle increases. The predicted values are in satisfactory agreement with the experimental measurements available in the literature.[89,90]

Influence of Temperature. The temperature dependence of the cmc and of the average aggregation number of the micelle has been calculated for a number of surfactants. Figure 10 compares the predicted cmc values with the experimental data[85,86] for the zwitterionic surfactants *N*-alkylbetaines for three different alkyl chain lengths. In Figure 11, the predicted cmcs of the anionic surfactant sodium dodecyl sulfate have been plotted for two different concentrations of added NaCl electrolyte and compared with the experimental data.[92] The calculated and experimental[93] cmcs are shown in Figure 12 for the homologous family of sodium alkyl sulfonates. In all cases, the predictions show reasonable agreement with the experimental data. However, one may note that the predicted values show a monotonically decreasing cmc with decreasing temperature. In contrast, the experiments indicate some increase in the cmc as the temperature is decreased below about 25 °C. This has been qualitatively attributed to the possible dehydration of the ionic head

(92) Moroi, Y.; Nishikido, N.; Uehara, H.; Matuura, R. *J. Colloid Interface Sci.* **1975**, *50*, 254.
(93) Volkov, V. A. *Colloid J. USSR (Engl. Transl.)* **1976**, *38*, 610.

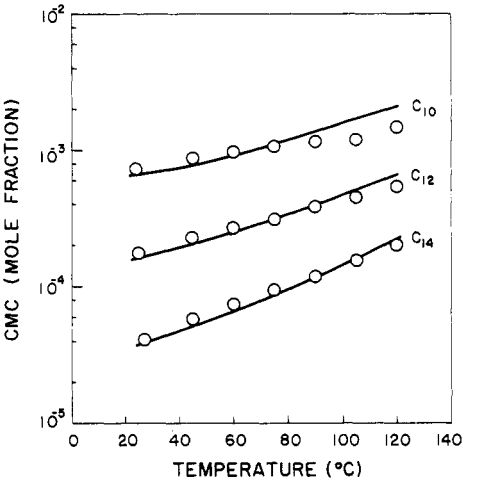

Figure 12. Dependence of cmc on temperature for sodium alkyl sulfonates having C_{10}, C_{12}, and C_{14} as surfactant tails. The lines are predictions of the present theory while the points are experimental data.

groups of the surfactants in the micelles when compared to their singly dispersed state as the temperature is lowered below 25 °C. Free energy contributions accounting for such an effect cannot be calculated at the present time with any precision, and therefore have not been included in the theory presented here.

Sphere to Rod Transition. A continuing increase in ionic strength beyond that in Figure 9 is expected to contribute to the transition from globular micelles to large spherocylindrical micelles. This is examined in some detail for the anionic sodium alkyl sulfates with NaCl as the added electrolyte. As shown by eq 17, the average aggregation number of spherocylindrical micelles and the change in this aggregation number with changing surfactant concentration are both determined by the parameter K. As noted earlier, the parameter K, which indicates the propensity for the presence of a surfactant in the cylindrical part of the micelle rather than in the spherical endcaps, has an extremely sensitive dependence on the standard free energy difference between the molecules located in those regions. One may observe from eq 12 that a small variation of $0.05kT$ in the standard free energy difference $\Delta\mu^{\circ}_{cyl} - \Delta\mu^{\circ}_{cap}$ causes a change in K by a factor of about $e^{4.5} = 90$, because g_{cap} is close to 90 for a typical system considered in this paper. Consequently, an ability to predict ln K with deviations of about 4.5 or less from the measurements can be considered very satisfactory. The predicted values for the sphere to rod transition parameter K are plotted in Figure 13 against the added concentration of electrolyte for the anionic sodium dodecyl sulfate. The predicted values are compared with those provided by light scattering measurements.[59] The comparison is exceptionally good, given the sensitivity of the parameter K to the free energy estimates. The predicted radius of the cylindrical part of the aggregate is smaller than the fully extended length of the surfactant tail. It increases from 14.5 to 14.9 Å as the electrolyte concentration is increased from 0.45 to 1.25 M at 25 °C. For this range of ionic strengths, the radius of the endcaps remains unaltered and has the value equal to the extended length of the surfactant tail. The predicted cmc, as defined by eq 18, decreases from 0.38 to 0.204 mM over this range of added salt concentration.

The temperature dependence of the parameter K has been calculated for sodium dodecyl sulfate for two concentrations of the added NaCl electrolyte. The predicted values of K are shown in Figure 14 along with experimental estimates based on dynamic light scattering

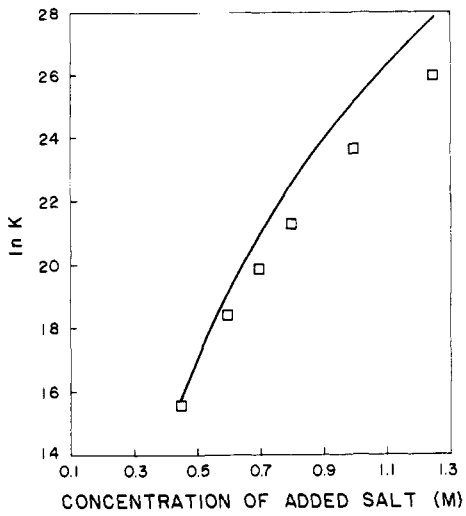

Figure 13. Dependence of the sphere to rod transition parameter K for sodium dodecyl sulfate on the concentration of added electrolyte NaCl. The points are from measurements, and the line represents the predictions, both at 25 °C.

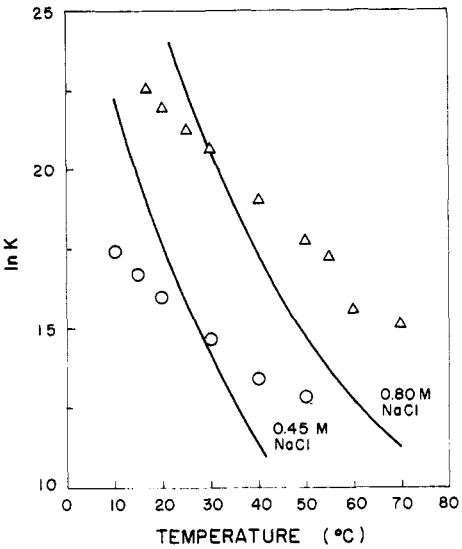

Figure 14. Influence of temperature on the sphere to rod transition parameter K of sodium dodecyl sulfate in solutions containing 0.45 and 0.80 M added NaCl electrolyte. The lines denote the predicted values while the points are experimental data.

measurements.[59] Again the comparison is satisfactory. Figure 15 presents the predicted values of K as a function of the added electrolyte concentration for the homologous family of sodium alkyl sulfates having 10–13 carbon atoms in their hydrophobic tails. One may see that even the largest deviation in ln K between the predicted and the experimental values[59] is smaller than 4.

V. Model for Surfactants with Poly(oxyethylene) Head Groups

Nonionic surfactants with poly(oxyethylene) chains as their polar head groups are among the most extensively used surfactants. In our earlier work,[23,24,45] these surfactants have been viewed as being similar to other nonionic surfactants with compact head groups. As a result, the steric interactions between the polar head groups have been evaluated using the van der Waals excluded area approach (eq 66). The effective cross-sectional area of the polar head group a_p was taken as the ratio between the volume of the poly(oxyethylene) chain and its root mean square end to end distance estimated assuming a random

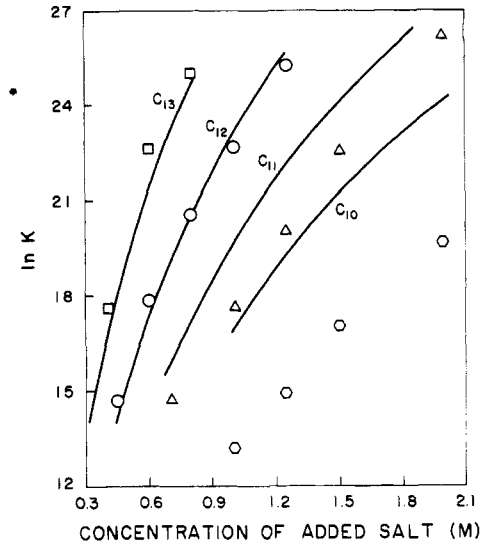

Figure 15. Dependence of the sphere to rod transition parameter K on the surfactant tail length and on the concentration of added electrolyte NaCl for sodium alkyl sulfates. The lines are predictions obtained from the present theory while the points denote the experimental data, both at 30 °C. The predicted lines are labeled, and the corresponding experimental data are indicated by squares, circles, triangles, and hexagons, respectively.

coil conformation. Such a definition for a_p ensured a systematic variation (increase) of the head group effective area with increasing length of the poly(oxyethylene) chain. Using that approach, the cmc and the average aggregation number for micelles of poly(oxyethylene) surfactants having from 6 to 63 ethylene oxide units have been computed. The calculations showed that the aggregation number decreases while the cmc increases with increasing poly(oxyethylene) chain length. This is in agreement with the expected increase in the steric repulsion between the head groups with increasing size of the polar head group. Whereas the predicted aggregation numbers showed reasonable agreement with the experimental data,[94-98] the predicted critical micelle concentrations were found to deviate from measurements up to 2 orders of magnitude, depending upon the poly(oxyethylene) chain length.

A similar computation of the steric interactions among the poly(oxyethylene) chains was also recently adopted by Puvvada and Blankschtein[41] who, in addition, consider that the effective cross-sectional area a_p is temperature dependent because of the decrease in the extent of hydration of the head group with increasing temperature. The calculations presented by Puvvada and Blankschtein involved short-chain poly(oxyethylene) head groups, with 4–8 oxyethylene units and surfactant tails made of decyl or dodecyl hydrocarbon chains ($C_{10}E_x$ and $C_{12}E_x$). Over this range of poly(oxyethylene) chain lengths, they calculated cmcs, critical micellar concentrations for phase separations, and other thermodynamic properties such as osmotic compressibility and obtained satisfactory agreement with experiments.

Irrespective of the agreement or disagreement between predicted and experimental results, the visualization of the poly(oxyethylene) chains consisting of 6–63 oxyethylene units as compact molecular systems characterized by a hard core cross-sectional area a_p is not completely

(94) Becher, P. In *Non-Ionic Surfactants*; Schick, M. J., Ed.; Marcel Dekker: New York, 1967.
(95) Barry, B. W.; El-Aini, D. I. D. *J. Colloid Interface Sci.* **1976**, *54*, 339.
(96) Barry, B. W.; El-Aini, D. I. D.; Rhodes, C. T. *Colloid Interface Sci.* **1976**, *54*, 348.
(97) Elworthy, P. H.; MacFarlane, C. B. *J. Chem. Soc.* **1962**, 537.
(98) Elworthy, P. H.; MacFarlane, C. B. *J. Chem. Soc.* **1963**, 907.

satisfactory. For sufficiently large poly(oxyethylene) chain lengths, it is more appropriate to treat the head group as a polymeric chain and calculate the free energy of their mutual interactions by considering in detail the states of this polymeric chain in singly dispersed surfactants and in micellar aggregates. For the shorter poly(oxyethylene) chains the use of polymer statistics is probably less satisfactory.

Approach to Modeling Head Group Interactions. The poly(oxyethylene) head group of the singly dispersed surfactant molecule can be viewed as an isolated free polymer coil swollen in water. In micelles, the region surrounding the hydrophobic core (denoted as the micellar shell) can be viewed as a polymer solution consisting of poly(oxyethylene) chains and water. The difference in the free energy per molecule of a poly(oxyethylene) chain in the micellar shell and one present as an isolated, free coil in water provides an additional contribution to the free energy of micelle formation. This contribution can be computed by considering the free energy of mixing of the polymer segments with water as well as the free energy of polymer chain deformation. The above approach to the calculation of the head group interaction energy has been employed in the treatment of micellization of block copolymers in selective solvents[99] and in the treatment of solubilization in block copolymer micelles.[56]

Two limiting models for the micellar shell region are developed in this paper. One model considers the micellar shell region to be characterized by a uniform concentration of polymer segments. Given the spherical and spherocylindrical shapes of micelles, the maintenance of such a uniform concentration in the micellar shell is possible only if the polymer chains deform nonuniformly along the radial coordinate characterizing the micelle geometry. The second model considers the polymer chains to be deformed uniformly. This gives rise to a radial concentration variation of polymer segments in the micellar shell region.

The quantitative results from either of the above models are expected to be affected by the polymer solution theory used for the calculation of the mixing free energies. Some available approaches include the scaling theory of de Gennes,[100] the mean field approach such as that of Flory,[73] the equation of state theories such as those of Flory[101] or Sanchez and Lacombe,[102] and the structural theory for aqueous poly(ethylene oxide) solutions developed by Kjellander and Florin.[103] The results based on any of these treatments are expected to be qualitatively similar while differing quantitatively. The choice of a polymer solution theory in this paper was dictated by the fact that, for the lengths of the polar head groups considered, the polymer segment concentration in the micellar shell (the region surrounding the micellar core) is large enough for the micellar shell to be viewed as a concentrated polymer solution. This rules out the use of the scaling approach valid for semidilute solutions as well as the structural model that is valid for polymer volume fractions smaller than about 0.10. The equation of state theories have not yet been applied to the quantitative description of aqueous poly(ethylene oxide) solutions, and their use requires the estimation of a number of equation of state parameters and mixing parameters from experimental data on poly(oxyethylene), water, and their solutions. This makes their use less convenient for the theory of micellization developed here. The mean field approach of Flory[73] is suitable for polymer solutions that are not dilute or semidilute. It has also some simplicity, since only a polymer segment–solvent interaction parameter is needed for calculating the free energies. Therefore, we employ this approach in this paper for the calculation of the mixing free energies. As will be discussed later, even this approach is beset with problems since the experimental activity data for poly(oxyethylene) in water cannot be represented by a single value for the segment–water interaction parameter.

An alternate model of micellization of poly(oxyethylene) surfactants can also be developed utilizing the analogy between micelles and star polymers whose conformational properties have been described by Daoud and Cotton.[104] Such a model for the micellization of poly(oxyethylene) surfactants will be examined in a latter paper.

A. Uniform Concentration/Nonuniform Deformation Model. In this model, the micellar shell region is assumed to have a uniform concentration. Given the spherical and cylindrical geometries of micelles, this requires the poly(oxyethylene) chains to deform nonuniformly along the radial coordinate characterizing the micelle geometry so as to maintain the concentration homogeneity in the shell region of the micelles. In lamellar aggregates curvature effects are absent and hence a uniform concentration in the shell region can be maintained by a uniformly deformed polymer chain.

In the present treatment, the poly(oxyethylene) head group of the surfactant is described as a polymer chain whose characteristic segment has the volume L^3, similar to the segments of the polymethylene chains present in the micellar core. For a poly(oxyethylene) chain containing E_x oxyethylene units, the number of segments N_E consistent with the lattice definition (segment size L) is given by

$$N_E = E_x v_E / L^3 \tag{80}$$

where v_E is the volume of an oxyethylene unit. On the basis of available density data,[105] the volume of an oxyethylene unit at 25 °C has been estimated to be $v_E = 63$ Å^3. The polymer–water interactions are accounted for by an interaction free energy parameter χ_{wE} of the van Laar or the Flory–Huggins type.[73]

In micelles, the region surrounding the hydrophobic core is viewed as a polymer solution. The thickness of this region is denoted by D. The volume of this shell region per surfactant molecule can be calculated from

$$V_{SH}/g = (V_g/g)[(1 + D/R_s)^3 - 1] \tag{81}$$

for spherical micelles

$$V_{SH}/g = (V_g/g)[(1 + D/R_s)^2(1 + D/b) - 1] \tag{82}$$

for globular aggregates

$$V_{SH}/g = (V_g/g)[(1 + D/R_c)^2 - 1] \tag{83}$$

for infinite rods, and

$$\frac{V_{SH}}{g} = \frac{V_g}{g}\left[\frac{8\pi(R_s + D)^3}{3gv_s} - \frac{2\pi}{3gv_s}\{3(R_s + D) - (H + D)\} - 1\right] \tag{84}$$

for the endcaps of the spherocylindrical aggregates. Since the concentration is homogeneous in the micellar shell,

(99) Nagarajan, R.; Ganesh, K. *J. Chem. Phys.* **1989**, *90*, 5843.
(100) de Gennes, P. G. *Scaling Concepts in Polymer Physics*; Cornell University Press: Ithaca, NY, 1979.
(101) Flory, P. J. *J. Am. Chem. Soc.* **1965**, *87*, 1833.
(102) Sanchez, I. C.; Lacombe, R. H. *Macromolecules* **1978**, *11*, 1145.
(103) Kjellander, R.; Florin, E. *J. Chem. Soc., Faraday Trans. 1* **1981**, *77*, 2053.
(104) Daoud, M.; Cotton, J. P. *J. Phys.* **1982**, *43*, 531.
(105) Mulley, B. A. In *Nonionic Surfactants*; Schick, M. J., Ed.; Marcel Dekker: New York, 1967.

the volume fraction of the polymer segments is given by

$$\phi_{Eg} = gE_x v_E / V_{SH} = gN_E L^3 / V_{SH} \quad (85)$$

Head Group Mixing Free Energy. The change in the free energy of mixing of the poly(oxyethylene) head group and water when an isolated free polymer coil is transferred to the micellar shell is calculated using the mean field approach of Flory.[73] For this purpose, one can represent the segment density of the poly(oxyethylene) in the micellar shell as a function of the radial coordinate r of the spherical or spherocylindrical aggregate by a smooth field $\phi(r)$. Given the concentration homogeneity in the micellar shell, $\phi(r)$ is independent of the radial coordinate and is given by

$$\phi(r) = \phi_{Eg} = g(N_E L^3 / V_{SH}) \quad (86)$$

Because of the interactions between the segments of a single molecule with the segments of all the other molecules, each molecule experiences a potential $U(r)$. This potential is taken in the mean field approach to be proportional to the total segment density arising from all the molecules of the micelle. The influence of the solvent is also incorporated in this mean potential via the excluded volume factor.[73,100] Thus, the mean potential can be written as

$$U(r) = kT\phi(r)(^1/_2 - \chi_{wE}) \quad (87)$$

where χ_{wE} is the Flory–Huggins-type interaction parameter for the water–poly(oxyethylene) system. The mixing free energy of a poly(oxyethylene) head group in the micellar shell of spherical aggregates with respect to the reference state of an isolated, free polymer coil is given by

$$\frac{(\Delta\mu_g^o)_{mix,E}}{kT} = \frac{1}{g}\frac{1}{L^3}\int_R^{R+D} \phi(r)\frac{U(r)}{kT} 4\pi r^2 \, dr = N_E\phi_{Eg}(^1/_2 - \chi_{wE}) \quad (88)$$

Here, R refers to the location of the micelle core–water interface and thus represents the core radius R_s of the spherical micelles. Equation 88 is used to calculate the head group mixing free energy for the globular aggregates and the endcaps of spherocylinders, as well. For the cylindrical part of the spherocylinders, one can write

$$\frac{(\Delta\mu_g^o)_{mix,E}}{kT} = \frac{1}{g}\frac{1}{L^3}\int_R^{R+D} \phi(r)\frac{U(r)}{kT} 2\pi r \, dr = N_E\phi_{Eg}(^1/_2 - \chi_{wE}) \quad (89)$$

where R now stands for the core radius R_c of the cylindrical part of the micelle.

Head Group Deformation Free Energy. The deformation free energy of the poly(oxyethylene) chains in the shell region of the micelle is calculated by employing the approach used in section III, for estimating the deformation free energy of the surfactant tail. Again, we adapt the analytical results obtained for pure block copolymers by Semenov[55] to the polymer solution in the shell region of the micelle.

Consider the shell region of thickness D surrounding the hydrophobic core of the micelle. The core–water interface is located at R, where R stands for the radius R_s in the case of spheres, the radius R_c in the case of cylinders, the half-thickness of the hydrophobic lamellae in the case of planar bilayers. One end of the polar head group is fixed at a radial distance R, namely, at the hydrophobic core–water interface. The free end of the head group is located at a radial distance r_o which has a value between R and $R + D$. Let $r(n)$ designate the location of the nth segment, with r lying between R and $R + D$. Therefore, $r(N_E) = r_o$. The local extension of the segments at a distance r is defined by the function $E(r,r_o) = dr/dn$. The function $G(r_o)$ is the density distribution function for the terminal segments. $G(r_o)\,dr_o$ represents the number of polymer molecules whose terminal segments lie in the region dr_o located at the radial distance r_o. The free energy of the micellar shell associated with the chain deformation can be written as

$$\frac{F}{kT} = \frac{3}{2}\frac{1}{L^2}\int_R^{R+D} dr_o \int_R^{R+r_o} dr\, E(r,r_o)\, G(r_o) \quad (90)$$

The functions $E(r,r_o)$ and $G(r_o)$, which remain to be determined, should satisfy the following constraints:

$$\int_R^{R+r_o} dr/E(r,r_o) = N_E \quad (91)$$

$$\int_R^r dr_o\, L^3[G(r_o)/E(r,r_o)] = 4\pi r^2\phi_{Eg},\ 2\pi r\phi_{Eg},\ 2\phi_{Eg} \quad (92)$$

The first constraint specifies that there are N_E segments associated with each poly(oxyethylene) head group, and the second states that the concentration of the polymer segments in the shell region of the micelle is uniform. The three quantities in the right-hand side of eq 92 correspond to spherical aggregates, infinite cylindrical aggregates, and infinite lamellar aggregates, respectively. By minimizing the deformation free energy eq 90 subject to the constraints eqs 91 and 92, one can determine the functional forms of $E(r,r_o)$ and $G(r_o)$, and thus, the minimum value of F for an arbitrary aggregation number g. The equations are similar to those encountered before in the calculation of the deformation free energy of the surfactant tail where exact analytical solutions were obtained for spherical, cylindrical, and lamellar geometries. For lamellar aggregates, the core and the shell regions are similar, and hence, an exact analytical solution for the head group deformation free energy can be obtained as for the tail deformation free energy. For spheres and cylinders, the exact solution for the head group deformation free energy is complicated, but as suggested by Semenov,[55] a very good approximate solution can be obtained if one considers that all the terminal segments of the poly(oxyethylene) head groups lie at the distance D from the core–water interface. In other words, the distribution of the terminal segments within the shell region of the micelle is simplified by the specification that all free ends of the head groups are located at the distance D from the micelle core. Therefore

$$G(r_o) = g\delta(r_o - (R + D)) \quad (93)$$

where δ is the δ function. The local chain deformation function $E(r,r_o)$ is now a function only of r and is obtained by combining eqs 92 and 93. This yields

$$E(r,r_o) = \frac{gL^3}{4\pi r^2\phi_{Eg}},\ \frac{gL^3}{2\pi r\phi_{Eg}},\ \frac{gL^3}{2\phi_{Eg}} \quad (94)$$

for spheres, infinite cylinders, and infinite lamellae, respectively.

Substituting the above expressions for the local chain extension function $E(r,r_o)$ and the terminal segment distribution function $G(r_o)$ in eq 90, one obtains for spheres, cylinders, and lamellae the following estimates for the head group deformation free energy:

$$\frac{1}{g}\frac{F}{kT} = \frac{3}{2}\frac{LR}{a\phi_{Eg}}\frac{D}{R+D},\ \frac{3}{2}\frac{LR}{a\phi_{Eg}}\ln\left(1+\frac{D}{R}\right),\ \frac{3}{2}\frac{LR}{a\phi_{Eg}}\frac{D}{R} \quad (95)$$

As mentioned earlier, the following exact analytical solution for lamellar aggregates can be written, in analogy with the expression eq 58 for the surfactant tail deformation free energy:

$$\frac{1}{g}\frac{F}{kT} = \frac{10\pi^2}{80}\frac{D^2}{N_E L^2} = \frac{\pi^2}{8}\frac{LR}{a\phi_{Eg}}\frac{D}{R} \text{ since } Da = \frac{N_E L^3}{\phi_{Eg}} \quad (96)$$

This differs from the approximate solution provided by eq 95 by the constant factor of $\pi^2/12$ hence by about 20%. The area per molecule of the hydrophobic core surface, a, that appears in the above equations has already been defined for various geometries. Consequently, one can estimate the free energy contribution arising from the head group deformation in the micellar shell region from

$$\frac{(\Delta\mu_g^o)_{def,E}}{kT} = \frac{3}{2}\frac{LR_s}{a\phi_{Eg}}\left[\frac{D}{D+R_s}\right] \quad (97)$$

for spheres, globular aggregates, and the endcaps of the spherocylinder and by

$$\frac{(\Delta\mu_g^o)_{def,E}}{kT} = \frac{3}{2}\frac{LR_c}{a\phi_{Eg}}\ln\left[1+\frac{D}{R_c}\right] \quad (98)$$

for the cylindrical part of the spherocylinder.

Head Group Steric Interaction Free Energy. The interactions among the poly(oxyethylene) groups in the micellar shell region have already been accounted for by the mixing and the deformation free energy contributions. A minor additional contribution is that due to the steric repulsions at the sharp interface between the micellar core and shell regions. This contribution, which is independent of the length of the poly(oxyethylene) chain, arises because one end of the long-chain poly(oxyethylene) is localized at this sharp interface. This steric repulsion free energy can be calculated using eq 66. The hard core cross-sectional area a_p represents the cross-sectional area of a polymer segment located at the core surface. Since the lattice spacing required to accomodate one polymer segment is L, a_p is equal to L^2.

Aggregate Core–Water Interfacial Free Energy. The chain deformation and mixing free energies for the poly(oxyethylene) chains considered above refer to the shell region of the micelle whereas the interfacial free energy contribution refers to the sharp interface between the micellar core and the micellar shell. The free energy of formation of this sharp interface can be calculated as before from eq 61. In the case of surfactants with compact head groups, the aggregate core–water interface has been taken to be the interface between the hydrophobic tails of the surfactant and water. Consequently, the characteristic interfacial tension at the aggregate core is taken to be $\sigma_{agg} = \sigma_{sw}$. However, the nature of the interface is modified for surfactants with poly(oxyethylene) head groups. In these systems, the micellar core–water interface is that between one phase made up of the surfactant tails and another phase made up of a solution of poly(oxyethylene) segments in water. This implies that σ_{agg} in eq 61 should be different from σ_{sw} and affected by the concentration of the poly(oxyethylene) segments in the micellar shell region as well as by the surfactant tail–poly(oxyethylene) interfacial tension σ_{sE}.

The interfacial tension between a polymer solution (poly(oxyethylene) plus water in the micellar shell) and an immiscible liquid (surfactant tails in the micellar core) can be calculated using the Prigogine theory[106,107] for the surface tensions of solutions. According to this theory, the surface is treated as a distinct phase. The surface phase composition is determined as a function of the bulk solution composition by equating the chemical potentials of the surface and bulk phases. The surface phase compositions, in turn, determine the effective interfacial tension between the two bulk phases. The Prigogine theory has been shown to predict[108] reasonably well the surface tensions of polymer solutions as well as the interfacial tensions between polymer solutions and pure liquids. The theory can also be used to predict the surface and interfacial tensions for mixtures of low molecular weight liquids. This theory is applied for the calculation of σ_{agg}. In the present case, the micellar shell region is considered to be a polymer solution with a uniform bulk concentration ϕ_{Eg}. Corresponding to this bulk composition ϕ_{Eg}, the concentration ϕ^S of polymer segments in the surface monolayer is determined by solving the implicit equation

$$\ln\left[\frac{(\phi^S/\phi_{Eg})^{1/N_E)}}{(1-\phi^S)/(1-\phi_{Eg})}\right] = \frac{(\sigma_{sw}-\sigma_{sE})}{kT}v_s^{2/3} + \chi_{wE}(3/4)[(1-\phi_{Eg})-\phi_{Eg}] - \chi_{wE}(1/2)[(1-\phi^S)-\phi^S] \quad (99)$$

Once the surface monolayer composition is known, the interfacial tension σ_{agg} can be calculated from the explicit equation

$$\left(\frac{\sigma_{agg}-\sigma_{sw}}{kT}\right)v_s^{2/3} = \ln\left(\frac{1-\phi^S}{1-\phi_{Eg}}\right) + \left(\frac{N_E-1}{N_E}\right)(\phi^S-\phi_{Eg}) + \chi_{wE}[{}^1/_2(\phi^S)^2 - {}^3/_4(\phi_{Eg})^2] \quad (100)$$

The interfacial tension between poly(oxyethylene) and surfactant tails σ_{sE}, which appears in the above equation, can be calculated in terms of the surface tension σ_s of the surfactant tails and the surface tension σ_E of poly(oxyethylene) using the following relation between surface and interfacial tensions:[74]

$$\sigma_{sE} = \sigma_s + \sigma_E - 2.0\psi(\sigma_s\sigma_E)^{1/2} \quad (101)$$

The constant ψ depends upon the nature of the interactions between the two components[74] and is close to unity if the types of self-interactions are very similar. For water–alcohol, water–ether, and water–ketone systems, ψ is close to unity.[74] The polarity of poly(oxyethylene) as indicated by solubility parameter values is similar to that of alcohols, ethers, and ketones.[109] Thus, from the point of view of interfacial tensions, the polarities of water and poly(oxyethylene) are very similar. Consequently, the ψ parameter for water–surfactant tail interactions must be comparable to that for poly(oxyethylene)–surfactant tail interactions. Since for the water–surfactant tail system considered in eq 62, $\psi = 0.55$, we estimate that $\psi = 0.55$ also for the poly(oxyethylene)–surfactant tail system in eq 101. The surface tension σ_s is calculated from eq 64. The surface tension of poly(oxyethylene) as a function of its molecular weight and temperature is estimated on the basis of the information given in ref 110 using the equation

$$\sigma_E = 42.5 - 19E_x^{-2/3} - 0.098(T-293) \quad (102)$$

where E_x represents the number of oxyethylene units of the head group.

B. Uniform Deformation/Nonuniform Concentration Model. In this model, the micellar shell region is considered to have a radial concentration gradient that is consistent with a uniform deformation of the poly(oxyethylene) chain in this region. As in the previous model, N_E denotes the number of effective segments in the head group containing E_x oxyethylene units, with the segment

(106) Prigogine, I.; Marechal, J. *J. Colloid Sci.* **1952**, *7*, 122.
(107) Defay, R.; Prigogine, I.; Bellemans, A.; Everett, D. H. *Surface Tension and Adsorption*; Wiley: New York, 1966.
(108) Siow, K. S.; Patterson, D. *J. Phys. Chem.* **1973**, *77*, 356.
(109) Barton, A. F. M. *Handbook of Solubility Parameters and Other Cohesion Parameters*; CRC Press: Boca Raton, FL, 1983.
(110) Wu, S. *Polymer Interface and Adhesion*; Marcel Dekker: New York, 1982.

size given by the lattice parameter L. The polymer–water interactions are expressed via the Flory–Huggins interaction parameter χ_{wE}. One end of the head group is located at the hydrophobic core–water interface while the other free end is assumed to be located at a distance D from this interface.

Head Group Mixing Free Energy. To calculate the mixing free energy, the polymer concentration in the micellar shell region should be known. This is determined from the requirement that the polymer chains be uniformly deformed over D, which implies that the local chain deformation is a constant. Hence

$$dr/dn = \text{constant} = D/N_E \tag{103}$$

With $\phi(r)$ denoting the smooth radial concentration profile of the polymer segments in the micellar shell, one can write for the spherical micelles

$$4\pi r^2\phi(r)\,dr = g\,dn\,L^3 \tag{104}$$

Combining the above two equations, the radial variation of polymer concentration is given by

$$\phi(r) = \left(\frac{N_E L^3}{D}\right)\frac{g}{4\pi r^2} \tag{105}$$

Similarly for infinite cylinders

$$2\pi r\phi(r)\,dr = g\,dn\,L^3 \tag{106}$$

and hence, the radial variation of the concentration of polymer segments has the form

$$\phi(r) = \left(\frac{N_E L^3}{D}\right)\frac{g}{2\pi r} \tag{107}$$

The polymer concentration at the micellar core–water interface (where $r = R$) is denoted by ϕ_R. For both spheres and infinite cylinders, one obtains

$$\phi_R = N_E L^3/Da \tag{108}$$

where a is the micellar core area per surfactant molecule defined earlier in section II.

Each of the polymer molecules interacts with all the molecules present in the micellar shell with an interaction potential $U(r)$. In the framework of the mean field approach, the potential $U(r)$ is given by

$$U(r) = kT\phi(r)\,(^1/_2 - \chi_{wE}) \tag{109}$$

This equation is identical to eq 87 considered in the previous model, except for the fact that here $\phi(r)$ is not a constant but depends on the radial distance r. As in the previous model, the mixing free energy of a poly(oxyethylene) head group in the micellar shell with respect to the reference state of an isolated, free polymer coil is given for spherical micelles by

$$\frac{(\Delta\mu_g^\circ)_{mix,E}}{kT} = \frac{1}{g}\frac{1}{L^3}\int_R^{R+D}\phi(r)\frac{U(r)}{kT}4\pi r^2\,dr = N_E\phi_R(^1/_2 - \chi_{wE})\frac{1}{(1 + D/R)} \tag{110}$$

Here, R refers to the location of the micellar core–water interface and thus represents the core radius R_s of the spherical micelles. Equation 110 can be used to calculate the head group mixing free energy for both the globular aggregates and the endcaps of spherocylinders. For the cylindrical part of the spherocylinders, one can use the expression

$$\frac{(\Delta\mu_g^\circ)_{mix,E}}{kT} = \frac{1}{g}\frac{1}{L^3}\int_R^{R+D}\phi(r)\frac{U(r)}{kT}2\pi r\,dr = N_E\phi_R(^1/_2 - \chi_{wE})(R/D)\ln(1 + D/R) \tag{111}$$

where R now stands for the core radius R_c of the cylindrical part of the micelle.

Head Group Deformation Free Energy. The polymer chain has been assumed to deform uniformly along the chain length. The micellar shell region may be viewed as a network of poly(oxyethylene) chains with all the chains linked to the micellar core. No other cross-linking between the chains exists. One may apply the results of rubber elasticity theory developed by Flory[73] to estimate the deformation free energy for each chain in the network. For the elongation of a chain at constant volume, the entropy of deformation has been evaluated by Flory.[73] Using this equation, and considering that no cross-linking exists between the chains present in the shell region, the free energy of deformation can be calculated from

$$\frac{(\Delta\mu_g^\circ)_{def,E}}{kT} = \frac{1}{2}\left(\frac{D^2}{N_E L^2} + \frac{2N_E^{1/2}L}{D} - 3\right) \tag{112}$$

This equation is used for all the aggregate geometries.

Head Group Steric Interaction Free Energy. As in the previous model, a minor additional contribution arising from the steric repulsions at the micellar core surface can be calculated using eq 66. The hard core cross-sectional area a_p represents the cross-sectional area of a polymer segment located at the core surface. Since the lattice spacing required to accomodate one polymer segment is L, a_p is equal to L^2.

Aggregate Core–Water Interfacial Free Energy. The free energy of formation of the aggregate core–water interface can be calculated as in the previous model using eq 61. The characteristic interfacial tension σ_{agg} which appears in eq 61 should be affected in the present model, by the concentration ϕ_R of the poly(oxyethylene) segments in the region close to the hydrophobic core. Consequently, σ_{agg} is calculated on the basis of the Prigogine theory using eqs 99 and 100 but with ϕ_R replacing ϕ_{Eg}. Thus, the concentration of polymer segments in the surface monolayer ϕ^S is determined by solving the implicit equation

$$\ln\left[\frac{(\phi^S/\phi_R)^{1/N_E)}}{(1-\phi^S)/(1-\phi_R)}\right] = \frac{(\sigma_{sw} - \sigma_{sE})}{kT}v_s^{2/3} + \chi_{wE}(3/4)[(1-\phi_R) - \phi_R] - \chi_{wE}(1/2)[(1-\phi^S) - \phi^S] \tag{113}$$

The interfacial tension σ_{agg} is calculated from the explicit equation

$$\left(\frac{\sigma_{agg} - \sigma_{sw}}{kT}\right)v_s^{2/3} = \ln\left(\frac{1-\phi^S}{1-\phi_R}\right) + \frac{N_E - 1}{N_E}(\phi^S - \phi_R) + \chi_{wE}[^1/_2(\phi^S)^2 - {}^3/_4(\phi_R)^2] \tag{114}$$

The expressions needed to calculate the interfacial tensions σ_{sw} and σ_{sE} have already been presented in eqs 62 and 101.

VI. Predictions of the Model for Poly(oxyethylene) Surfactants

Computational Approach. For spherical or globular aggregates, the dispersion of sizes is small and hence the equilibrium micelles are predicted from the condition of maximum aggregate concentration X_g. In the present case, the aggregate concentration X_g depends on two independent variables, the aggregation number g, and the thickness of the micellar shell region D. In contrast, for surfactants with compact head groups, X_g depends only on one variable, namely, the aggregation number g. Therefore,

for spherical or globular micelles, the average aggregation number and the shell thickness D can be calculated from the condition of maximum of X_g with respect to g and D.

If the aggregates are spherocylindrical, the standard chemical potential difference per molecule $\Delta\mu^{\circ}_{cyl}$ for the surfactant present in the cylindrical part is minimized with respect to the two independent variables R_c and D to obtain the minimum value for $\Delta\mu^{\circ}_{cyl}$ and also the corresponding values of R_c and D. Also the standard chemical potential difference per molecule $\Delta\mu^{\circ}_{cap}$ for the surfactant present in the endcaps is minimized with respect to the two independent variables g_{cap} and D. From the values of the standard chemical potential differences $\Delta\mu^{\circ}_{cyl}$, $\Delta\mu^{\circ}_{cap}$, and of g_{cap}, one can calculate the sphere to rod transition parameter K (eq 12), the average aggregation numbers at any total surfactant concentration (eq 17), and the cmc (eq 18). The IMSL subroutine ZXMWD was used for the optimizations involving two independent variables.

The poly(oxyethylene)–water interaction parameter χ_{wE} can, in principle, be obtained from thermodynamic properties of poly(oxyethylene)–water solutions (such as activity data or phase diagram). The activity data[111] for poly(oxyethylene)–water solution, represented in the framework of the Flory–Huggins theory indicate that the magnitude of the interaction parameter is dependent on the composition of the polymer solution.[112] The observed phase behavior of the poly(oxyethylene)–water system includes both a lower critical solution temperature and an upper critical solution temperature.[103,111] This phase behavior indicates that χ_{wE} first increases and then decreases with increasing temperature; in other words, it exhibits a maximum. An explicit expression for the dependence of the poly(oxyethylene)–water interaction parameter χ_{wE} on polymer concentration, temperature, and polymer molecular weight is presently not available.

The head group of the surfactant contains besides the oxyethylene groups another functional group that terminates the polymer chain such as a hydroxyl group. The presence of this terminal group may alter somewhat the magnitude of the interaction parameter when compared to the interaction parameter of the high molecular weight poly(oxyethylene)–water systems. This alteration may be relevant for surfactant head groups containing only a small number (4–10) of oxyethylene units. The polarity of the functional group contributes to increased compatibility with water, and this is reflected in a lower value of χ_{wE}. Here, calculations have been carried out for two different values of the interaction parameter, namely, χ_{wE} = 0.1 and 0.3. Since water is a good solvent for poly(oxyethylene), values for χ_{wE} smaller than 0.5 (which corresponds to a θ solvent) have been chosen for the illustrative calculations. One may also note that a value for χ_{wE} close to 0.1 in the structural model of Kjellander and Florin[103] described the activity data well at low polymer concentrations. Somewhat larger values for this parameter are expected at higher polymer concentrations in view of the experimental activity data.[111] Hence, the choice of the range 0.1–0.3 is meaningful for the examination of the influence of χ_{wE} on the calculated aggregation properties.

Predictions of the Cmc and Micellar Size. Predicted cmc values for a surfactant with dodecyl hydrocarbon tail and 6–53 oxyethylene units ($C_{12}E_x$) are presented in Figure 16. The cmc values are calculated on the basis of the two

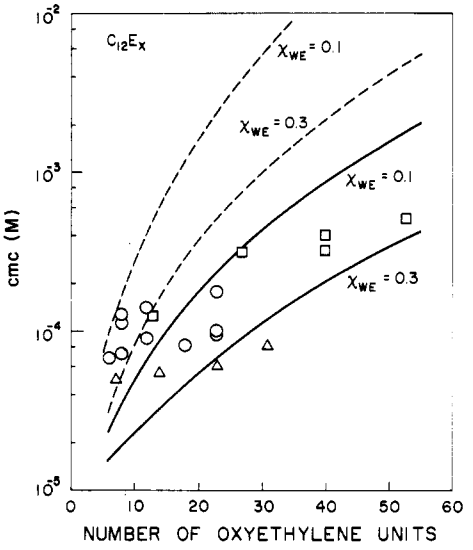

Figure 16. Dependence of the cmc on the length of the poly(oxyethylene) head group of nonionic surfactants containing a dodecyl chain as the surfactant tail ($C_{12}E_x$). The points refer to measured values while the lines denote predictions of the present model, both at 25 °C. The continuous lines represent the results from the uniform deformation/nonuniform concentration model while the dotted lines denote the predictions based on the uniform concentration/nonuniform deformation model. Calculated results are shown for two different values of the poly(oxyethylene)–water interaction parameter. Circles refer to commercial poly(oxyethylene) glycol ethers,[113–116] triangles represent commercial samples where the distribution of oxyethylene chain lengths is reduced by molecular distillation,[117] and squares correspond to purified poly(oxyethylene) methyl ethers.[118]

models developed in this paper, namely, the uniform concentration/nonuniform deformation model and the nonuniform concentration/uniform deformation model. Also, the cmcs calculated for two values of the poly(oxyethylene)–water interaction parameter are given in the plot. The experimental data shown for comparison are those obtained on poly(oxyethylene) glycol ethers[94,113–117] and poly(oxyethylene) methyl ethers.[118] One may observe from Figure 16 that there is considerable scatter in the measured cmc values. This is partly a consequence of the heterogeneity of some of the surfactant samples that have been used, the samples having included a range of poly(oxyethylene) chain lengths distributed around the reported mean value. The predicted cmc values based on the uniform concentration/nonuniform deformation model show significantly increasing deviations from experiments as the number of oxyethylene units in the surfactant is increased. The uniform deformation/nonuniform concentration model provides cmc values relatively closer to the measurements.

Figure 17 presents predicted as well as measured cmc data for a surfactant with hexadecyl hydrocarbon tail and 8–63 oxyethylene units ($C_{16}E_x$). The experimental data shown for comparison are those obtained with poly(oxyethylene) glycol ethers[95–98] and poly(oxyethylene) methyl ethers.[118] The smaller scatter in the experimental data shown in Figure 17 compared to the data in Figure 16 is

(111) Malcolm, G. N.; Rowlinson, J. S. *Trans. Faraday Soc.* **1957**, *53*, 921.

(112) Sheu, J. Thermodynamics of Phase Separation in Aqueous Polymer-Surfactant-Electrolyte Solutions. Ph.D. Dissertation, The Pennsylvania State University, University Park, PA, 1983.

(113) Becher, P. In *Chemistry, Physics and Application of Surface Active Substances*; Overbeek, J. Th. G., Ed.; Gordon and Breach Science Publishers: New York, 1964; p 621.

(114) Becher, P.; Arai, H. *J. Colloid Interface Sci.* **1968**, *27*, 634.

(115) Meguro, K.; Ueno, M.; Esumi, K. In *Nonionic Surfactants Physical Chemistry*; Schick, M. J., Ed.; Marcel Dekker: New York, 1987; p 109.

(116) Woodhead, J. L.; Lewis, J. A.; Malcolm, J. N.; Watson, I. D. *J. Colloid Interface Sci.* **1981**, *79*, 454.

(117) Schick, M. J.; Gilber, A. H. *J. Colloid Sci.* **1965**, *20*, 464.

(118) Reddy, N. K.; Foster, A.; Styring, M. G.; Booth, C. *J. Colloid Interface Sci.* **1990**, *136*, 588.

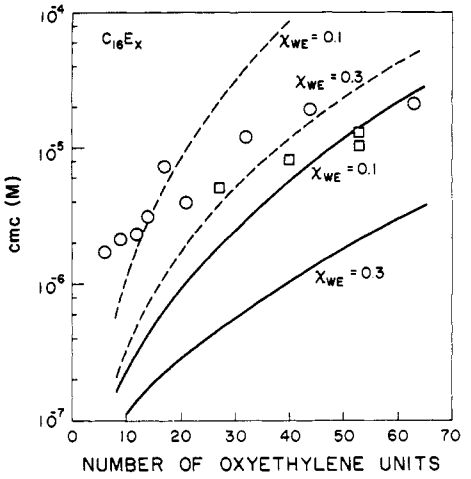

Figure 17. Dependence of the cmc on the length of the poly(oxyethylene) head group of nonionic surfactants containing a hexadecyl chain as the surfactant tail ($C_{16}E_x$). The points refer to measured values while the lines denote predictions of the present model, both at 25 °C. The continuous lines represent the results from the uniform deformation/nonuniform concentration model while the dotted lines denote the predictions based on the uniform concentration/nonuniform deformation model. Calculated results are shown for two different values of the poly(oxyethylene)–water interaction parameter. Circles denote poly(oxyethylene) glycol ethers[95-98] while the squares represent purified poly(oxyethylene) methyl ethers.[118]

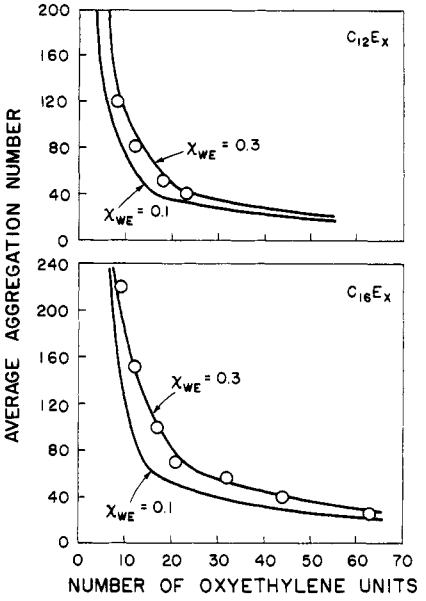

Figure 18. Influence of the poly(oxyethylene) head group size on the average aggregation number of micelles. The two surfactants contain dodecyl and hexadecyl hydrophobic tails, respectively. The points are experimental data (25 °C), and the lines represent the predictions of the present theory. The calculated results are based on the uniform deformation/nonuniform concentration model.

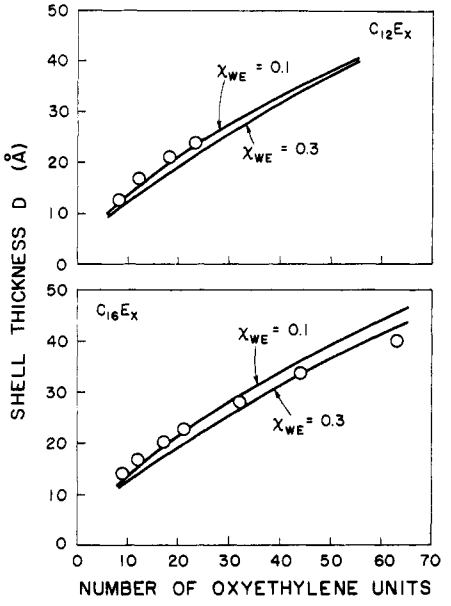

Figure 19. Influence of the poly(oxyethylene) head group size on the shell thickness of the micelles. The two surfactants are $C_{12}E_x$ and $C_{16}E_x$. The points are experimental data (25 °C), and the lines represent the predictions of the present theory. The calculated results are based on the uniform deformation/nonuniform concentration model.

primarily due to the fewer cmc measurements available for the $C_{16}E_x$ surfactants. Predicted cmc values are based on the two models and the two values of the poly(oxyethylene)–water interaction parameter. As before, the uniform concentration/nonuniform deformation model predicts a higher rate of increase of the cmc with poly(oxyethylene) chain length than that observed experimentally. The predictions based on the uniform deformation/nonuniform concentration model provide a rate of change of cmc closer to the measurements.

The predicted aggregation numbers based on the uniform deformation/nonuniform concentration model are shown in Figure 18 for both $C_{12}E_x$ and $C_{16}E_x$ surfactants. Measured aggregation numbers[94-98] are also plotted for comparison. The calculated aggregation numbers for both values of the poly(oxyethylene)–water interaction parameters show qualitative agreement with the experimental values. The predicted aggregation numbers are larger if the parameter χ_{wE} assumes a larger magnitude. The agreement between the predicted and measured aggregation numbers is also satisfactory when quantitative comparisons are made.

The predicted thickness D of the micellar shell region containing the poly(oxyethylene) head groups is plotted in Figure 19 for both $C_{12}E_x$ and $C_{16}E_x$ surfactants. The calculations are based on the uniform deformation/nonuniform concentration model and assume two different values for the poly(oxyethylene)–water interaction parameter. The shell thicknesses have been estimated by Tanford et al.[119] from intrinsic viscosity measurements.[95-98] They found that the shell thickness calculated assuming a random coil conformation for the poly(oxyethylene) chain is consistent with the measured intrinsic viscosities. The estimated shell thicknesses are presented for comparison in Figure 19. The values of D predicted in this paper are in reasonable agreement with the estimates obtained from intrinsic viscosity data for both $C_{12}E_x$ and $C_{16}E_x$ surfactants. As one may expect, the shell thickness D calculated assuming a smaller value for the poly(oxyethylene)–water interaction parameter ($\chi_{wE} = 0.1$, implying a better solvent) is larger than that calculated assuming a larger value for the interaction parameter ($\chi_{wE} = 0.3$, implying a relatively poorer solvent).

The predicted aggregation numbers and shell thicknesses based on the uniform concentration/nonuniform deformation model are presented in Figures 20 and 21 for both $C_{12}E_x$ and $C_{16}E_x$ surfactants. The experimental aggregation numbers[94-98] and shell thicknesses[119] are also presented for comparison. The predicted dependence of the micelle aggregation numbers on the poly(oxyethylene) chain length is in reasonable agreement with the measurements, but the calculated aggregation numbers are uniformly smaller than the experimental values. The

(119) Tanford, C.; Nozaki, Y.; Rhode, M. F. *J. Phys. Chem.* **1977**, *81*, 1555.

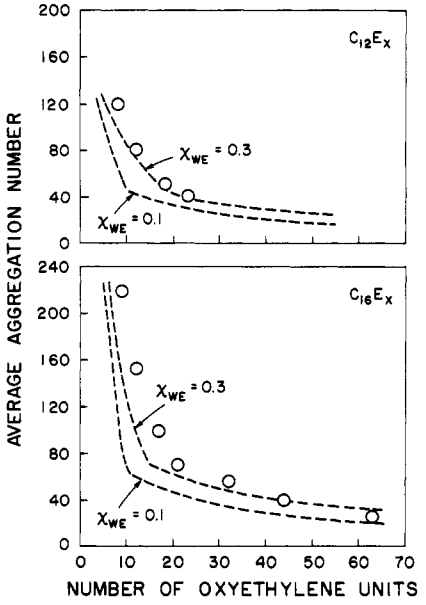

Figure 20. Influence of the poly(oxyethylene) head group size on the average aggregation number of micelles. The two surfactants contain dodecyl and hexadecyl hydrophobic tails, respectively. The points are experimental data (25 °C), and the lines represent the predictions of the present theory. The calculated results are based on the nonuniform deformation/uniform concentration model.

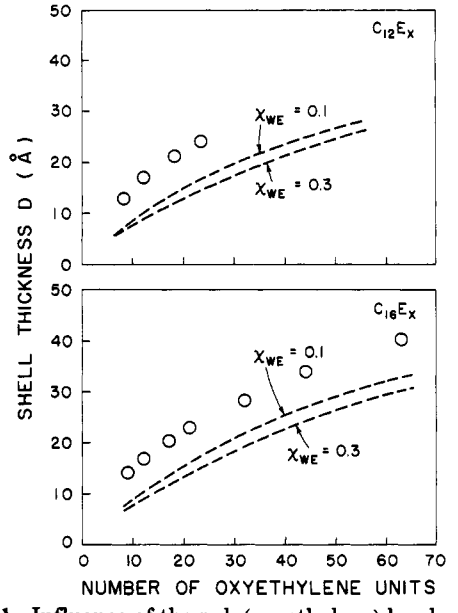

Figure 21. Influence of the poly(oxyethylene) head group size on the thickness of the micellar shell for the $C_{12}E_x$ and $C_{16}E_x$ surfactants. The points are experimental data (25 °C), and the lines represent the predictions of the present theory. The calculated results are based on the nonuniform deformation/uniform concentration model.

comparison of shell thicknesses D in Figure 21 shows that the model predicts considerably smaller values for the thickness D than that estimated from intrinsic viscosity measurements.[119]

From a comparison between the predicted and experimental values for the cmcs, aggregation numbers, and shell thicknesses of the $C_{12}E_x$ and $C_{16}E_x$ surfactants, over an extended range of oxyethylene chain lengths shown in Figures 16–21, one may conclude that the uniform deformation/nonuniform concentration model is in somewhat better agreement with the experiments than the uniform concentration/nonuniform deformation model. Improved correspondence between predicted and experimental micellar properties should await a more satisfactory treatment of poly(oxyethylene)–water solutions than that presently available. However, it is essential that any model for nonionic surfactants be tested by considering all the micellar characteristics, namely, the cmc, the aggregation number, and the shell thickness over the extended range of poly(oxyethylene) chain lengths as has been attempted here.

The temperature dependence of the aggregation behavior of surfactants with poly(oxyethylene) head groups must differ from that of ionic and zwitterionic surfactants because of the way the interactions between poly(oxyethylene) head groups depend on the temperature. For ionic and zwitterionic surfactants, the various contributions to the free energy of micellization display a temperature dependence which leads to a lowering of the aggregation number with increasing temperature. In addition to these free energy contributions, one has to now also consider the interactions involving the poly(oxyethylene) head groups and water in the micellar shell region. These interactions are affected by the temperature dependence of the poly(oxyethylene)–water interaction parameter. As suggested by the observed phase behavior of the poly(oxyethylene)–water systems,[103,111,112] the interaction parameter χ_{wE} should first increase as the temperature is increased (giving rise to a lower critical solution temperature, LCST), pass through a maximum, and then decrease with increasing temperature (giving rise to an upper critical solution temperature, UCST). Thus, for temperatures smaller than the LCST (which is the temperature range for which the aggregation behavior is examined), the interaction parameter χ_{wE} increases with an increase in temperature. The calculations discussed above show that the aggregation numbers increase with increasing poly(oxyethylene)–water interaction parameter, χ_{wE}, if none of the other variables are modified (Figures 18 and 20). Consequently, one may conclude that head group interactions promote aggregate growth with increasing temperature for nonionic poly(oxyethylene) surfactants. The remaining free energy contributions favor a decrease in the aggregation number. The net effect on the equilibrium aggregation number can be an increase or a decrease depending on the relative importance of the different free energy contributions. Thus, because of the temperature dependence of the head group interaction free energy in the case of surfactants with poly(oxyethylene) head groups, these surfactants can form micelles of increasing aggregation number with increasing temperature,[120–122] in contrast to the behavior of ionic and zwitterionic surfactants. It is interesting to observe that an increase in the polymer–water interaction parameter χ_{wE} which promotes the phase separation of the polymer solution (LCST) also promotes the growth of the micelles to large sizes.

VII. Thermodynamics of Solubilization

The phenomenon of solubilization in aqueous media refers to the enhanced solubility of hydrophobic solutes because of the presence of surfactant aggregates. Experimental studies of solubilization have provided information about the maximum amount of solubilization possible for a given surfactant concentration and, in some cases, the micellar aggregation numbers as well. It has been found that, within a homologous family of solubilizate molecules, the molar solubilization ratio (the ratio between the number of solubilizate and surfactant molecules in the

(120) Ottewill, R.; Storer, C. C.; Walker, T. *Trans. Faraday Soc.* **1967**, *63*, 2796.
(121) Zana, R.; Weill, C. J. *Phys. Lett.* **1985**, *46*, L-953.
(122) Nishikido, N. *Langmuir*, **1990**, *6*, 1225.

aggregate) decreases with an increase in the size of the solubilizate molecules. Further, the aromatic molecules are solubilized to a larger extent than the aliphatic molecules of comparable molecular volume.[2,3] Also, most interesting, the aromatic molecules are selectively solubilized compared to aliphatic molecules when binary mixtures of hydrocarbons are solubilized.[123]

Solubilization in surfactant aggregates can give rise to two types of structures. The aggregates designated type I in our earlier work[52] are those in which the solubilizate molecules are present entirely within the region of surfactant tails. They are referred to as swollen aggregates in this paper (Figure 2). In contrast, the aggregates designated type II are those in which the solubilizate molecules are present both within the region of the surfactant tails and also in a core containing only solubilizate molecules. Such aggregates are referred to in this paper as microemulsions (Figure 3).

Geometrical Characteristics of Aggregates. The geometrical characteristics of the swollen micelles are virtually the same as those discussed in section II, except for the fact that the total aggregate volume V_g consists now of both surfactant and solubilizate molecules. We denote by Z the mole fraction of the solubilizate and by η the volume fraction of the solubilizate, both within the surfactant tail region. The volume fraction η can be readily calculated from

$$\eta = \frac{Zv_o}{Zv_o + (1-Z)v_s} \tag{115}$$

where v_o denotes the molecular volume of the solubilizate. Obviously, for swollen aggregates Z and η also represent the mole fraction and the volume fraction of the solubilizate in the entire aggregate. For swollen aggregates of all the shapes considered in section II, the expressions derived before for the volume V_g of the aggregate, the total surface area of the aggregate A_g, the area $A_{g\delta}$ evaluated at a distance δ, and the packing factor P all remain unchanged and are given by eqs 19–38. However, the volume of the aggregate can now be related to molecular characteristics via

$$V_g = gv_s/(1-\eta) \tag{116}$$

The packing factor P is therefore given by the relation

$$P = V_g/A_gR_s = v_s/a(1-\eta)R_s \tag{117}$$

for spheres, globular aggregates, and the endcaps of spherocylinders and by the relation

$$P = V_g/A_gR_c = v_s/a(1-\eta)R_c \tag{118}$$

for the cylindrical part of spherocylinders. One may note that, for spherocylindrical aggregates, the parameters Z and η are allowed to assume different values in the cylindrical middle part and in the spherical endcaps of the aggregate. The molar solubilization ratio in swollen aggregates is obtained from

$$(j/g)_{avg} = Z/(1-Z) \tag{120}$$

For microemulsions, we denote the thickness of the surfactant tail region by R and the overall radius of the spherical aggregate by R_s. The volume of the surfactant tail region is denoted by V_g and the total surface area of the aggregate by A_g:

$$V_g = \frac{4\pi R_s^3}{3} - \frac{4\pi(R_s-R)^3}{3} = \frac{gv_s}{(1-\eta)} \tag{121}$$

The surface area of the aggregate–water interface of microemulsions is

$$A_g = 4\pi R_s^2 = ga \tag{122}$$

while the aggregate surface area at a distance δ from the hydrophobic core–water interface is

$$A_{g\delta} = 4\pi(R_s+\delta)^2 = ga_\delta \tag{123}$$

The packing factor P in the surfactant tail region is defined as

$$P = V_g/A_gR = v_s/a(1-\eta)R \tag{124}$$

The molar solubilization ratio in a microemulsion system is estimated by accounting for the solubilizate present in both the surfactant tail region and the core region:

$$\left(\frac{j}{g}\right)_{avg} = \frac{Z}{(1-Z)} + \frac{1}{g}\frac{4\pi(R_s-R)^3}{3v_o} \tag{125}$$

where the first term accounts for the contribution from the surfactant tail region and the second term that from the core region of the microemulsion. Having defined the geometrical characteristics of the aggregates, one can now consider the aggregate size distribution at equilibrium, from which the molar solubilization ratio $(j/g)_{avg}$ and the average size of the micelles can be determined.

Size Distribution of Aggregates Containing Solubilizates. The surfactant solution consists of singly dispersed surfactant and solubilizate molecules, aggregates of surfactants in which solubilizate molecules are incorporated, and solvent water molecules. The minimization of the Gibbs free energy of the solution for given total amounts of surfactant and solubilizate in the system leads to an expression for the size distribution of aggregates similar to eq 2. The mole fraction of aggregates containing g surfactant molecules and j solubilizate molecules is given by the relation

$$X_g = X_1^g X_{1o}^j \exp\left(-\frac{\mu_{gj}^\circ - g\mu_1^\circ - j\mu_{1o}^\circ}{kT}\right) \tag{126}$$

Here, X_{1o} refers to the mole fraction of the singly dispersed solubilizate molecules in the solution, μ_{1o}° refers to the standard chemical potential of singly dispersed solubilizate molecules in the aqueous phase at infinite dilution, and μ_{gj}° denotes the standard chemical potential of an aggregate at infinite dilution, containing g surfactant and j solubilizate molecules. The mole fraction of aggregates denoted for simplicity by X_g is obviously also dependent on the variable j.

The concentration of the singly dispersed solubilizate molecules can assume its largest value X_{1o}^* when the surfactant solution is saturated in solubilizate and an excess solubilizate phase coexists at equilibrium. For this condition, the concentration of the singly dispersed solubilizate molecules can be obtained from the equilibrium between a pure solubilizate phase and the aqueous solution. Equating the chemical potential of the solubilizate in the pure solubilizate phase to that of the singly dispersed solubilizate molecules in the aqueous phase, one obtains

$$\mu_o^H = \mu_{1o}^\circ + kT \ln X_{1o}^* \tag{127}$$

where μ_o^H is the chemical potential of the pure solubilizate phase. The ratio between the mole fraction of the singly dispersed solubilizate in the surfactant solution and that when the surfactant solution is saturated in solubilizate

(123) Chaiko, M. A.; Nagarajan, R.; Ruckenstein, E. *J. Colloid Interface Sci.* **1984**, *99*, 168.

is denoted by f:

$$X_{1o} = fX^*_{1o} \tag{128}$$

The aggregate size distribution function (eq 126) can be written now in a form analogous to eq 2 by introducing eqs 127 and 128:

$$X_g = X_1^g \exp(-g\Delta\tilde{\mu}^o_g/kT) \tag{129}$$

where

$$\frac{\Delta\tilde{\mu}^o_g}{kT} = \frac{\Delta\mu^o_g}{kT} - \frac{j}{g}\ln f \qquad \Delta\mu^o_g = \frac{\mu^o_{gj}}{g} - \mu^o_1 - \frac{j}{g}\mu^H_o \tag{130}$$

In the above equation, $\Delta\mu^o_g$ is the difference in the standard chemical potential for a surfactant molecule and j/g solubilizate molecules present in an aggregate with respect to a singly dispersed surfactant molecule in aqueous phase and j/g solubilizate molecules in the bulk solubilizate phase. The number and the weight average aggregation numbers can be calculated from the aggregate size distribution via eq 3, while the average molar ratio of surfactant to solubilizate can be obtained from

$$(j/g)_{avg} = \sum jX_g / \sum gX_g \tag{131}$$

Obviously, the average quantities are obtained by carrying out the summations in eqs 3 and 131 over both g and j where g varies between 2 and ∞ while j can change from 0 to ∞.

The maximum amount of solubilization is reached when the concentration of the singly dispersed solubilizate assumes its maximum possible value. This corresponds to a value of unity for the ratio f defined by eq 128. All predictions of the molar solubilization ratio corresponding to the maximum amount of solubilization possible are thus obtained by taking f equal to unity in the size distribution eq 129.

Sphere to Rod Transition. The formation of swollen spherocylindrical micelles can be analyzed in a manner similar to that considered in section II in the absence of solubilizates. The size distribution equation in the presence of solubilizates (eq 129) is formally identical to eq 2 considered earlier. One should note, however, that the standard chemical potential difference term $\Delta\mu^o_g$ is different since it includes contributions arising from the presence of the solubilizate molecule. Given the formal equivalence in the size distribution expressions, the formation of spherocylindrical micelles swollen by solubilizates can be completely described by eqs 10–18. The overall molar solubilization ratio in the spherocylinder depends upon the amounts both in the middle cylindrical part and in the spherical endcaps. Combining the definition for the molar solubilization ratio $(j/g)_{avg}$ given by eq 131 and the size distribution equation for spherocylindrical aggregates (eq 13), one obtains

$$\left(\frac{j}{g}\right)_{avg} = \left(\frac{Z}{1-Z}\right)_{cyl} + \frac{g_{cap}}{g_n}\left(\frac{Z}{1-Z}\right)_{cap} \tag{132}$$

where the subscripts cyl and cap refer to the cylindrical middle part and the spherical endcaps of the aggregate.

VIII. Model for the Free Energy of Solubilization

In order to predict the solubilization behavior of surfactants, explicit expressions for $\Delta\mu^o_g$ must be developed. This free energy difference is made up of a number of contributions, many of which have already been identified in the treatment of micellization. The presence of the solubilizate affects the standard free energy difference in a number of ways. Firstly, a new contribution $(\Delta\mu^o_g)_{mix}$ must be introduced to account for the entropy and the enthalpy of mixing of the solubilizates with the surfactant tails in the swollen micelles as well as in the surfactant tail region of microemulsions. Secondly, the contribution of the tail deformation free energy $(\Delta\mu^o_g)_{def}$ and of the micelle–water interfacial free energy $(\Delta\mu^o_g)_{int}$ must be modified to account for the presence of the solubilizate. Finally, all the remaining free energy contributions are affected by the presence of the solubilizate since the incorporation of the solubilizate modifies the aggregate geometry and thus the free energies that depend on the geometrical characteristics. Only the transfer free energy of the surfactant tail, $(\Delta\mu^o_g)_{tr}$, which is unrelated to the presence of solubilizates as well as to the aggregate geometry, remains unaffected. One can write the free energy of solubilization decomposed into various contributing terms as

$$\Delta\mu^o_g = (\Delta\mu^o_g)_{tr} + (\Delta\mu^o_g)_{def} + (\Delta\mu^o_g)_{int} + (\Delta\mu^o_g)_{steric} + (\Delta\mu^o_g)_{dipole} + (\Delta\mu^o_g)_{ionic} + (\Delta\mu^o_g)_{mix} \tag{133}$$

In the case of poly(oxyethylene) surfactants, additional free energy contributions, $(\Delta\mu^o_g)_{def,E}$ and $(\Delta\mu^o_g)_{mix,E}$, arise from the interactions between the poly(oxyethylene) head groups. The expressions for $(\Delta\mu^o_g)_{tr}$, $(\Delta\mu^o_g)_{steric}$, $(\Delta\mu^o_g)_{dipole}$, and $(\Delta\mu^o_g)_{ionic}$ are identical to those presented in section III, while the expressions for $(\Delta\mu^o_g)_{def,E}$ and $(\Delta\mu^o_g)_{mix,E}$ are identical to those presented in section V, with the difference that the new geometrical relations corresponding to solubilization should be included in all these expressions. The remaining free energy contributions that are modified in a more substantial manner by the presence of solubilizates are discussed below.

Deformation Free Energy of the Surfactant Tail. The deformation free energy of the surfactant tail was modeled in section III, by visualizing the surfactant tail as a polymer molecule containing N segments of characteristic size L. The presence of solubilizate in the hydrophobic region of the aggregates transforms the representation of this region from that of a pure polymer to that of a polymer solution, with the solubilizate swelling the polymer. Thus, in the present calculations, the micellar core region is treated as a uniform solution of the surfactant tail and the solubilizate.

The deformation free energy of the tail can be calculated by following the approach employed for solubilizate-free micelles in section III. Accordingly, the free energy of the aggregate core associated with the nonuniform chain deformation can be written as

$$\frac{F}{kT} = \frac{3}{2}\frac{1}{L^2}\int_0^R dr_o \int_0^{r_o} dr\, E(r,r_o)\, G(r_o) \tag{134}$$

As before, the functions $E(r,r_o)$ and $G(r_o)$ are unknown, but they should satisfy the following relations:

$$\int_0^{r_o} dr/E(r,r_o) = N \tag{135}$$

and

$$\int_r^R dr_o\, L^3[G(r_o)/E(r,r_o)] = 4\pi(R-r)^2(1-\eta), 2\pi(R-r)(1-\eta), 2(1-\eta) \tag{136}$$

where $1-\eta$ is the volume fraction of surfactant chains in the micelle core. Equation 135 specifies that there are N segments in the surfactant chain while eq 136 states that the concentration of segments (or of solubilizate) in the core of the aggregate is uniform. The three quantities on the right-hand side of eq 136 correspond to spherical, infinite cylindrical, and infinite lamellar aggregates, re-

spectively. The minimization of the deformation free energy eq 134 subject to the constraints eqs 135 and 136 allows the determination of the functional forms of $E(r,r_o)$ and $G(r_o)$, and thus of the minimum value of F for any arbitrary aggregation number. Following the approach of section III, one obtains

$$E(r,r_o) = \pi(r_o^2 - r^2)^{1/2}/2N \quad (137)$$

which coincides with eq 51.

For spherical aggregates

$$G(r) = (8\pi R^2/NL^3)(1-\eta)u[\tanh^{-1}(1-u^2)^{1/2} - (1-u^2)^{1/2}] \quad (138)$$

where u denotes r/R. Introducing eqs 137 and 138 in eq 134, one obtains

$$\frac{F}{kT} = \left(\frac{3\pi^2}{80}\right)\left(\frac{4\pi R^3(1-\eta)}{3NL^3}\right)\left(\frac{R^2}{NL^2}\right) = \left(\frac{3\pi^2}{80}\right)g\left(\frac{R^2}{NL^2}\right) \quad (139)$$

Equation 138 differs from eq 52 by the presence of the factor $1-\eta$. The free energy expression eq 139 formally coincides with eq 53 developed for the solubilizate free micelles. Similar results are obtained for the infinite cylindrical and infinite lamellar aggregates. For infinite cylinders

$$G(r) = (2\pi R/NL^3)(1-\eta)u\tanh^{-1}(1-u^2)^{1/2} \quad (140)$$

and

$$\frac{F}{kT} = \left(\frac{5\pi^2}{80}\right)\left(\frac{\pi R^2(1-\eta)}{NL^3}\right)\left(\frac{R^2}{NL^2}\right) = \left(\frac{5\pi^2}{80}\right)g\left(\frac{R^2}{NL^2}\right) \quad (141)$$

For infinite lamellae

$$G(r) = \frac{2}{NL^3}(1-\eta)\frac{u}{(1-u^2)^{1/2}} \quad (142)$$

and

$$\frac{F}{kT} = \left(\frac{10\pi^2}{80}\right)\left(\frac{2R(1-\eta)}{NL^3}\right)\left(\frac{R^2}{NL^2}\right) = \left(\frac{10\pi^2}{80}\right)g\left(\frac{R^2}{NL^2}\right) \quad (143)$$

One can estimate the chain deformation free energy of the swollen micellar core per surfactant molecule for spheres, cylinders, and lamellae, respectively, from

$$\frac{1}{g}\frac{F}{kT} = \left(\frac{3\pi^2}{80}\right)\left(\frac{R^2}{NL^2}\right), \left(\frac{5\pi^2}{80}\right)\left(\frac{R^2}{NL^2}\right), \left(\frac{10\pi^2}{80}\right)\left(\frac{R^2}{NL^2}\right) \quad (144)$$

By introducing explicitly in the above equation the geometrical packing factor P defined for micelles containing solubilizate, the free energy expressions for the three geometries become practically unified since the numerical values 3, 5, and 10 become $9P$ for spheres, and $10P$ for cylinders as well as lamellae. Consequently, we estimate the contribution of the chain deformation in the aggregate core to the free energy of solubilization in spherical micelles by

$$\frac{(\Delta\mu_g^o)_{def}}{kT} = \frac{9P\pi^2}{80}\frac{R_s^2}{NL^2} \quad (145)$$

the same relation also being employed for globular micelles and for the spherical endcaps of the spherocylinders. The relation valid for infinite cylindrical rods

$$\frac{(\Delta\mu_g^o)_{def}}{kT} = \frac{10P\pi^2}{80}\frac{R_c^2}{NL^2} \quad (146)$$

is employed for the middle cylindrical part of the spherocylinder.

In the case of microemulsion structures, the surfactant tails are in an environment similar to that of swollen spherical micelles when the amount of solubilization is small. When the amount of solubilization is extremely large, the environment of the tails approaches that in swollen lamellar aggregates. Therefore, the coefficient in the expression for the deformation free energy must lie between $9P$ (as for swollen spheres) and $10P$ (as for swollen lamellae). Since the amount of solubilization typically encountered is not too large, we write for microemulsions

$$\frac{(\Delta\mu_g^o)_{def}}{kT} = \frac{9P\pi^2}{80}\frac{R^2}{NL^2} \quad (147)$$

Micelle Core–Water Interfacial Free Energy. The interfacial tension at the aggregate core–water interface σ_{agg} is also affected by the solubilizate. For a uniform distribution of solubilizate with a volume fraction η in the surfactant tail region, the interfacial tension of the aggregate core–water interface may be viewed as that between a solution of surfactant tails and solubilizate on the one hand and water on the other. Interfacial tensions between two solutions can be readily estimated in terms of the interfacial tensions between pure components using the Prigogine theory discussed in section V. Accordingly, the micellar core region is considered to be a solution with a uniform solvent concentration η. Corresponding to this bulk composition, the concentration of solvent in the surface monolayer η^S is determined by the implicit equation

$$\ln\left[\frac{(\eta^S/\eta)^{v_s/v_o}}{(1-\eta^S)/(1-\eta)}\right] = \frac{(\sigma_{sw}-\sigma_{ow})}{kT}v_s^{2/3} + \chi_{os}(3/4)[(1-\eta)-\eta] - \chi_{os}(1/2)[(1-\eta^S)-\eta^S] \quad (148)$$

Here, σ_{sw} is the surfactant tail–water interfacial tension considered in section III while σ_{ow} is the interfacial tension between the solubilizate and water. The parameter χ_{os} denotes the van Laar or the Flory–Huggins-type interaction parameter between the solubilizate and the surfactant tail. Once the surface monolayer composition is obtained by solving eq 148, the interfacial tension σ_{agg} is calculated from the explicit equation

$$\left(\frac{\sigma_{agg}-\sigma_{sw}}{kT}\right)v_s^{2/3} = \ln\left(\frac{1-\eta^S}{1-\eta}\right) + \left(1-\frac{v_s}{v_o}\right)(\eta^S-\eta) + \chi_{os}[{}^1/_2(\eta^S)^2 - {}^3/_4\eta^2] \quad (149)$$

The estimation of the interfacial tension between surfactant tails and water σ_{sw} has already been discussed in section III. The interfacial tension between solubilizate and water σ_{ow} can be expressed in terms of the surface tension σ_o of the solubilizate and the surface tension σ_w of water using the relation[69]

$$\sigma_{ow} = \sigma_o + \sigma_w - 2.0\psi(\sigma_o\sigma_w)^{1/2} \quad (150)$$

The constant ψ depends upon the nature of interactions between the two components[74] and will be close to unity if the types of self-interactions are very similar. For water–alcohol, water–ether, and water–ketone systems, ψ is close to unity. For water–aliphatic hydrocarbons, it is about 0.55, and for water–aromatic hydrocarbons, ψ is approximately 0.71.[74]

When solubilization takes place in surfactants possessing poly(oxyethylene) chains as head groups, the interface is

that between a solution of surfactant tails and solubilizate on the one side and a solution of poly(oxyethylene) head groups and water on the other side. For such a case, the Prigogine theory can be again employed for the calculation of the interfacial tension at the aggregate core. σ_{agg} will now depend upon the four individual interfacial tensions σ_{sw}, σ_{ow}, σ_{sE}, and σ_{oE}, as well as the volume fraction η of the solubilizate in the micelle core and the volume fraction of the poly(oxyethylene) in the micellar shell (ϕ_{Eg} in the case of uniform concentration/nonuniform deformation model and ϕ_R in the case of nonuniform concentration/uniform deformation model). Here, σ_{oE} represents the interfacial tension between the solubilizate and the poly(oxyethylene) head group, while the remaining quantities have already been defined. The method involves computing first the interfacial tension σ_{sEw} between the surfactant tails and a solution of poly(oxyethylene) in water by solving the system of two equations

$$\ln\left[\frac{((\phi^S/\phi_{Eg})^{1/N_E})}{(1-\phi^S)/(1-\phi_{Eg})}\right] = \frac{(\sigma_{sw}-\sigma_{sE})}{kT}\upsilon_s^{2/3} + \chi_{wE}(3/4)[(1-\phi_{Eg})-\phi_{Eg}] - \chi_{wE}(1/2)[(1-\phi^S)-\phi^S] \quad (151)$$

$$\left(\frac{\sigma_{sEw}-\sigma_{sw}}{kT}\right)\upsilon_s^{2/3} = \ln\left(\frac{1-\phi^S}{1-\phi_{Eg}}\right) + \left(\frac{N_E-1}{N_E}\right)(\phi^S - \phi_{Eg}) + \chi_{wE}[{}^1/_2(\phi^S)^2 - {}^3/_4(\phi_{Eg})^2] \quad (152)$$

Similarly, the interfacial tension σ_{oEw} between the solubilizate and a solution of poly(oxyethylene) in water can be estimated by solving the two equations

$$\ln\left[\frac{(\phi^S/\phi_{Eg})^{1/N_E})}{(1-\phi^S)/(1-\phi_{Eg})}\right] = \frac{(\sigma_{ow}-\sigma_{oE})}{kT}\upsilon_s^{2/3} + \chi_{wE}(3/4)[(1-\phi_{Eg})-\phi_{Eg}] - \chi_{wE}(1/2)[(1-\phi^S)-\phi^S] \quad (153)$$

$$\left(\frac{\sigma_{oEw}-\sigma_{ow}}{kT}\right)\upsilon_s^{2/3} = \ln\left(\frac{1-\phi^S}{1-\phi_{Eg}}\right) + \left(\frac{N_E-1}{N_E}\right)(\phi^S - \phi_{Eg}) + \chi_{wE}[{}^1/_2(\phi^S)^2 - {}^3/_4(\phi_{Eg})^2] \quad (154)$$

Finally, the interfacial tension σ_{agg} at the micellar core surface can be estimated using the expressions

$$\ln\left[\frac{(\eta^S/\eta)^{\upsilon_s/\upsilon_o})}{(1-\eta^S)/(1-\eta)}\right] = \frac{(\sigma_{sEw}-\sigma_{oEw})}{kT}\upsilon_s^{2/3} + \chi_{os}(3/4)[(1-\eta)-\eta] - \chi_{os}(1/2)[(1-\eta^S)-\eta^S] \quad (155)$$

$$\left(\frac{\sigma_{agg}-\sigma_{sEw}}{kT}\right)\upsilon_s^{2/3} = \ln\left(\frac{1-\eta^S}{1-\eta}\right) + \left(1-\frac{\upsilon_s}{\upsilon_o}\right)(\eta^S-\eta) + \chi_{os}[{}^1/_2(\eta^S)^2 - {}^3/_4\eta^2] \quad (156)$$

The above two equations are written as for the surface tension of a binary solution whose components (surfactant tail and solubilizate) have the surface tensions of σ_{sEw} and σ_{oEw}, respectively, and a component (solubilizate) volume fraction η. Equations 151–154 have been written for the uniform concentration/nonuniform deformation model of the poly(oxyethylene) head groups. By replacing the volume fraction ϕ_{Eg} (defined by eq 85) in these equations by the volume fraction ϕ_R (defined by eq 108), one can estimate the interfacial tension at the micellar core for the nonuniform concentration/uniform deformation model of the micellar shell.

Head Group Interactions for Poly(oxyethylene) Surfactants. The interactions among poly(oxyethylene) head groups have been modeled in section V by considering the free energy of mixing and the free energy of deformation of the polymeric head group in the shell region of the micellar aggregates and also the steric interactions between the oxyethylene segments at the micellar core surface. All the equations developed in section V for micellization remain valid for solubilization as well. One may note that, for swollen aggregates, the volume of the shell region of the aggregates made up of poly(oxyethylene) chains and water is givenby eqs 81–84 for different geometries. While these equations remain unaltered for solubilization, one has to recognize that the factor V_g/g which appears in these equations is now given by

$$V_g/g = \upsilon_s/(1-\eta) \quad (157)$$

For microemulsion droplets, the volume per molecule in the shell region is given by

$$V_{SH}/g = [\upsilon_s/(1-\eta) + 4\pi(R_s-R)^3/3g][(1+D/R_s)^3 - 1] \quad (158)$$

Using the volume of the shell region estimated from the above equation, the volume fraction ϕ_{Eg} of the poly(oxyethylene) segments in the shell region can be estimated from eq 85.

Surfactant Tail–Solubilizate Mixing Free Energy. The presence of the solubilizate molecules in the surfactant tail region of the aggregates gives rise to a free energy of mixing. In swollen aggregates, all the solubilizate molecules mix with the surfactant tails, while in microemulsions, only the solubilizate molecules in the surfactant tail region mix with the surfactant molecules. The free energy of mixing is written using the Flory–Huggins expression[73] which accounts for both the entropy and the enthalpy of mixing. For a solution containing a mole fraction Z and a volume fraction η of solubilizate, the free energy of mixing per surfactant molecule is given by

$$(\Delta\mu_g^o)_{mix}/kT = [\ln(1-\eta) + [Z/(1-Z)]\ln\eta] + [\chi_{os}(\upsilon_s/\upsilon_o)\eta] \quad (159)$$

In the above expression, the first term represents the entropy of mixing and the second term represents the enthalpy of mixing written in the van Laar form as used by Flory and Huggins.

Table II. Molecular Properties of Solubilizates

solubilizate	X_{lo}	υ_o, Å^3	σ_{ow}, dyn/cm	δ_o, MPa$^{1/2}$	χ_{os}
benzene	4.3×10^{-4}	146	33.9	18.7	0.128
toluene	1.1×10^{-4}	176	36.1	18.3	0.096
cyclohexane	1.7×10^{-5}	179	50.2	16.8	0.0
n-hexane	2.2×10^{-6}	217	50.5	14.9	0.19
n-decane	5.6×10^{-9}	323	51.9	15.8	0.079

IX. Predictions of the Solubilization Model

Properties of Solubilizates. For illustrative purposes, the solubilization behavior in ionic and nonionic micelles is computed for benzene, toluene, hexane, decane, and cyclohexane as solubilizates. In this manner, one can investigate the effects of molecular size, aromaticity, and interfacial activity, as well as the interaction parameter of solubilizate on solubilization in micellar solutions. The relevant physical properties of the solubilizates are listed in Table II. All the physical properties listed are estimated at 25 °C. The molecular volumes have been calculated using liquid density data,[72] and the solubility data have been obtained from refs 70–72 and 124, the surface tension data from refs 74–76, and the solubility parameters from

(124) *American Petroleum Institute Technical Data Book*; American Petroleum Institute: Washington, DC, 1979.

ref 109. Concerning the solubility parameters listed in the table, it is worth noting that several compilations are available in the literature[109] and that they recommend different solubility parameter values for aromatic hydrocarbons. As noted in the *Handbook of Solubility Parameters*,[109] as long as the solubility parameters are taken from a single compilation and the mutual interaction energies are computed in a consistent way, equivalent results will be obtained regardless of the compilation selected. The interaction parameters for solubilizate (o)–surfactant tail (s) interactions are calculated using the expression

$$\chi_{os} = v_o(\delta_o - \delta_s)^2/kT \qquad (160)$$

where δ_o and δ_s represent the solubility parameters of the solubilizate and surfactant tail, respectively. The solubility parameter for the dodecyl hydrocarbon tail of the surfactant is estimated (in SI units) to be 16.8 $MPa^{1/2}$.[109]

Computational Approach. The equilibrium characteristics of the aggregates that incorporate solubilizates are obtained in a way similar to that described in sections IV and VI. As noted earlier, for the swollen spherical and globular aggregates as well as for microemulsions, the equilibrium characteristics are those corresponding to an aggregate for which the concentration X_g is a maximum because the dispersion in sizes is small. However, for swollen spherocylindrical aggregates, the dispersion of sizes is large and therefore the average aggregation number must be calculated on the basis of the entire size distribution. The parameters characterizing the size distribution are obtained from the minimum in the standard chemical potential per surfactant molecule for the infinite cylinders and for the endcaps of spherocylinders.

Consequently, for ionic surfactants that generate swollen spherical or globular aggregates, the aggregation number g and the mole fraction Z of the solubilizate in the aggregate are determined from the condition of maximum of X_g with respect to these two independent variables. For microemulsions, the maximization of X_g is carried out with respect to the overall radius R_s of the sphere, the thickness R of the surfactant tail region, and the mole fraction Z of the solubilizate in the surfactant tail region. In the case of swollen spherocylinders, the standard chemical potential difference $\Delta\mu^o_{cyl}$ of the cylindrical middle part is minimized with respect to the radius R_c and the mole fraction Z_{cyl} of solubilizate, while the standard chemical potential difference $\Delta\mu^o_{cap}$ of the endcaps is minimized with respect to the aggregation number g_{cap} of the endcaps as well as the mole fraction Z_{cap} of the solubilizate. Thus, in the case of ionic surfactants, there are two independent variables for swollen spherical, globular, and spherocylindrical aggregates and three independent variables for microemulsions. For surfactants with poly(oxyethylene) head groups, yet another independent variable is involved in the optimization, namely, the thickness D of the micellar shell region that contains the poly(oxyethylene) segments and water. All the optimization problems involving the search for two, three, or four parameters have been performed using the subroutine ZXMWD referred to earlier.

Solubilization in Ionic Surfactant Solutions. The solubilization of the hydrocarbons listed in Table II in solutions of the ionic surfactant sodium dodecyl sulfate has been calculated for 25 °C. The results reveal that the microemulsion structure is preferred to the swollen aggregate. This result differs from that obtained in our earlier treatment[52,53] where we found that the swollen aggregate is the preferred shape. The preference for the microemulsion structure predicted by the present model can be traced to the inclusion of the shape- and size-dependent surfactant tail deformation free energy. This free energy contribution was assumed independent of size in our earlier treatment and thus had no effect on the characteristics of the aggregate. In contrast, the inclusion of the shape- and size-dependent deformation free energy favors the microemulsion structure because the surfactant tails are not forced to become fully stretched.

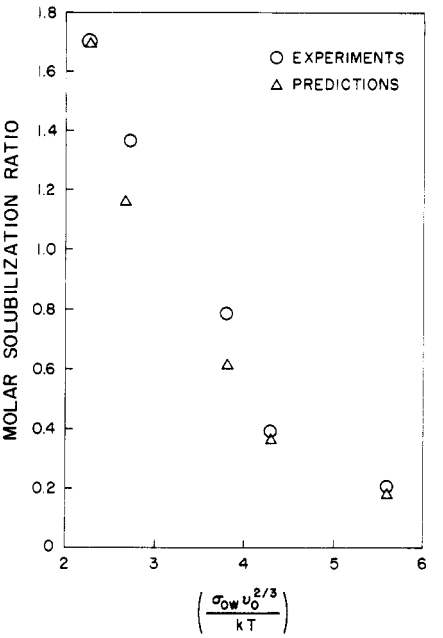

Figure 22. Molar solubilization ratio of hydrocarbons in 0.1 M solutions of sodium dodecyl sulfate at 25 °C, plotted as a function of the volume–polarity parameter (see text for discussion about its significance). The experimental data are shown by circles while predictions of the model for the five solubilizates are identified by triangles.

The calculated molar solubilization ratio and the measured molar solubilization ratio[123] are both correlated against the parameter $\sigma_{ow}v_o^{2/3}/kT$ in Figure 22. This parameter was suggested in our earlier work[123] as an indicator for the polarity and the molecular size of the solubilizate. The importance of these two variables is obvious from the present theory in which the free energy contributions associated with the presence of the solubilizate are dependent on these two variables. The smaller the molecular volume and the larger the interfacial activity (indicated by a smaller value for σ_{ow}), the smaller is the volume–polarity parameter and the larger the molar solubilization ratio. The agreement between the molar solubilization ratios measured at 0.1 M solutions of sodium dodecyl sulfate and the present predictions is reasonably good.

The predicted critical micelle concentrations are plotted in Figure 23 for the solubilization of the five hydrocarbons. The cmc values have been normalized with respect to the predicted cmc in the absence of solubilizate. The aggregation number for microemulsions (namely, the number of constituent surfactant molecules) normalized with respect to the aggregation number of the solubilizate free micelle is also included in the figure. The molecular volume–polarity parameter has been used in this plot as well, as the correlating variable. Qualitatively, one finds that the depression in cmc is larger and the relative aggregation number increases as the volume–polarity parameter decreases. Detailed experimental measurements of the changes in cmc and aggregation number in the presence of solubilizates are not available in the literature for a more systematic comparison to be made.

The present model predicts a small increase in the molar solubilization ratio with an increase in the total surfac-

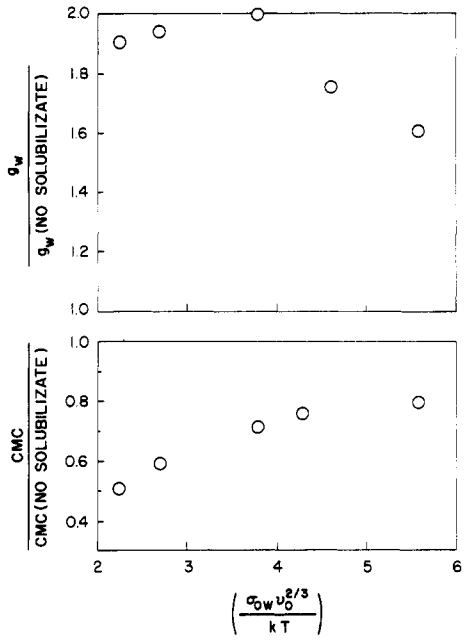

Figure 23. Dependence of the cmc and the average aggregation number (at 0.1 M surfactant concentration) of sodium dodecyl sulfate aggregates at 25 °C on the volume–polarity parameter of the solubilizates. The values of cmc and the aggregation numbers are shown in normalized form with respect to the soluibilizate free system. All the points represent calculated values.

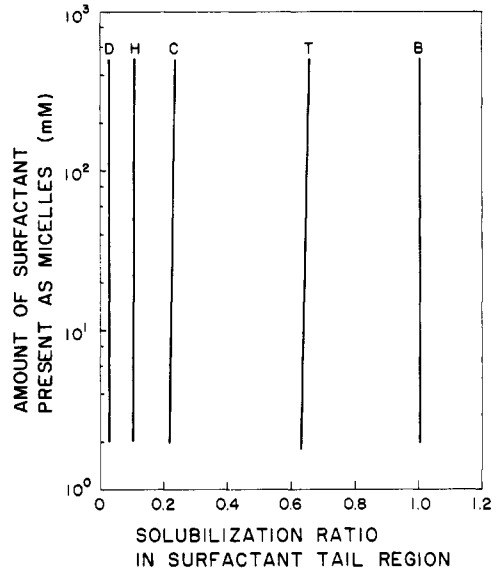

Figure 24. Dependence of molar solubilization ratio in the surfactant tail region of microemulsion aggregates on the concentration of sodium dodecyl sulfate present in aggregated form. All five lines corresponding to the labeled solubilizates (D, decane; H, hexane; C, cyclohexane; T, toluene; B, benzene) represent the predictions of the present theory.

tant concentration. This can be seen from Figures 24 and 25 where the two contributions to the total molar solubilization ratio (one from the surfactant tail region of the microemulsions and the other from the core of the microemulsion) are plotted. Figure 24 shows how the calculated molar solubilization ratio in the surfactant tail region depends on surfactant concentration for all five solubilizates. Figure 25 presents the calculated molar solubilization ratio in the core region of the microemulsion for the same solubilizates.

In our earlier treatment of solubilization,[52,53] the molar solubilization ratio was found to be practically independent of the surfactant concentration as long as the concentration was not very close to the cmc. This result is explained by

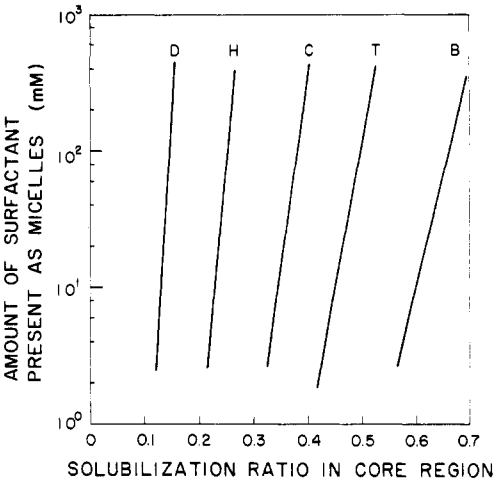

Figure 25. Dependence of molar solubilization ratio in the core region of microemulsion aggregates on the concentration of sodium dodecyl sulfate present in aggregated form. All five lines corresponding to the labeled solubilizates (D, decane; H, hexane, C, cyclohexane; T, toluene; B, benzene) represent the predictions of the present theory.

the observation from Figure 24 that the contribution to the molar solubilization ratio from the surfactant tail region is practically independent of surfactant concentration. In our earlier treatment the swollen aggregates were preferred and hence the surfactant tail region covered the entire volume of the aggregate. Thus, the predicted small dependence of $(j/g)_{avg}$ on the total surfactant concentration noted in this paper (which is, however, greater than that predicted by our previous model) arises entirely because the solubilization occurs also in the core region of the microemulsion (Figure 25). Thus, the concentration dependence of the molar solubilization ratio predicted in the present model is a consequence of the preference for the microemulsion structure.

The calculated results in Figures 24 and 25 also show that it is important to account for the presence of the solubilizate in the surfactant tail region in any quantitative model of microemulsions. Indeed, the penetration of the solubilizate in the surfactant tail region is significant when the molecular size of the solubilizate is small and some polarity is associated with the solubilizate. The ratio of the molar solubilization ratio in the surfactant tail region to the total molar solubilization ratio is found to be 0.17 for decane, 0.3 for hexane, 0.38 for cyclohexane, 0.56 for toluene, and 0.61 for benzene in 0.1 M sodium dodecyl sulfate micellar solutions.

Solubilization in Micelles of Poly(oxyethylene) Surfactants. The solubilization behavior of the five solubilizates listed in Table II has been calculated for solutions of a nonionic surfactant having a dodecyl hydrocarbon tail and a head group containing 23 oxyethylene units. The calculations are based on both the uniform concentration/nonuniform deformation model and the uniform deformation/nonuniform concentration model for the micellar shell region described earlier in section V. Both measured[125] and predicted molar solubilization ratios in a solution of nonionic surfactant with 20 wt % surfactant are presented in Table III for all the solubilizates. Included in the table are the calculated molar solubilization ratios for two assumed values of the poly(oxyethylene)–water interaction parameter.

In solubilizate free systems examined in section VI, it was found that the uniform deformation/nonuniform

(125) Barry, M. Solubilizate and Surfactant Structural Effects on Single Component and Binary Solubilization. M.S. Thesis, Department of Chemical Engineering, The Pennsylvania State University, University Park, PA, 1986.

Table III. Predicted Molar Solubilization Ratios in Nonionic Micelle[a]

solubilizate	experiment	$\chi_{wE} = 0.1$	$\chi_{wE} = 0.2$	$\chi_{wE} = 0.3$
Uniform Concentration/Nonuniform Deformation Model				
benzene	3.47	1.55	1.93	2.84
toluene	2.03	1.16	1.47	2.21
cyclohexane	1.04	0.52	0.68	1.00
n-hexane	0.62	0.32	0.43	0.66
n-decane	0.21	0.16	0.18	0.29
Nonuniform Concentration/Uniform Deformation Model				
benzene	3.47	1.49	1.74	2.27
toluene	2.03	1.08	1.26	1.69
cyclohexane	1.04	0.52	0.67	0.97
n-hexane	0.62	0.32	0.36	0.62
n-decane	0.21	0.14	0.18	0.28

[a] 20 wt % solution of $C_{12}E_{23}$ at 25 °C.

concentration model showed somewhat better agreement with experimentally determined cmc, aggregation number, and micellar shell thickness. The calculated molar solubilization ratios based on this model are in reasonable agreement with measurements for decane, hexane, and cyclohexane but are smaller than the measured values for benzene and toluene. The significant discrepency for benzene and toluene can be readily explained by the fact that aromatic solubilizates have very good compatibility with poly(oxyethylene) and hence could also be solubilized in the shell region of the micelle.[126] Since the present model does not consider any solubilization in the shell region, it is natural to underpredict the measurements. The uniform concentration/nonuniform deformation model predicts larger molar solubilization ratios in better agreement with experiments. Nevertheless, this model provides somewhat poorer agreement with the other measured micellar properties as discussed in section VI.

The calculations show that larger values for the molar solubilization ratios are predicted when the poly(oxyethylene)–water interaction parameter is larger. This implies that an increase in temperature (which increases the magnitude of the interaction parameter) will cause an increase in the amount solubilized. This is qualitatively consistent with experimental data.[126]

Solubilization-Induced Rod to Sphere Transition. For the surfactants examined until now, calculations show that small spherical or globular micelles of solubilizate free systems transform into microemulsions in the presence of solubilizates. It is of interest to investigate what will be the predicted change in spherocylindrical micelles as a result of solubilization. Hoffmann et al.[127,128] noted a transition from spherocylinders to spheres by solubilizing hydrocarbons in a solution of the cationic surfactant tetradecyltrimethylammonium bromide ((TTA)Br) in the presence of sodium salicylate (NaSal) as electrolyte. They observed an initial growth in the size of the swollen spherocylindrical aggregates when toluene was solubilized before the eventual transition to spherical aggregates at larger solubilizate concentrations. In contrast, when decane was solubilized, the transition to spheres occurred at very low amounts of solubilizates and the spherical aggregates grew in size with increasing solubilizate concentration.

For illustrative purposes, we have carried out calculations for the solubilization of benzene and decane in solutions of sodium dodecyl sulfate at an added electrolyte (NaCl) concentration of 0.6 M. The micellar characteristics have been predicted in section IV for such conditions, and it was found that large polydispersed spherocylindrical micelles form. The sphere to rod transition parameter K was predicted to be $K = 1.04 \times 10^8$. Here, the aggregate characteristics are computed as a function of the amount of solubilizate present from a value of 0 to the maximum possible molar solubilization ratio. The total concentration of surfactant is kept constant at 0.1 M. For various values of the molar solubilization ratio below the maximum possible value, the concentration of the singly dispersed surfactant in solution is calculated assuming either swollen spherocylindrical aggregates or spherical microemulsions in solution. Obviously, the shape for which the concentration of the singly dispersed surfactant is smaller is the preferred aggregate shape because the free energy of the system is the smallest.

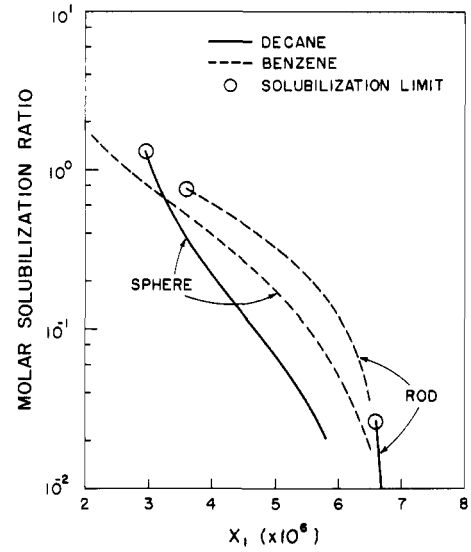

Figure 26. Calculated concentration of the singly dispersed surfactant as a function of the molar solubilization ratio in a solution containing 0.1 M sodium dodecyl sulfate and 0.6 M NaCl. Spheres refer to microemulsions, and rods refer to swollen spherocylindrical aggregates. The points indicate maximum possible molar solubilization ratios.

Figure 26 shows the equilibrium concentrations of the singly dispersed surfactant when different amounts of benzene or decane are incorporated into the aggregates. The surfactant solution saturated with the solubilizate is indicated by a point (the saturation condition for benzene solubilized in spherical structures falls outside the diagram and hence is not shown). The calculations show that, at any molar solubilization ratio of both benzene and decane, the monomer concentration X_1 is substantially lower when spherical microemulsions form. Thus, in all cases, the spherical microemulsions are favored over the swollen rods. Indeed, the predictions suggest that rodlike micelles are transformed into spherical microemulsions even when only a small amount of solubilizate is introduced.

The radius R_s of the hydrophobic core of the microemulsion is plotted in Figure 27 for the solubilization of benzene and decane in a 0.1 M solution of sodium dodecyl sulfate containing 0.6 M NaCl. In the absence of any solubilizate in this surfactant system, the hydrodynamic radius of the hydrophobic core of the spherocylindrical micelle calculated from

$$R_h = (3V_g/4\pi)^{1/3} \qquad (161)$$

is 43 Å. From the calculated results in Figure 27 one can see that the hydrodynamic radius sharply decreases to 21 Å at low concentrations of solubilizates; this corresponds to a rod to sphere transition. With subsequent addition

(126) Mackay, R. A. In *Nonionic Surfactants*; Schick, M. J., Ed.; Marcel Dekker: New York, 1987.
(127) Bayer, O.; Hoffman, H.; Ulbricht, W.; Thurn, H. *Adv. Colloid Interface Sci.* **1986**, *26*, 177.
(128) Hoffmann, H.; Ulbricht, W. *J. Colloid Interface Sci.* **1989**, *129*, 388.

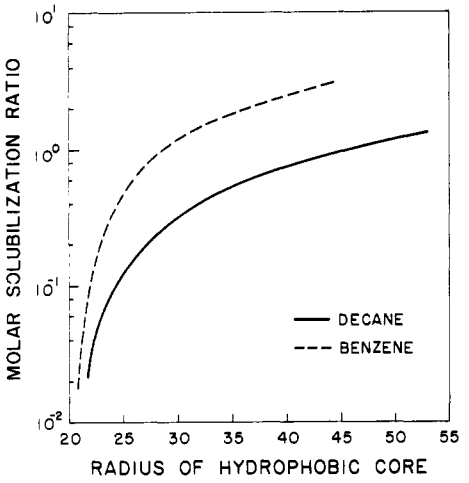

Figure 27. Calculated radius of the hydrophobic core of microemulsions in a solution containing 0.1 M sodium dodecyl sulfate and 0.6 M NaCl. The hydrodynamic radius is 43 Å when the molar solubilization ratio is zero. The radius of 21 Å calculated at low molar solubilization ratios indicates the transition of solubilizate free rods to spheres.

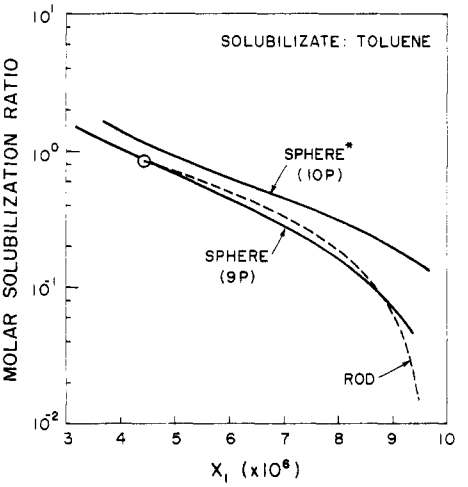

Figure 28. Calculated concentration of the monomeric surfactant as a function of the molar solubilization ratio for toluene in a solution containing 10 mM TTASal. Spheres refer to microemulsions, and rods refer to swollen spherocylindrical aggregates. The point indicates the maximum possible molar solubilization ratio. The sphere with an asterisk refers to calculated results when the factor $9P$ in eq 147 is replaced by $10P$. See text for discussion.

of solubilizate, the microemulsion aggregate grows in size. For both aromatic and aliphatic solubilizates, essentially the same trend is predicted. The preference for the microemulsion structure over that of swollen spherocylindrical aggregates is a consequent of the smaller interfacial free energy and surfactant tail deformation free energy (both expressed per surfactant molecule) in a microemulsion structure. The larger size of the microemulsion aggregate containing benzene than that containing decane predicted here can be principally attributed to the lower interfacial tension of benzene.

To explore the Hoffmann effect wherein micelles remain rodlike on the addition of solubilizates before eventually transforming into spheres, calculations have been carried out for the surfactant system employed in his experimental study.[127,128] The solution contained equimolar amounts (10 mM) of the cationic surfactant tetradecyltrimethylammonium bromide ((TTA)Br) and the electrolyte sodium salicylate (NaSal). The salicylate counterion is very hydrophobic, and hence, one may expect that it is strongly adsorbed at the micellar surface. Thus, this surfactant system can be visualized for all practical purposes not as ionic but as zwitterionic tetradecyltrimethylammonium salicylate (TTASal). Therefore, in the present calculations, the surfactant is considered to be zwitterionic with a dipole length d estimated from atomic dimensions of approximately 3 Å. Further, the area of the head group a_p is estimated to be 35 Å^2, and therefore, the area of the micellar core shielded from water is taken to be a_o = 21 Å^2.

The concentrations of the singly dispersed surfactant for different amounts of toluene solubilized in a 10 mM solution of TTASal are calculated assuming spherical microemulsion and swollen rod structures, and the results are presented in Figure 28. The calculated results show that, at molar solubilization ratios below 0.1, the monomer concentration is smaller for rodlike micelles than for microemulsions. Therefore, the initial addition of toluene to the surfactant solution does not cause a change in the shape of the aggregate, and swollen rodlike aggregates persist in solution. For molar solubilization ratios greater than 0.1, the monomer concentration is smaller for spherical microemulsions than for swollen rods. Hence, the addition of toluene above the molar solubilization ratio of 0.1 gives rise to the transition from swollen rods to spherical microemulsions. At yet larger molar solubilization ratio, closer to the maximum value possible for swollen rodlike structures, the monomer concentrations are comparable whether rodlike aggregates or spherical microemulsions form. Under such conditions, one expects both structures to coexist. The region of coacervation experimentally observed by Hoffmann et al.[128] may correspond to such a situation. At higher molar solubilization ratios (above the maximum for rodlike micelles), only spherical microemulsions are present. All these predictions are in qualitative agreement with the experimental results[128] obtained by Hoffmann. More detailed considerations regarding the hydrophobic salicylate counterion and its effects are necessary before quantitative comparisons can be made.

A comparison between the calculated results plotted in Figure 28 for TTASal with those in Figure 26 for sodium dodecyl sulfate is instructive. The monomer concentrations corresponding to spherical and rodlike shapes are quite close to one another in the case of TTASal when compared to the case of SDS. This suggests that small alterations in the standard free energy changes for either of the two aggregate shapes may favor rodlike aggregates over spherical microemulsions in the case of TTASal. To examine this, calculations have been repeated for a marginally different estimate of the surfactant tail deformation energy in the microemulsion. As noted earlier in the derivation of the tail deformation energy for the microemulsion structure, the coefficient in eq 147 must lie between $9P$ (as for swollen spheres, when the amount of solubilization is small) and $10P$ (as for swollen lamellae, when the amount of solubilization is very large), where P is the packing factor. Since the molar solubilization ratios in various systems considered in this study are small, the value of $9P$ is more suitable and hence has been used in the calculations. To examine the effect of an increase in the coefficient from the value of $9P$, calculated results for spherical microemulsions are presented in Figure 28 also using the value of $10P$ for the coefficient in eq 147. One can notice from the figure the qualitative change in predictions arising because of this modification. The calculations show that the monomer concentration is smaller when swollen rods are formed rather than spherical microemulsions. Consequently, up to a molar solubilization ratio of 0.83 (corresponding to the maximum possible value for rods in this system), swollen rodlike

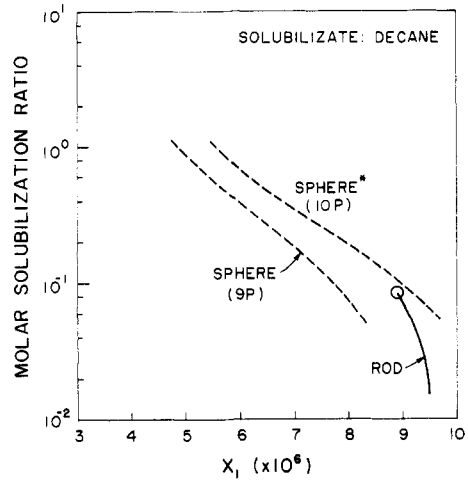

Figure 29. Calculated concentration of the monomeric surfactant as a function of the molar solubilization ratio for decane in a solution containing 10 mM TTASal. Spheres refer to microemulsions while rods refer to swollen spherocylindrical aggregates. The point indicates the maximum possible molar solubilization ratio. The sphere with an asterisk refers to results obtained when the factor $9P$ in eq 147 is replaced by $10P$. See text for discussion.

aggregates persist in the solution. Only on the addition of further toluene to the surfactant solution, spherical microemulsions are generated. In contrast, the calculations based on the value of $9P$ in eq 147 indicate that swollen rods will persist only up to a molar solubilization ratio of 0.1 for toluene. On further addition of toluene, transition to spheres occurs. Thus, the actual solubilization behavior may span the range predicted for the two different free energy estimates chosen for illustrative purposes.

Figure 29 presents the calculated results when decane is solubilized in TTASal. In this case, the monomer concentration is smaller when spherical structures rather than swollen rods form. This is similar to the behavior observed with toluene as solubilizate. When the free energy of the surfactant tail deformation is slightly increased in spherical microemulsions (by making the coefficient in eq 147 $10P$ in place of $9P$), the monomer concentration becomes smaller for swollen rods than for microemulsions. This behavior is also similar to that observed in Figure 28 for the solubilization of toluene. However, the results for the two solubilizates differ in the maximum amount of solubilization possible in swollen rodlike aggregates. For decane, the maximum possible molar solubilization ratio in swollen rods is 0.083 while for toluene it is 0.83. Consequently, even when swollen rods are favored (calculations using $10P$ in eq 147), the swollen rods can persist only up to a molar solubilization ratio of 0.083 for decane and further addition of decane causes the transition from swollen rods to spherical microemulsions. In contrast, for toluene the swollen rods will persist up to a molar solubilization ratio of 0.83 before the transition to spheres will occur. These calculated results, which emphasize the different behaviors of toluene and decane regarding the transition from swollen rods to spheres, are in qualitative agreement with the results of Hoffmann et al.[127,128]

X. Solubilization of Binary Hydrocarbon Mixtures

On the basis of model calculations carried out earlier for the solubilization of binary hydrocarbon mixtures,[51] we had proposed the utilization of solubilization to carry out chemical separations. The calculations showed that when mixtures of benzene and hexane were dissolved in micellar solutions, benzene was selectively solubilized. The predictions based on model simulations were confirmed by our experiments which demonstrated that indeed selective solubilization occurs.[52,53] This feature of micellar systems has since been exploited in a number of investigations focusing on chemical separations.[129] Here, we present a quantitative model for the solubilization of binary mixtures of solubilizates by extending the treatment described in sections VII and VIII for a single solubilizate.

Thermodynamics of Solubilization of Binary Mixtures. The surfactant solution consists of singly dispersed surfactant molecules, singly dispersed solubilizates (designated A and B), surfactant aggregates containing both solubilizates (A and B), and the solvent water. At equilibrium, the condition of minimum total Gibbs free energy leads to an equation for the size distribution of aggregates in solution. Here by size, we imply variations in the numbers of surfactant, solubilizate A, and solubilizate B molecules in the aggregates. The size distribution expression is a simple extension of eq 126 for a single solubilizate and has the form

$$X_g = X_1^g X_{1oA}^{j_A} X_{1oB}^{j_B} \exp\left(-\frac{\mu_{gj}^\circ - g\mu_1^\circ - j_A\mu_{1oA}^\circ - j_B\mu_{1oB}^\circ}{kT}\right) \quad (162)$$

Here, X_{1oA} and X_{1oB} refer to the concentrations of the singly dispersed solubilizate molecules A and B in the aqueous phase, while μ_{1oA}° and μ_{1oB}° refer to their standard chemical potentials corresponding to the infinitely dilute reference state. The standard chemical potential μ_{gj}° refers to an aggregate containing g surfactants, j_A solubilizates of type A, and j_B solubilizates of type B, j denoting the sum $j_A + j_B$.

As for single component solubilization, we will focus on the determination of the maximum amount of solubilization possible in the micellar solution. Such a situation is achieved when the aqueous surfactant phase is in equilibrium with the bulk solubilizate phase. Let ϕ_A and ϕ_B denote the volume fractions of solubilizates A and B in the bulk solubilizate phase. Since this phase is in equilibrium with the aqueous phase, one can determine the concentrations of the singly dispersed solubilizate molecules in the aqueous phase from the condition of equilibrium (similar to eq 127 for single solubilizate):

$$\mu_{1oA}^\circ + kT \ln X_{1oA}^* = \mu_{oA}^H + kT \ln a_A \quad (163)$$

$$\mu_{1oB}^\circ + kT \ln X_{1oB}^* = \mu_{oB}^H + kT \ln a_B \quad (164)$$

Here, μ_{oA}^H and μ_{oB}^H are the standard chemical potentials of A and B defined using the pure components (A or B) as the reference states while a_A and a_B are the activities of A and B in the solubilizate phase. The activities can be written using the Flory–Huggins equation:

$$\ln a_A = [\ln \phi_A + (1 - v_{oA}/v_{oB})\phi_B + \chi_{AB}\phi_B^2] \quad (165)$$

$$\ln a_B = [\ln \phi_B + (1 - v_{oB}/v_{oA})\phi_A + \chi_{BA}\phi_A^2] \quad (166)$$

The interaction parameters χ_{AB} and χ_{BA} are related to one another via the respective molecular volumes v_{oA} and v_{oB}:

$$\chi_{AB}/v_{oA} = \chi_{BA}/v_{oB} \quad (167)$$

Introducing eqs 163 and 164 in the size distribution relation

(129) Scamehorn, J. F., Harwell, J. H., Eds. *Surfactant Based Separation Processes*; Marcel Dekker: New York, 1988.

eq 162, one can rewrite the size distribution of aggregates in a form similar to eqs 2 and 129.

$$X_g = X_1^g \exp(-g\Delta\tilde{\mu}_g^\circ/kT) \quad (168)$$

where

$$\frac{\Delta\tilde{\mu}_g^\circ}{kT} = \frac{\Delta\mu_g^\circ}{kT} - \frac{j_A}{g}\ln a_A - \frac{j_B}{g}\ln a_B \quad (169)$$

and

$$\Delta\mu_g^\circ = \frac{\mu_{gj}^\circ}{g} - \mu_1^\circ - \frac{j_A}{g}\mu_{oA}^H - \frac{j_B}{g}\mu_{oB}^H \quad (170)$$

The free energy difference $\Delta\mu_g^\circ$ represents the difference between the standard chemical potential per surfactant molecule between an aggregate containing g surfactant and j_A and j_B solubilizate molecules of kind A and B on one hand and a singly dispersed surfactant in water, j_A/g molecules of solubilizate A, and j_B/g molecules of solubilizate B, the latter two in their pure phases, on the other hand.

The number and the weight average aggregation numbers can be calculated from the aggregate size distribution as before using eq 3, while the average molar ratio of the solubilizate to the surfactant is calculated from

$$\left(\frac{j_A}{g}\right)_{avg} = \frac{\sum j_A X_g}{\sum g X_g} \qquad \left(\frac{j_B}{g}\right)_{avg} = \frac{\sum j_B X_g}{\sum g X_g} \quad (171)$$

The summations in the above equation as well as the summations while employing eq 3 are now to be carried out over all allowed values of g, j_A, and j_B.

Solubilization in Spherocylindrical Aggregates. The size distribution equation for aggregates containing two solubilizates (eq 168) is formally identical to the size distribution in the absence of solubilizates (eq 2). Consequently, the formation of swollen spherocylindrical micelles can be analyzed by using the equations in section II, developed for aggregates in the absence of solubilizates. Specifically, we can calculate the sphere to rod transition parameter K and the parameter Y using eq 12, the cmc from eq 18, the aggregate size distribution from eq 13, the average aggregation numbers from eq 17, and the total surfactant concentration from eq 16.

Geometrical Characterization of the Aggregates. The swollen spherical, globular, and spherocylindrical aggregates contain the two solubilizates A and B in the surfactant tail region. The aggregates with a microemulsion structure incorporate the solubilizates both in the surfactant tail region of the aggregate and in a domain made up only of the solubilizate phase. We denote by Z_A and Z_B the mole fractions of the solubilizates A and B in the surfactant tail region. The corresponding volume fractions are denoted by η_A and η_B. These volume fractions are related to the mole fractions by the equations

$$\eta_A = \frac{Z_A v_{oA}}{(Z_A v_{oA} + Z_B v_{oB} + (1 - Z_A - Z_B)v_s)} \quad (172)$$

$$\eta_B = \frac{Z_B v_{oB}}{(Z_A v_{oA} + Z_B v_{oB} + (1 - Z_A - Z_B)v_s)} \quad (173)$$

The total mole fraction of the solubilizates Z is the sum $Z_A + Z_B$ while the total volume fraction of the solubilizates η is the sum $\eta_A + \eta_B$, both for the region of the surfactant tails. The aggregate geometrical properties are given by expressions summarized in section VII for a single solubilizate, with the difference that now η accounts for the sum of the volume fractions of the two solubilizates.

The molar ratio of the solubilizate to the surfactant is readily obtained for each solubilizate from

$$(j_A/g)_{avg} = Z_A/(1 - Z) \qquad (j_B/g)_{avg} = Z_B/(1 - Z) \quad (174)$$

for swollen spherical and globular aggregates. For swollen spherocylindrical aggregates, the solubilizates A and B are allowed to be distributed differently in the cylindrical middle portion and the spherical endcaps of the aggregate. For these aggregates

$$\left(\frac{j_A}{g}\right)_{avg} = \left(\frac{Z_A}{1 - Z}\right)_{cyl} + \frac{g_{cap}}{g_n}\left(\frac{Z_A}{1 - Z}\right)_{cap} \quad (175)$$

$$\left(\frac{j_B}{g}\right)_{avg} = \left(\frac{Z_B}{1 - Z}\right)_{cyl} + \frac{g_{cap}}{g_n}\left(\frac{Z_B}{1 - Z}\right)_{cap} \quad (176)$$

For the microemulsion structure, the surfactant free domain of solubilizate in the interior of the aggregate has the same composition as the bulk solubilizate phase with which the aqueous phase is in equilibrium. The compositions in the surfactant tail region of the microemulsion have been defined using the variables also employed in defining the composition of the swollen aggregates. Therefore, for the microemulsion, the overall molar solubilization ratio is found by adding the contributions from the surfactant tail region and from the surfactant free solubilizate domain. The resulting equation for the molar solubilization ratio constitutes a generalization of eq 125:

$$\left(\frac{j_A}{g}\right)_{avg} = \left(\frac{Z_A}{1 - Z}\right) + \frac{1}{g}\frac{4\pi(R_s - R)^3}{3}\frac{\phi_A}{v_{oA}} \quad (177)$$

$$\left(\frac{j_B}{g}\right)_{avg} = \left(\frac{Z_B}{1 - Z}\right) + \frac{1}{g}\frac{4\pi(R_s - R)^3}{3}\frac{\phi_B}{v_{oB}} \quad (178)$$

Free Energy of Solubilization of Binary Mixtures. The standard free energy difference associated with solubilization $\Delta\mu_g^\circ$ is the sum of various contributions that have already been identified in eq 133 while considering aggregates containing one solubilizate. All the free energy contributions discussed in section VII under solubilization of single components remain valid in the present case, with only minor modifications to account for the presence of both solubilizates. Only the modifications are examined in this section.

Deformation Free Energy of Surfactant Tail. The deformation free energy of the surfactant tail can be calculated from eqs 145–147 for the various aggregate structures. The packing factor P appearing in these expressions is now affected by the presence of the solubilizates as can be seen from eqs 117, 118, and 124. The packing factor is modified to account for the presence of two solubilizates A and B by simply defining η as $\eta = \eta_A + \eta_B$.

Aggregate–Water Interfacial Energy. The free energy of formation of the aggregate–water interface is written as the product of an interfacial area and the interfacial tension of this interface. For the case of a single solubilizate, this interfacial tension was written using the Prigogine theory (eqs 148 and 149). For the present situation, the interfacial tension should account for both components A and B. The two solubilizates considered are benzene and hexane. The aliphatic hexane has an interfacial tension with water that is practically identical to the interfacial tension of the surfactant tail with water.

Therefore, the interfacial tension of the aggregate interface can be estimated using the Prigogine model by accounting for the interfacial tension variations due to the presence of benzene whose interfacial tension with water is quite different. With η_B denoting the volume fraction of benzene in the surfactant tail region of the aggregate, one can find the surface monolayer composition η_B^S of benzene from the implicit equation

$$\ln\left[\frac{(\eta_B^S/\eta_B)^{v_s/v_{oB}})}{(1-\eta_B^S)/(1-\eta_B)}\right] = \frac{(\sigma_{sw}-\sigma_{oBw})}{kT}v_s^{2/3} + \chi_{oBs}(3/4)[(1-\eta_B)-\eta_B] - \chi_{oBs}(1/2)[(1-\eta_B^S)-\eta_B^S] \quad (179)$$

Here, σ_{sw} is the surfactant tail–water interfacial tension considered in section III while σ_{oBw} is the interfacial tension between the solubilizate B and water. The parameter χ_{oBs} denotes the Flory–Huggins-type interaction parameter between the solubilizate B and the surfactant tail. Once the surface monolayer composition is obtained by solving eq 179, the interfacial tension σ_{agg} is calculated from the explicit equation

$$\left(\frac{\sigma_{agg}-\sigma_{sw}}{kT}\right)v_s^{2/3} = \ln\left(\frac{1-\eta_B^S}{1-\eta_B}\right) + \left(1-\frac{v_s}{v_{oB}}\right)(\eta_B^S-\eta_B) + \chi_{oBs}[^1/_2(\eta_B^S)^2 - {}^3/_4(\eta_B)^2] \quad (180)$$

Surfactant Tail–Solubilizate Mixing Free Energy. For a single solubilizate, the free energy of mixing of the solubilizate and the surfactant tails in the surfactant tail region of the aggregates was calculated using eq 159. This expression is based on the Flory–Huggins model for the mixing of two components and thus accounts for both molecular size differences of the components and the interaction energies. This expression can be readily generalized to the case of two solubilizates. One obtains

$$\frac{(\Delta\mu_g^o)_{mix}}{kT} = \left[\ln(1-\eta) + \left(\frac{Z_A}{1-Z}\right)\ln\eta_A + \left(\frac{Z_B}{1-Z}\right)\ln\eta_B\right] + \left[\chi_{oAs}\frac{v_s}{v_{oA}}\eta_A + \chi_{oBs}\frac{v_s}{v_{oB}}\eta_B + \chi_{AB}\frac{v_s}{v_{oA}}\eta_A\eta_B\right] \quad (181)$$

In this expression, the first term stands for the entropy of mixing and the second term for the enthalpy of mixing, both referring to a ternary system consisting of the surfactant tail and the solubilizates A and B. In the above equation, χ_{oAs} and χ_{oBs} are the solubilizate A–surfactant tail and solubilizate B–surfactant tail interactions, respectively, while χ_{AB} is the solubilizate A–solubilizate B interaction parameter.

Predictions of the Binary Solubilization Model. The above model is used to compute the molar solubilization ratios and all the other aggregate properties when binary mixtures of benzene and hexane are solubilized in solutions of sodium dodecyl sulfate. The properties of the solubilizates have already been listed in Table II. The solubilizate–surfactant tail interaction parameters are calculated as for single solubilizates, using eq 160. The interaction parameter between solubilizates A and B is computed from

$$\chi_{AB} = v_{oA}(\delta_{oA}-\delta_{oB})^2/kT \quad (182)$$

One may note that $\chi_{AB}/v_{oA} = \chi_{BA}/v_{oB}$.

The computations of the equilibrium aggregation properties are carried out by the optimization procedures outlined before for the single component solubilizates. The only difference in the present case is that we have two variables, namely, Z_A and Z_B in place of the variable Z, with respective to which the optimization must be carried out. Thus, the optimization involves in this case the search for three, four, or five parameters depending upon the type of aggregate considered. The optimization was carried out using the IMSL subroutine ZXMWD in this case as well.

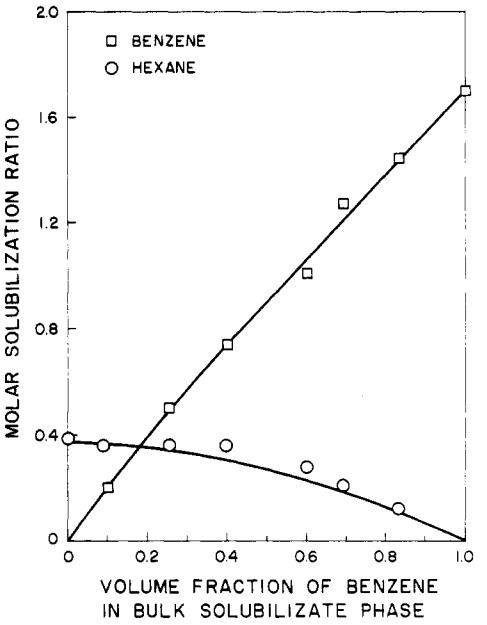

Figure 30. Dependence of the molar solubilization ratio of benzene and hexane on the composition of the solubilizate phase when binary mixtures of the two hydrocarbons are solubilized in 0.1 M solution of sodium dodecyl sulfate at 25 °C. Points are experimental data while the continuous lines represent the predictions of the present model.

The calculated molar solubilization ratios of benzene and hexane in 0.1 M solutions of sodium dodecyl sulfate are plotted in Figure 30 as a function of the composition of the bulk solubilizate phase that is in equilibrium with the aqueous surfactant solution. The predictions are also compared to our earlier experiments.[123] The comparison is quite satisfactory. Other properties such as the cmc and the average aggregation number have also been calculated but are not reported here since there are no measurements to compare them against.

XI. Conclusions

A predictive theory of surfactant self-assembly in aqueous solutions is developed free of any information derived from experiments on surfactant solutions. In addition, the number of molecular constants whose values can be determined from structural and physical property information is kept to a minimum. The thermodynamic model is developed by combining the well-established general principles of self-assembly with detailed molecular models for various contributions to the free energy of aggregation.

The molecular models for the free energy contributions contain a number of new features. Firstly, an analytical expression is derived for the conformational free energy of the surfactant tail inside the aggregates where the tail is in a state different from that of a liquid hydrocarbon. This expression depends on the aggregation number as well as the shape of the aggregate. Secondly, the head group interactions in nonionic poly(oxyethylene)-type surfactant systems are systematically modeled by taking into account the polymeric nature of the head group. The head group interaction free energy is computed by accounting for the mixing and elastic deformation free energy contributions. Thirdly, the ionic interaction free energy between the head groups of ionic surfactants is calculated

using an approximate analytical solution available in the literature for spherical and cylindrical geometries. This allows one to predict, not simply rationalize, the formation and properties of large rodlike micelles of ionic surfactants. Further, temperature-dependent expressions are provided for all the contributions to the free energy of aggregation. These permit computations of the temperature dependence of the cmc and the aggregation number. For solubilization, the differences in the molecular sizes of the solubilizate and the surfactant tail are accounted for as well as the nonideality in the mutual interaction energy.

Using the molecular free energy expressions derived here, the aggregation behaviors of illustrative nonionic, zwitterionic, and ionic surfactants have been predicted and compared with available experimental results. The cmc and the average aggregation number of micelles have been calculated as a function of the chain length of the surfactant tail when small, narrowly dispersed aggregates are formed. The change in the hydrodynamic radius of the aggregate has been computed as a function of the total surfactant concentration when polydispersed large spherocylindrical aggregates are formed. The dependence of the cmc and the average aggregation number have been predicted as a function of the ionic strength of the surfactant solution for ionic surfactants. The cmc and the aggregation numbers have also been predicted as a function of temperature for ionic and zwitterionic surfactants. The formation of polydispersed, large spherocylindrical micelles of ionic surfactants at various high electrolyte concentrations has been predicted. The sphere to rod transition parameter has been calculated as a function of the ionic strength, temperature, and tail length of the surfactant. The cmc, the average aggregation number, and the thickness of the poly(oxyethylene) head group region of nonionic micelles containing poly(oxyethylene) chains as head groups have been calculated as a function of the head group size. The molar solubilization ratios of a number of solubilizates in ionic and nonionic surfactants have been predicted. Also, the depression in cmc and the growth in the aggregation number accompanying solubilization have been calculated. The solubilization of hydrocarbons in rodlike aggregates has been examined. The solubilizate-induced transition to spherical aggregates and the influence of the solubilizates on this transition have been explained. Finally, the molar solubilization ratios of benzene and hexane in ionic micelles have been calculated when binary hydrocarbon mixtures are solubilized. In general, the predictions of the present model agree reasonably well with available experimental measurements.

Probably, the most significant feature of this work is that it offers a predictive approach in the vast literature regarding surfactant self-assembly. The ability to predict detailed features of aggregation opens up the opportunity and the need for corresponding detailed experimental measurements.